9-9-2015

Wireless communication system for data transfer and wireless power transmission

Timothy Buckley

Timothy Emmanuel Buckley
Candidate

Electrical and Computer Engineering
Department

This dissertation is approved, and it is acceptable in quality and form for publication:

Approved by the Dissertation Committee:

Dr. Christos Christodoulou, Chairperson

Dr. Mark Gilmore

Dr. Youssef Tawk

Dr. Steven Walsh

WIRELESS COMMUNICATION SYSTEM FOR

DATA TRANSFER AND WIRELESS POWER TRANSMISSION

by

TIMOTHY EMMANUEL BUCKLEY

DISSERTATION

Submitted in Partial Fulfillment of the
Requirements for the Degree of

Doctor of Philosophy

Engineering

The University of New Mexico
Albuquerque, New Mexico

December 2014

DEDICATION

I dedicate my Ph.D. to my mom, Angela Ortiz Buckley – Thank you Mom;

To my wife:

Raquel Buckley

To my boys and girl:

Austin Emmanuel Buckley,

Skyyler Ryder Buckley,

Dallas Hunter Buckley,

Dakota Buckley.

To Dr. Christos Christodoulou for giving me the opportunity, having patience, and allowing me to work with him.

To Dr. Wall, for believing in my math skills, providing guidance, and requiring that I major in electrical engineering in order to give me a book scholarship and provide me with tutors.

To Mr. Timbalo, without you explaining to me what an engineer was, taking the time out of your life to teach and tutor me in Algebra, Calculus I, II, III, and giving me the confidence to become an engineer, I never would have become an engineer or patent attorney.

To the Black Programs Department at New Mexico State University (No Black Programs Department – no Dr. Buckley).

To my brother Mychl, sisters Rachel and Jewel, and to my father, Bishop Buckley, Jr.

To Dr. Youssef Tawk and Firas Ayoub for all their gracious technical support in the lab.

To basketball and sports in general, for giving me the discipline and tenacity required to never give up.

I appreciate everything you have done for me. Thank you.

WIRELESS COMMUNICATION SYSTEM FOR

DATA TRANSFER AND WIRELESS POWER TRANSMISSION

By

Timothy Emmanuel Buckley

B.S., Electrical Engineering, New Mexico State University, 2001.

M.S., Electrical Engineering, National Technological University, 2002.

J.D., University of New Mexico, 2006.

M.B.A, University of New Mexico, 2010.

Ph.D., Engineering, University of New Mexico, 2014.

ABSTRACT

Powering wireless communication devices remotely is necessary when a user of the communication device has limited access to battery power or the resources necessary to constantly replace the batteries. This research is focused on remotely charging a communication device by using the power of the received signals at each antenna to dictate whether the system operates as a data transfer communication system or rectification device. The proposed communication system functions as a rectenna when the difference in power of the received signals is appreciable or as data transfer system when the received power is negligible. The WRCS system is also capable of harvesting energy that impinges the communication system. The size of the wireless communication system is designed based on the physical dimensions of the rectifier, the rectifier's impedance, as well as the operating frequency of the data transfer system. The overall objective is to maximize the power transferred to the system for storage while still being to operate effectively using the corresponding modulation system.

Table of Contents

LIST OF FIGURES

LIST OF TABLES

1 INTRODUCTION

Ever since Raytheon first demonstrated the ability to power a helicopter using microwaves in 1964 [1], engineers have been excited at the potential of remotely powering and harvesting energy to power electronic devices of all sorts. Since then wireless communication systems have become an integral part of everyday life in the United States and throughout the world. Due to both natural and man-made energy sources, an abundance of RF energy is propagating throughout the surrounding environment and constantly impinging on these wireless communication systems [10]. For example, atop the Golden Gate bridge in San Francisco wireless sensor networks have been deployed to collect various information related to the structure of the bridge [12]. Bridge related wireless sensor networks, such as the one depicted in the figure below, have been instituted to monitor the health of the bridge's infrastructure [12]. In wireless systems such as these where there is limited access to the device, it is often necessary to replenish dissipated energy without replacing the battery.

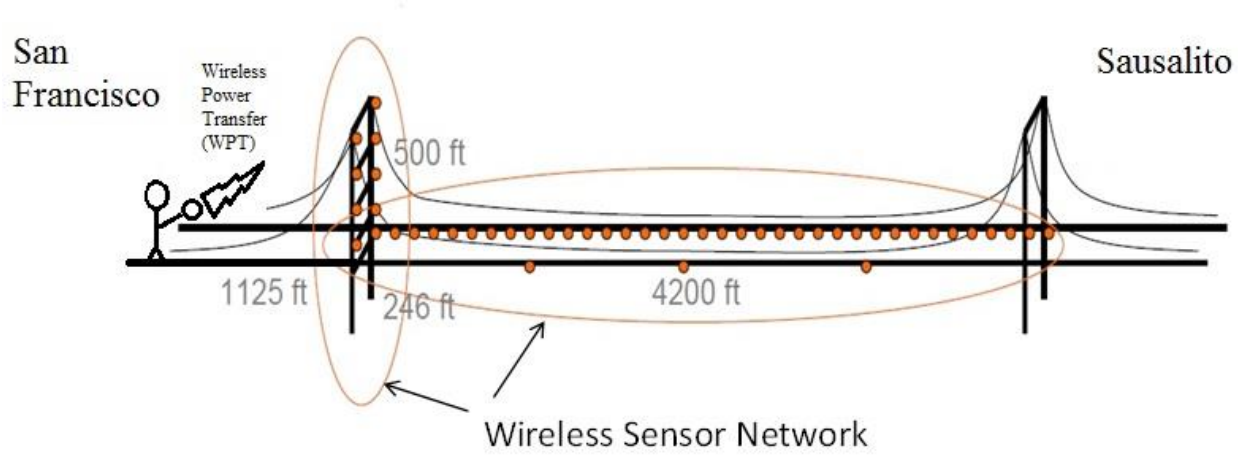

Figure 1" San Francisco's Golden Gate Bridge with Wireless Sensor Network (Adapted from [12] – Health Monitoring of Civil Infrastructures Using Wireless Sensor Networks)

Wireless sensors, such as those depicted above, are basically used to communicate with engineers and scientists on the ground to warn of any known dangers to the bridge. After a period of time, however, the batteries on these type of devices have to be replaced. Due to extensive traffic along the bridge and since the distance from the ground to the location of many of these devices located at the peak of the bridge is significant (550 feet in the case of the Golden Gate Bridge), it is not always feasible to easily replace the batteries.

Using wireless power transfer as a means of powering wireless devices allows the communication system to be self-sustainable for a longer period of time, relying less on the manual changing of batteries and reducing the need for the system to constantly be maintained. This can reduce the cost of maintenance for wireless communication systems, particularly those systems embedded in walls, buildings, bridges, etc. Thus, wireless power transfer has the potential to give wireless communication devices the ability to remotely-charge and obviate the need of the end user to constantly replace the batteries.

Ultra-low power sensors require 1.5 volts or 2.2 volts to operate [13]. For power sensors requiring 2.2 volts, storing power over a specified time frame can provide the power necessary to sustain the electronics for various tasks [13]. In order to power these sensors and better operate as an efficient wireless power transfer system, the receiving system should be able to rectify a maximum amount of energy within the antenna's frequency range and convert that energy to usable power.

Rectennas, which are a combination of an antenna and rectifier that convert received energy from alternating current (AC) to direct current (DC), can be used as means of wireless power transfer. However, because the overall objective of a rectenna system is to maximize the amount of power rectified, most rectenna systems do not provide for both wireless power

transfer and communication. This is because the energy collected for power storage is rendered useless for communication purposes after it is truncated at the point of rectification. Thus, for communication systems to operate effectively they require the ability to communicate. That is, the system must be able to transfer data using a specific modulation scheme and be able to demodulate the received signal. For a system to operate as both a rectenna and a communication system, the functionality of the communication system must remain intact.

The purpose of this research is to render a rectification device that maximizes power rectification and provides a communication system that provides for both communication and rectification while maintaining low cost. While the concept of energy rectification is not new (corporations such as Nokia and Intel are researching ways to maximize harvesting capability [8]), the ability of a communication system to utilize its antenna system both as a rectenna and communication device has not been studied in depth. For example, [1], [3], [4], [5] describe rectennas that focus on rectification alone. That is, they do not take into account that once the AC signal is converted to DC, it can no longer be utilized to transfer data. Others have studied the ability to use the same antennas for both data and power transfer [5, 14, 15]. However, they have not specifically focused on maximizing the rectified voltage through the use of power differences as opposed to forced phase differences. This research seeks to combine rectification and communication capabilities to maximize the rectified power while maintaining communication integrity.

In this research, a Wilkinson power combiner is manipulated using natural power differentiation to provide for both wireless power transfer and communication. A second broadband antenna can be added as part of the communication system to serve primarily as an

energy rectifier. The combination of energy obtained from the primary and secondary antenna systems combine to provide additional DC power to the communication system.

1.1 References

[1] W.C. Brown, J.R. Mims, N.I. Heenan, "An Experimental Microwave-Powered Helicopter", National Convention – IRE, 1965.

[2] W.C. Brown, "The History of Power Transmission by Radio Waves," *IEEE Trans. Microwave Theory and Techn.*, Vol. 32, No. 9, pp. 1230-1242, September 1984.

[3] D. Pozar, *Microwave and RF Design of Wireless Systems*, First Edition, Wiley, New York, 2001.

[4] D. Pozar, Microwave Engineering, 3rd Edition, Wiley, New York, 2005.

[5] H. Visser, *Approximate Antenna Analysis for CAD*, First Edition, Wiley, West Sussex, 2009.

[6] C.A. Balanis, *Antenna Theory: Analysis and Design*, Third Edition, Wiley, New York, 2005.

[7] Y.T. Lo, S.W. Lee, *Antenna Handbook: Theory, Applications, and Design*, Van Nostrand Reinhold Company Inc., New York, 1988.

[8] J.L. Volakis, C. Chen, K. Fujimoto, *Small Antennas: Miniaturization Techniques & Applications*, McGraw Hill, New York, 2010.

[9] J. Theeuwes, Simultaneous Wireless Transmission of Power and Data Using a Rectenna. *Eindhoven, University of Technology*. 2006.

[10] D. Bouchouicha, F. Dupont, M. Latrach, L. Ventura, *Ambient RF Energy Harvesting* . Granada : International Conference on Renewable Energies and Power Quality, 2010.

[11] A. Nimo, D. Grgic, L. Reindl, "Optimization of Passive Low Power Wireless Electromagnetic Energy Havesters", www.mpdi.com/journal/sensors, October 2012.

[12] S. Kim, S. Pakzad, D. Culler, J. Demmel, G. Fenves, S. Glaser, M. Turon, "Health Monitoring of Civil Infrastructures Using Wireless Sensor Networks", In *the Proceedings of the 6th International Conference on Information Processing in Sensor Networks (IPSN '07)*, Cambridge, MA, April 2007, ACM Press, pp. 254-263.

[13] C. Mikeka, H. Arai, Y. K. Tan, *Design Issues in Radio Frequency Energy Harvesting System - Sustainable Energy Harvesting Technologies - Past, Present and Future*, InTech, Available from: http://www.intechopen.com/books/sustainable-energy-harvestingtechnologies-past-present-and-future/design-issues-in-radio-frequency-energy-harvesting-system, 2011.

[14] M. Yang, R. Dougal, "A Wideband Circularly Polarized Rectenna for Wireless Power Transmission to Embedded Sensors",

[15] G. Yang, M. Islam, R. Dougal, M. Ali, "A Reconfigurable Stacked Patch Antenna for Wireless Power Transfer and Data Telemetry in Sensors", Progress in Electromagnetics Research C, Vol. 29, 67-81, 2012.

2 REVIEW OF RELATED LITERATURE

2.1 Introduction

Modern communication systems require an abundance of power in order to operate effectively. For example, RFID systems generally require 1.5 V to 2 V to operate effectively. There are many types of rectification systems that focus primarily on harvesting energy from ambient sources. A majority of the literature does not focus on using the same antennas for both wireless power transfer and wireless communication.

2.2 Rectenna, Rectenna Array Designs, and Data Telemetry for Wireless Power Transmission

The basic configuration of a rectenna consists of an antenna, a matching circuit, a bandpass filter, a diode model, a low-pass filter, and a load. The matching circuit matches the antenna to the impedance of the rectifier. The bandpass filter prevents harmonics generated by the diode from being reradiated by the antenna. The diode rectifies the energy received at the antenna. The low-pass filter prevents the RF signal from being radiated by the load and allows only the DC voltage to be provided to the load. A rectenna design is judged primarily by the amount of voltage rectified and the conversion efficiency of the rectifier.

In [1], a wireless power transmission rectenna was designed for RFID and Wireless Sensor Networks to operate at 2.45 GHz with a square patch antenna. The RFID rectenna consists of a rectangular patch antenna, an adaptation circuit, a bandpass filter, a diode, low-pass filter, and a load. For a microwave power transmission of 33 dBm and a receive power of 13 dBm with a 453 ohm load, the DC voltage across the load ranged between 1.6 V to 0.2 V for distances between 40 cm and 200 cm. The efficiency was calculated at 72%. A photograph of the RFID rectenna and corresponding rectified voltage are shown in the figures below.

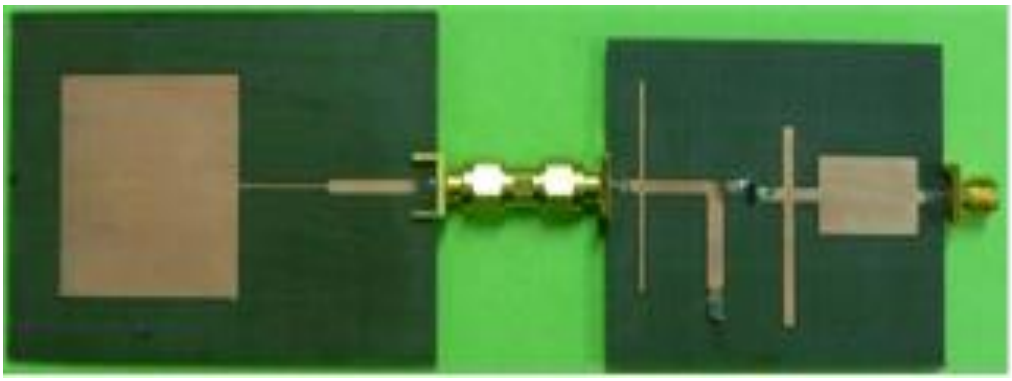

Figure 2: RFID Rectenna designed with a single diode at 2.45 GHz [1].

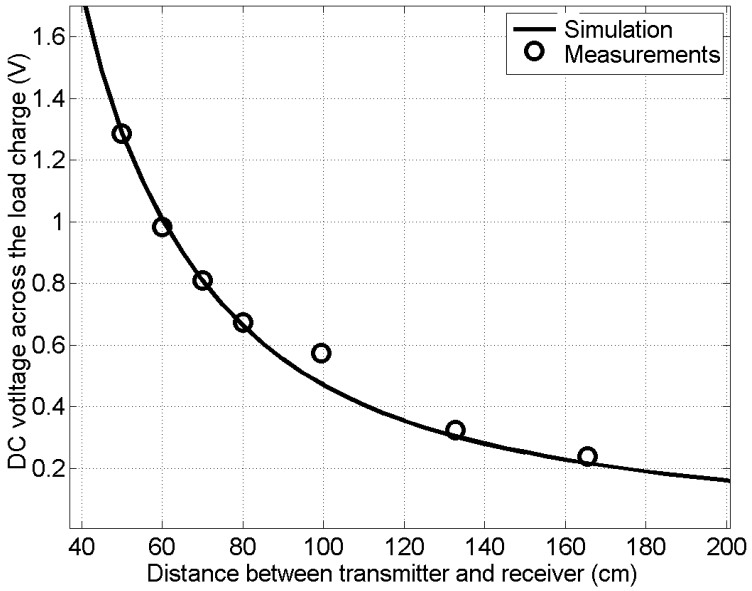

Figure 3: DC voltage measured at between 40 cm and 200 cm with a 453 ohm load, transmit power of 33 dBm, and receive power of 13 dBm [1].

RFID rectennas can be used to provide DC voltage to an RFID system having a battery for DC storage or a batteryless RFID using a capacitor to temporarily store energy. In [2], an RFID rectenna was designed for batteryless RFID sensors to operate at the 2.45 GHz ISM band to harvest ambient power. The RFID rectenna consists of an antenna, a transmission connected to a power divider, shorted stubs, and two voltage doublers. The RFID rectenna utilizes a two-stage Dickson zero-bias Schottky rectifier circuit. Using the HSMS-2852 diode in two voltage

doublers, the rectifier is able to provide a DC voltage of 1.6 V to the batteryless RFID sensor, exemplified by the powering of a 1.6 V LED. The PCB layout and circuit layout for the low-profile rectenna is shown in the figures below.

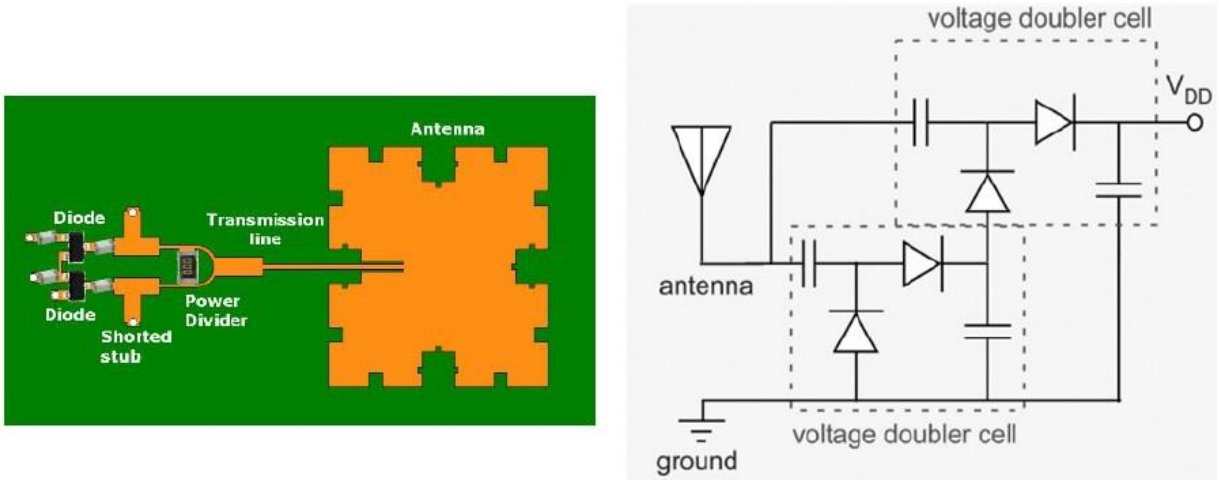

Figure 4: PCB layout and circuit layout for Low-Profile Rectenna for Batteryless RFID Sensors [2]

In [3], an RFID rectenna was designed to operate at 2.45 GHz for use in wireless power transportation. This paper focuses on identifying the areas of inefficiency in the rectenna and the means of improving the rectification circuit. The rectenna, as pictured below, includes a matching circuit, bandpass filter, the HSMS 2860 diode, and a low pass filter. For an RF input power of 15 dBm and 300Ω load, the efficiency obtained was 79.3%.

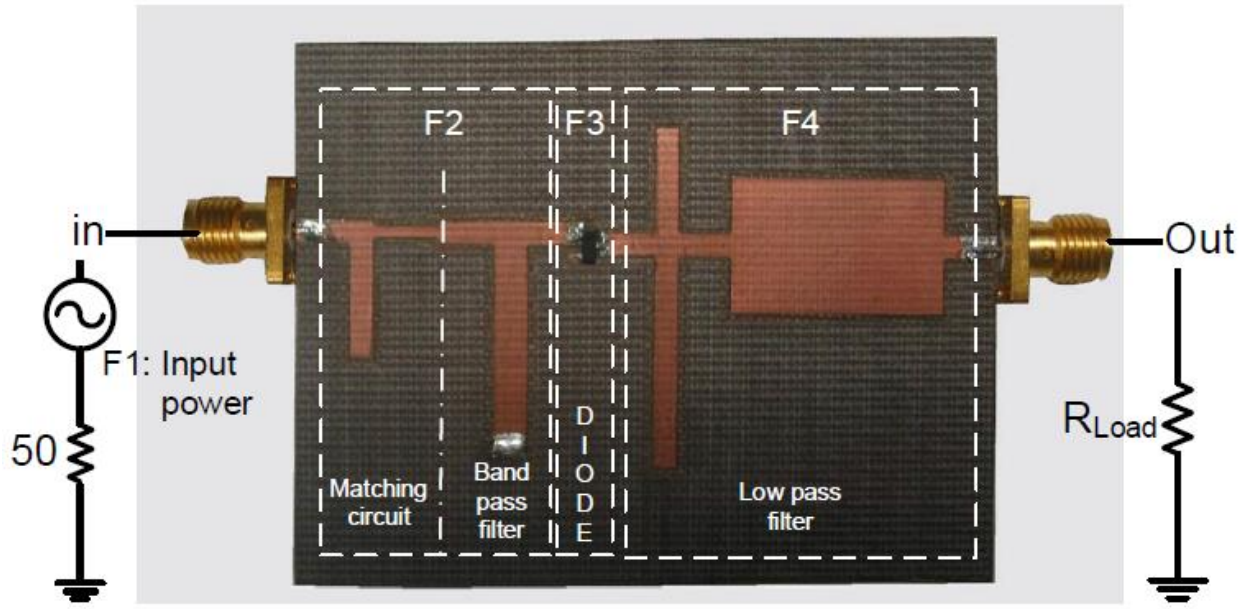

Figure 5: RFID Rectenna operating at 2.45 GHz with matching circuit, bandpass filter, diode, low-pass filter [3].

Rectennas have also been designed to operate in the unlicensed 5.8 GHz ISM band. In [4], a circularly polarized rectenna is designed with a single diode connected to a shorted annular ring-slot structure. The purpose of the design is to provide a rectenna having circular polarization, which is not typical in the majority of rectenna designs. The benefit of having a circularly polarized rectenna compared to a linearly polarized rectenna is that constant DC can be attained even when there is a change in the rotation angle of the rectenna compared to the transmitter. The shorted annular ring-slot structure rectenna operated at two frequencies, 2.45 GHz with a 49% efficiency and 5.8 GHz with a 14% efficiency. A schematic of the shorted annular ring-slot rectenna and the rectified DC voltage are depicted in the figures below.

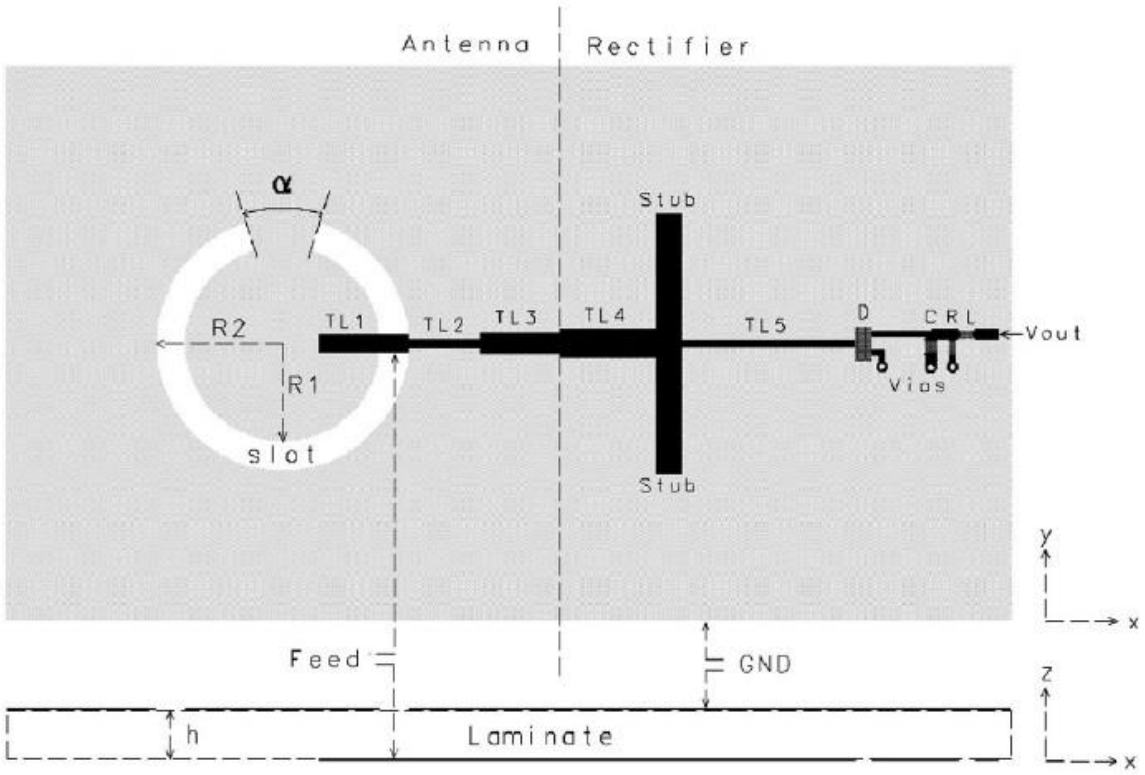

Figure 6: Shorted Annular Ring-slot Rectenna [4].

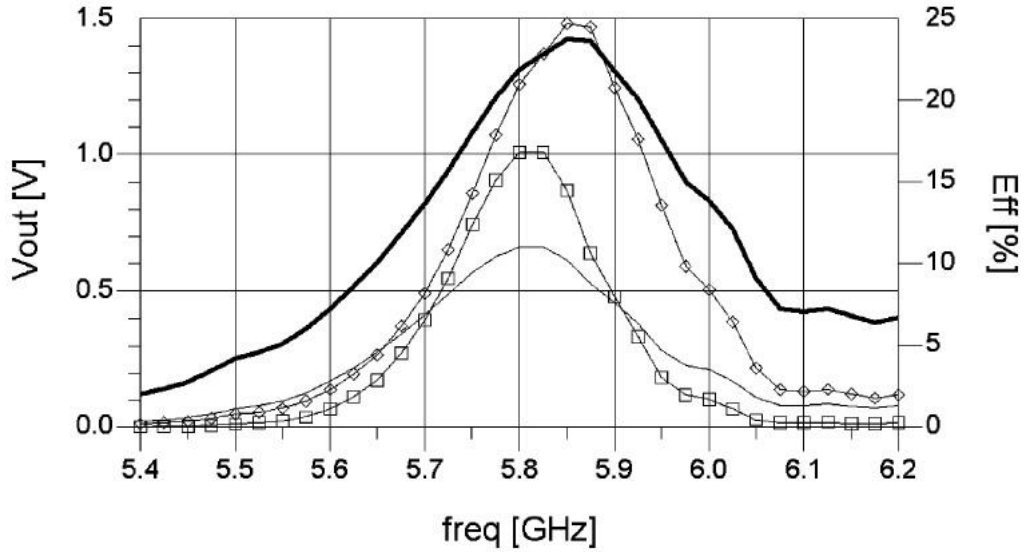

Figure 7:Measured rectifier output dc voltage (Vout) and efficiency (Eff) at two different input power (Pin) levels. Vout@Pin = - 5 dBm; Vout@Pin = 0 dBm; E_@Pin = - 5 dBm; _ E_@Pin = 0 dBm [4].

Wireless power transfer systems often utilize rectenna arrays in order to meet minimum power requirements. Rectenna arrays consist of a series of antennas whose output is rectified and combined using a rectifier. In one embodiment, each element of the antenna array has a diode at its output to rectify the voltage. The voltage is then combined in series, parallel, or a series-parallel combination. In another embodiment, an array of antennas may have a single diode rectifier at its output. There are a plethora of rectenna arrays that have been used to harvest energy at 5.8 GHz. However, like the single element rectennas, the majority of rectenna arays focus on using the antennas only to harvest energy, not for communication purposes.

In one example, in rectenna arrays are used for wireless power transmission in electric vehicles [5]. Powering the vehicle using a wireless power transmitter has the potential to eliminate the need for plugging in the vehicle into an electrical outlet in order to recharge the battery. The vehicle is equipped with a 4 x 4 rectenna array operating at 5.8 GHz. The electric vehicle utilizing wireless power transmission with the rectenna array configuration is shown in the figure below.

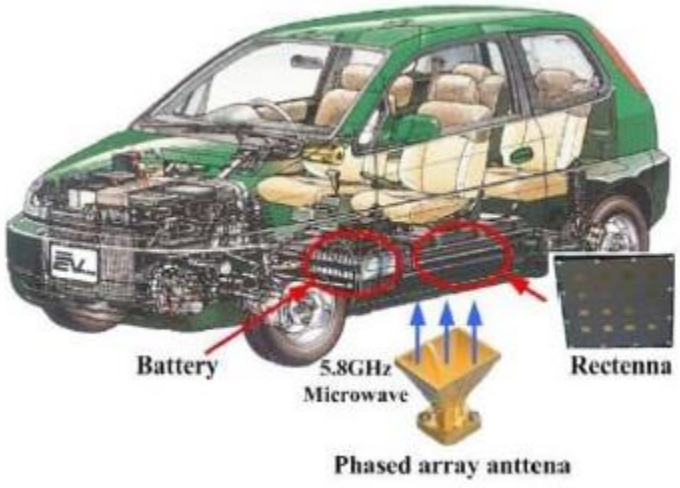

Figure 8: Electric vehicle using wireless power transfer at 5.8 GHz [5].

The rectification system uses the HSMS 8202 diode as a rectifier. The input power of the rectenna is 0 dBm and provided by a 4 horn antenna configuration. For the input power of 0 dBm, the rectified voltage is 230 mV. The efficiency was calculated as 49% at 200 mm and 75% at 400 mm. The experimental set-up as well as the 16 patch rectenna, wireless power transmitter, and output voltage are shown in the figures below.

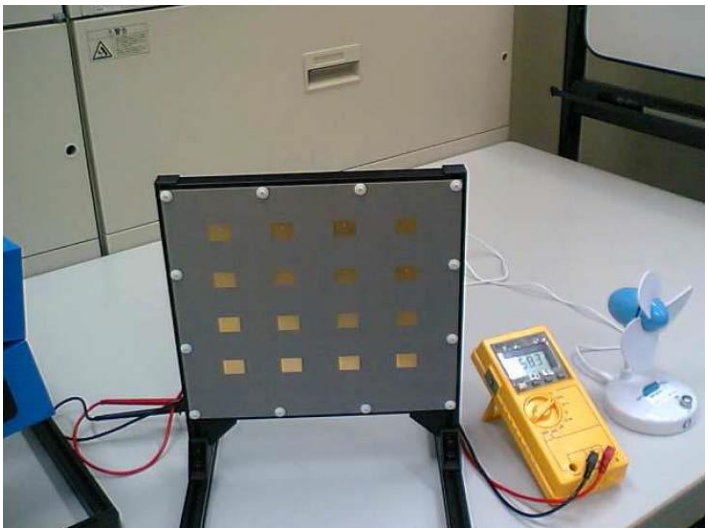

Figure 9: 4 x 4 Microstrip patch rectenna array operating at 5.8 GHz [5].

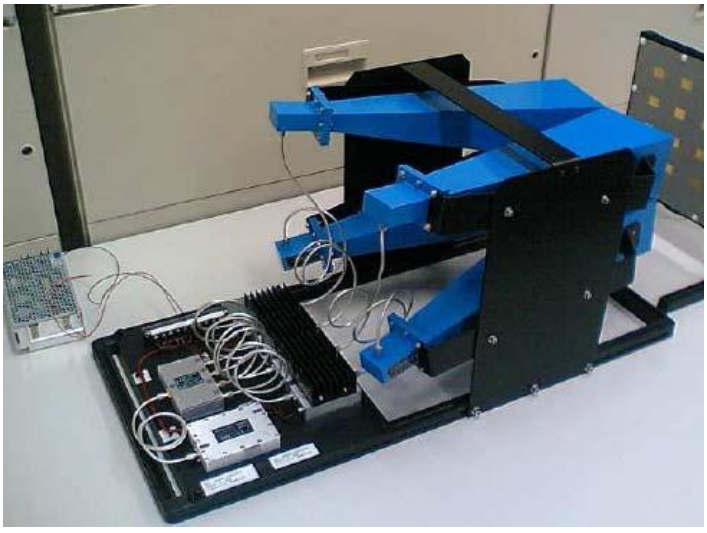

Figure 10: Wireless Power Transmitter at 5.8 GHz [5].

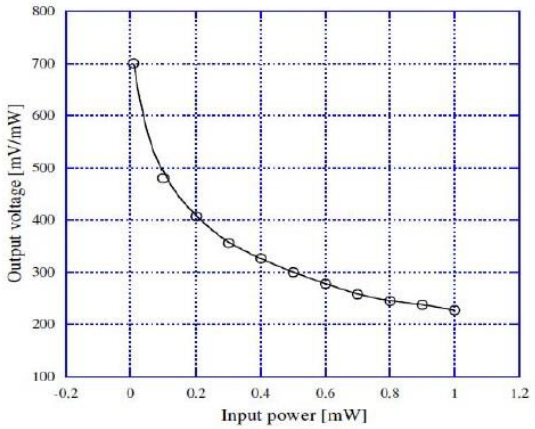

Figure 11: Output voltage for input power between -0.2 to 1.2 mW [5].

In [6], 5.8 GHz circularly polarized dual-patch, 6 patch, and 16 patch dual-diode rectenna and rectenna array are presented for microwave power transmission. The dual-diode configuration has a conversion efficiency of 76% and provides double the output voltage of the standard single diode rectenna. For DC combination, the rectenna uses a linear device model, which allows the dc combiner to work in series, in parallel, or in the series-parallel combination as shown below. A maximum output voltage of approximately 20 volts was achieved for the cascaded combination with a 150 ohm load and 18 mW/cm2.

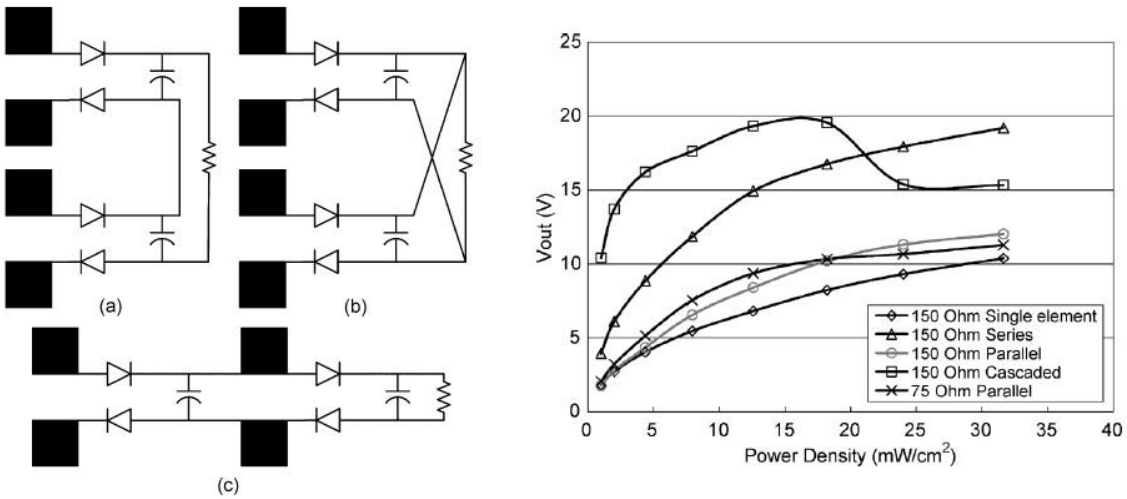

Figure 12: 4 Element Rectangular Patch Rectenna Array and corresponding rectified output voltage at 5.8 GHz [6].

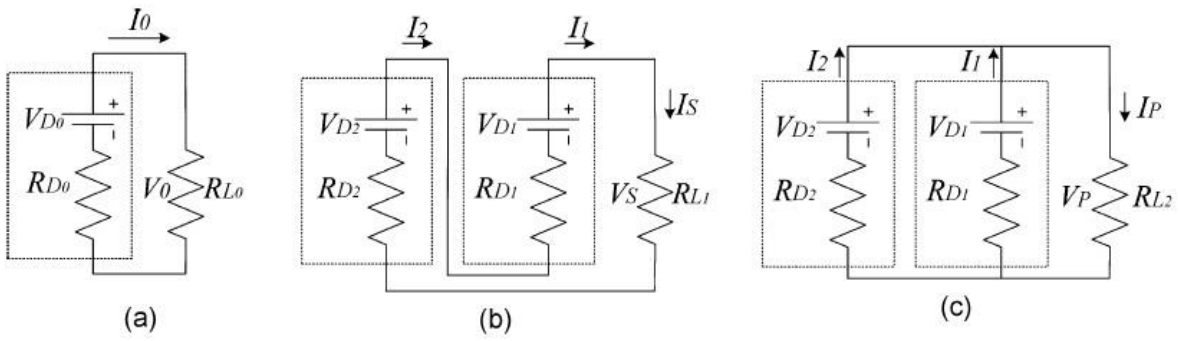

Figure 13: Linear Eq. Models used for combining the output voltages of rectenna array. (a) Single Element. (b) Series Connection. (c) Parallel connection. Vdi 7 Rdi are equivalent voltage & resistance of the rectifying circuit. Ii and Vi are the current and voltage provided from the rectifying circuit to the output load. RLi is the load resistance [6].

In [7], broadband circular dipole rectenna arrays are designed to increase the amount of rectified voltage compared to a single element rectenna. The voltage rectified from each dipole rectenna is combined in series. The four element array is designed to rectify voltage from 2.4 to 6.6 GHz. The peak rectified voltage for the 4 element array is around 75 mV with a conversion efficiency expected to be less that 50% (calculation of efficiency not completed at the time of publication). The amount of DC voltage rectified was less than the rectified voltage for a single rectenna and was attributed to the coupling between the antennas.

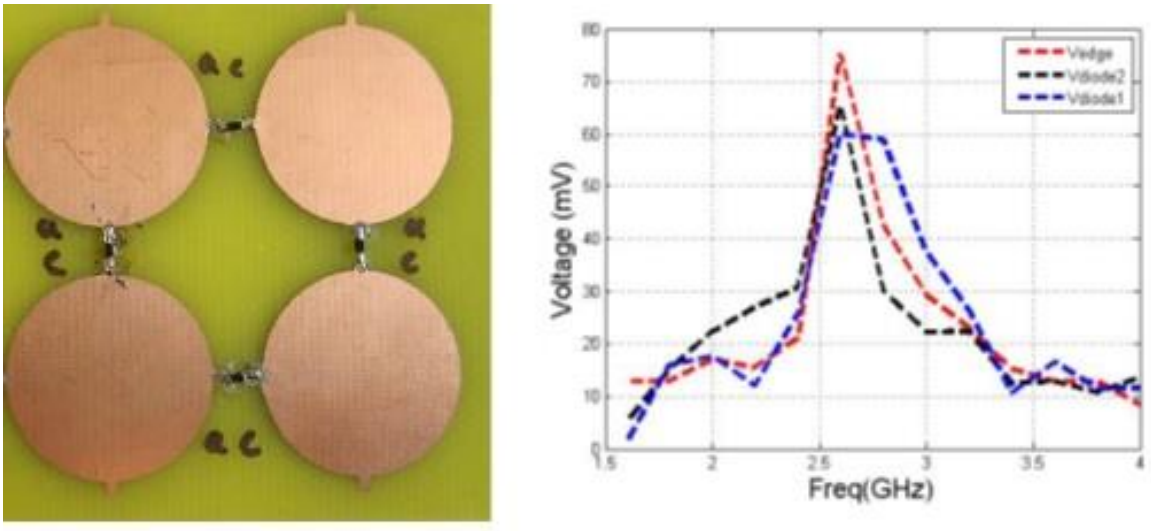

Figure 14: 2x2 Circular dipole rectenna array operating from 2.4 GHz to 6.6 GHz with a rectified voltage of 75 mV [7].

Spiral rectennas have also been used in wireless power transmission in order to rectify microwave power over a broad range of frequencies. In the spiral rectenna configuration, the rectifying diode is placed at the input feed of the spiral. There is no matching network placed between the diode and the arms of the antenna. The objective in the spiral rectenna design is to provide a constant impedance to the spiral over the specified frequency range. For example, in [8], a spiral rectenna is designed to operate between 1.5 GHz and 3 GHz. An HSMS 2850 diode is placed at the center of the spiral as depicted in the figure below.

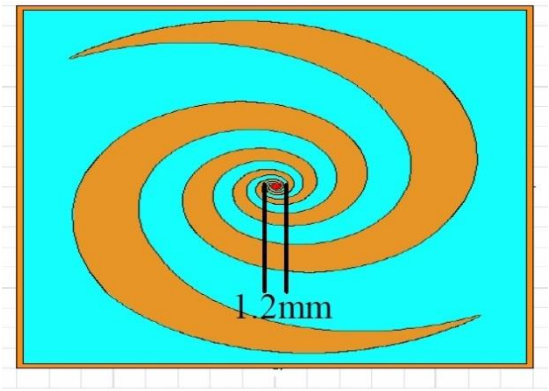

Figure 15: Spiral Rectenna with diode place in center for rectification [8].

The spiral antenna is heavily diode dependent because its center length is based on the size of the diode. Thus, the spiral rectenna must first consider the physical parameters of the diode when design the spiral rectenna. For the spiral rectenna designed in [8], a voltage doubler rectifier configuration was used with an 18 kΩ load place at the output. The fabricated design and corresponding DC output power are shown in the figures below.

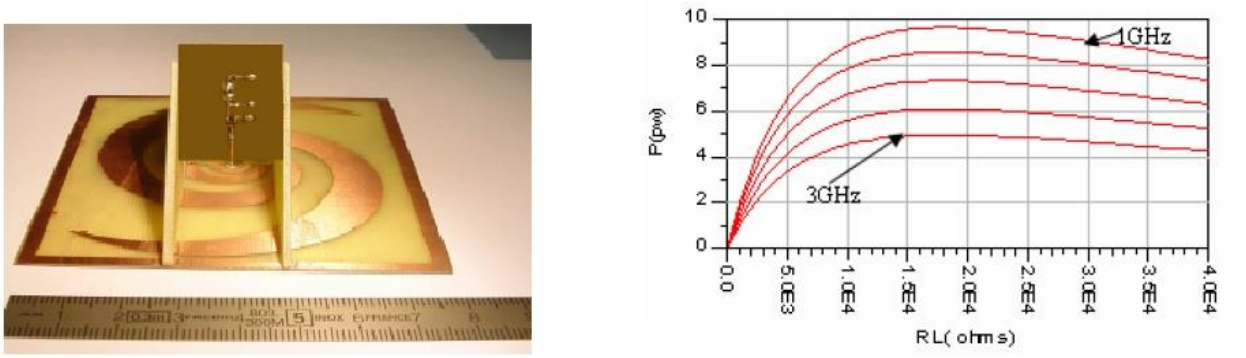

Figure 16: Spiral Rectenna operating from 1 to 3 GHz and the corresponding DC output power [8].

In [8], the DC output power as a function of the load resistance with an input power of -42 dBm is shown. As can be seen from the graph, the DC power output by the rectenna is extremely low (-83 dBm and -80 dBm) likely caused by mismatch between the HSMS 2850 diode and spiral antenna.

Spiral rectenna arrays are also used to increase the amount of DC power supplied to the load. An example of a spiral rectenna array is designed in [9]. The same principles for designing the single spiral rectenna relative to the physical parameters of the diode apply to the design of the spiral rectenna array, except that the output DC voltage must be combined using a DC combiner as depicted in the figure below.

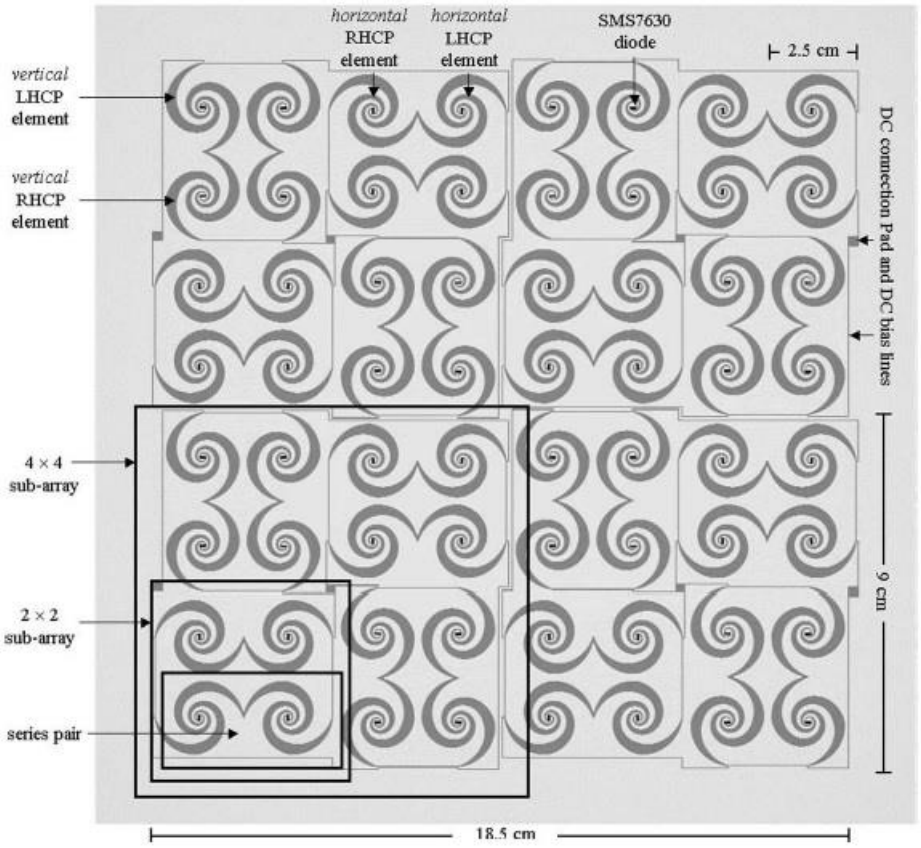

Figure 17: Example of Spiral Rectenna Array operating between 2-18 GHz [9].

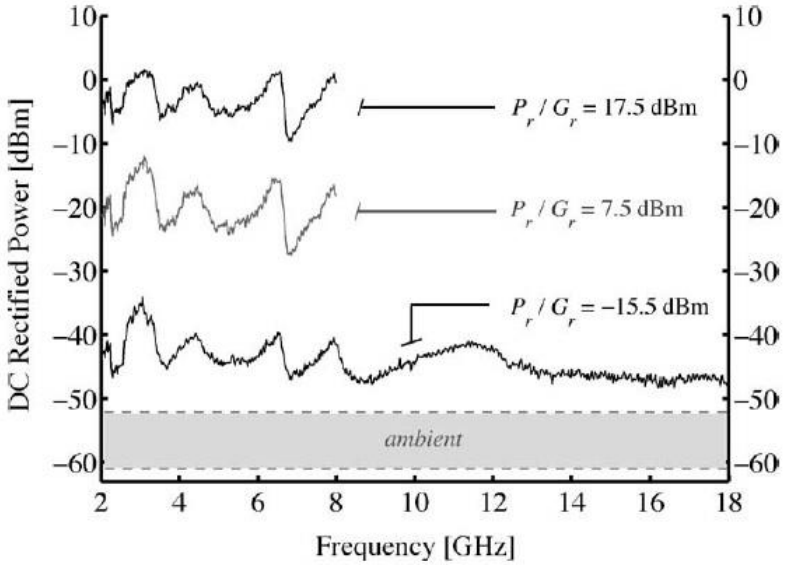

Figure 18: Rectified DC power for the 64 element spiral rectenna array between 2 GHz - 18 GHz [9].

Practical wireless communication systems designed for wireless power transmission must be able to generate DC voltage as well as perform necessary communication functions. For example, in [10] a wideband circularly polarized microstrip patch rectenna is designed to operate as a WLAN communication device at 5.15 GHz to 5.35 GHz and as a rectenna at 5.5 GHz. The circular polarization characteristic of the antennas allows the system to receive both left hand and right hand polarized signals. When the communication rectenna receives right hand polarized signals, it acts as a communication device. When the communication rectenna receives left hand polarization, it acts as a rectification device. In essence, the switching between communication and rectification is caused by the polarization of the received signal.

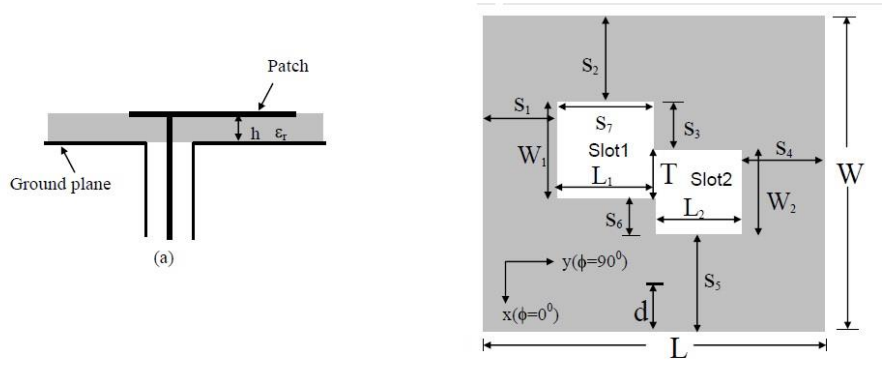

Figure 19: Circularly polarized microstrip patch rectenna is designed to operate as a WLAN communication device at 5.15 GHz to 5.35 GHz and as a rectenna at 5.5 GHz [10].

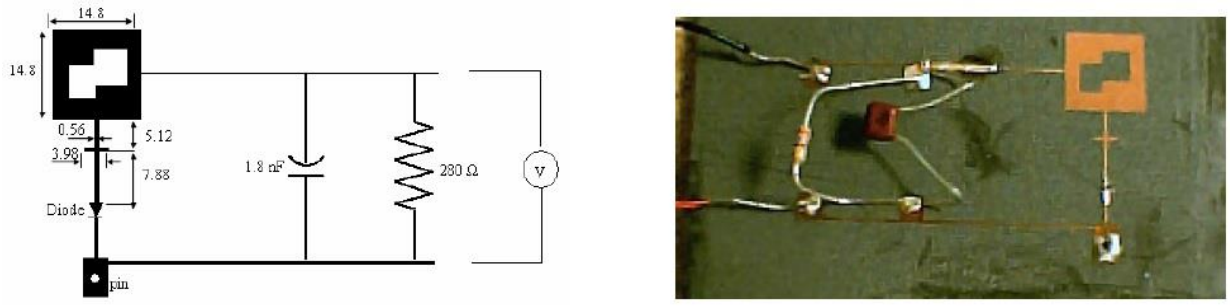

Figure 20: Circuit and fabrication of circularly polarized microstrip patch rectenna is designed to operate as a WLAN communication device at 5.15 GHz to 5.35 GHz and as a rectenna at 5.5 GHz [10].

In [11], a power and data system was designed to operate at 2.45 GHz using a technique used to force a phase shift between both antenna inputs. The system utilizes a Wilkinson combiner with an extended microstrip length in order to be able to the rectify voltage. To force a phase-shift difference at the combiner input ports, the transmission lines at input ports 1 and 2 were designed with unequal lengths as indicated in the figure below.

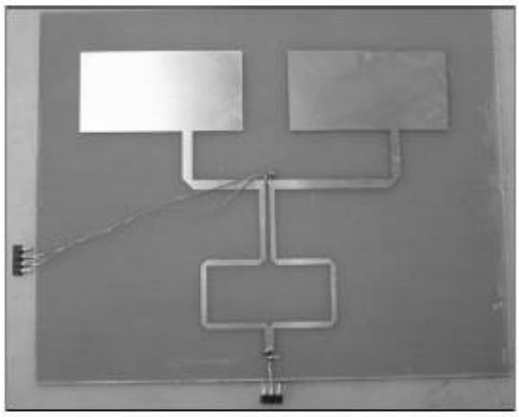

Figure 21: Power and data transfer circuit with forced-phased shifter operating at 2.45 GHz [11]

As can be seen from the figure below, using the HSMS 2852 diode, the system was able to rectify 0.7 volts at the resonant frequency with an input power of 3 mW (4.7 dBm).

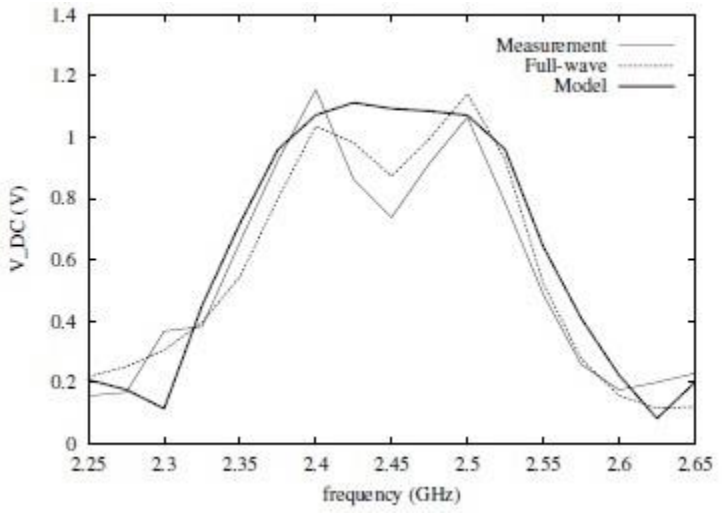

Figure 22: Results of power and data transfer circuit. [11]

Another example of a system that is able to perform both data transport and rectification is exemplified in [12]. In [12], a reconfigurable stacked patch antenna is designed for both wireless power reception and data telemetry. The reconfigurable rectifier and communication system operates as a rectenna at 5.8 GHz and as a communication device at 2.45 GHz. The communication rectenna switches between rectenna mode and telemetry mode using control circuitry. An HSMS 2862 is used as voltage doubler with a 200 ohm load. The reconfigurable stacked patch communication rectenna is shown in the figure below. For an input power density of 1 mW/cm^2, the conversion efficiency is 85.5% and the rectified voltage varies between 0.6 V and 2.8 V for distances ranging from 70cm to 160cm. When the designed reconfigurable circuit is place inside concrete, for a transmit power of 7 W the rectified voltage is 2.1 V. The circuit design for the reconfigurable stacked patch communication rectenna, the rectified DC voltage, and the conversion efficiency of the rectenna are depicted in the figures below.

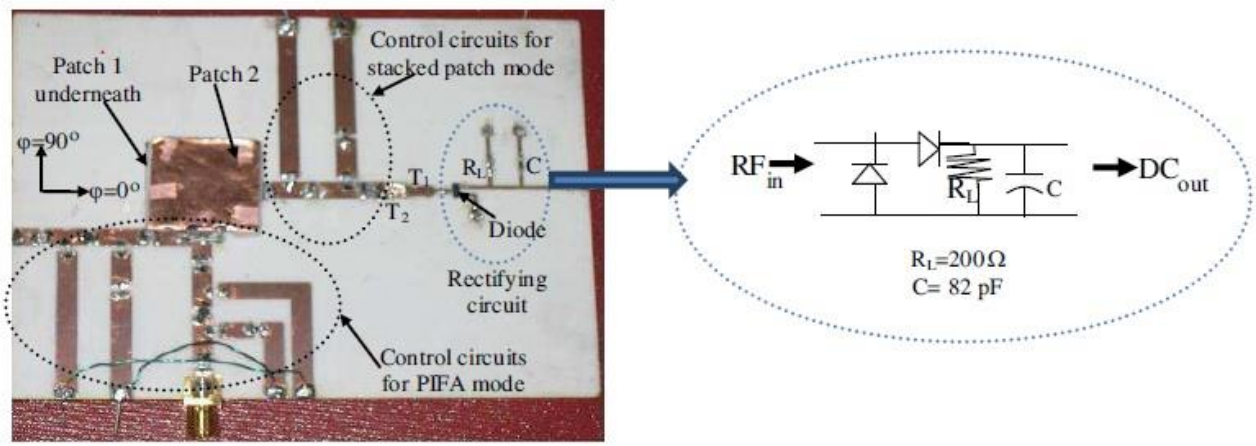

Figure 23: Reconfigurable stacked patch communication rectenna and voltage doubler for rectification at 5.8 GHz and communication at 2.45 GHz [12].

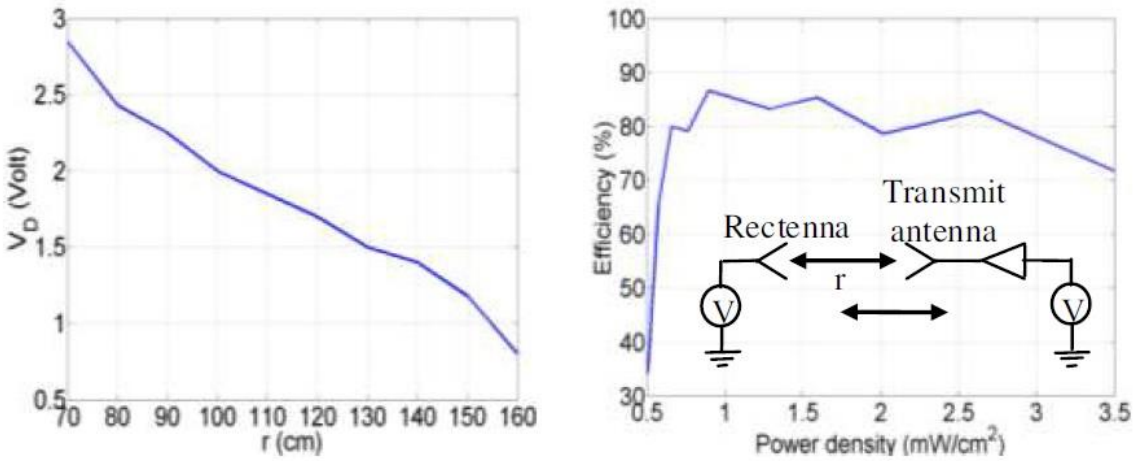

Figure 24: DC voltage and conversion efficiency for reconfigurable stacked patch communication rectenna for 3 V received voltage [12].

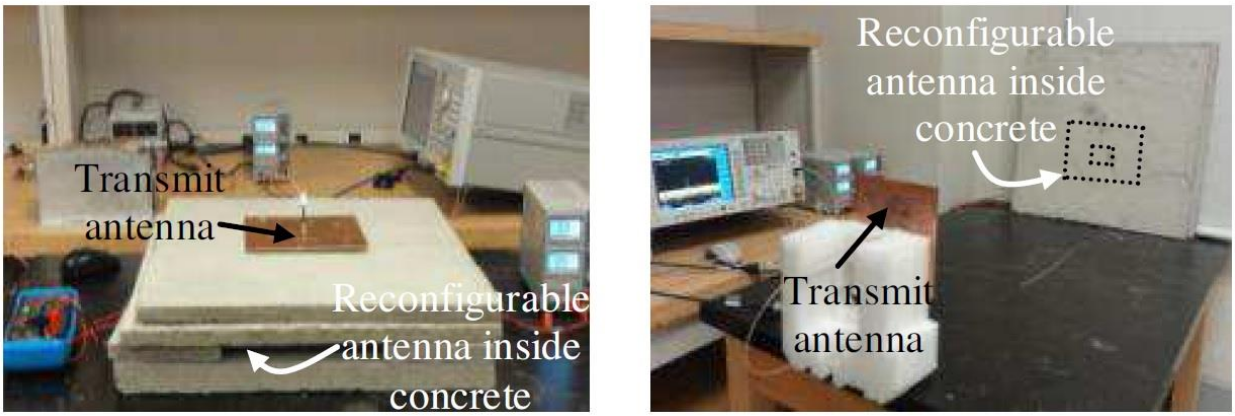

Figure 25: Example of the Reconfigurable stacked patch communication rectenna performing rectification and data communication in a concrete slab with a rectified voltage of 2.1 Volts [12].

A summary of the important parameters in this literature review for the rectenna, rectenna arrays, and communication rectenna configurations are shown in the table below.

Table 1: Summary of Literature Review and Related Research

Publication Title	Frequency	Input Power	Diode	Circuit Configuration	Rectifier Impedance	Load (Ohms)	Rectified Voltage	Efficiency	Antenna Type	Device Type	Author	Year
An integrated model of a wireless power transportation for RFID and WSN applications	2.45 GHz	13 dBm	HSMS 2860	Single Diode	-	453 Ω	1 V at 60 cm	0.72	Rectangular Patch	Rectenna	Riviere	2009
Low-profile planar rectenna for batteryless RFID sensors	2.45 GHz	-25 dBm to 10 dBm	HSMS 2852	Voltage Doubler	-	13 kΩ	1.6 V	60% to 70%	Fractal Microstrip Patch	Rectenna	Olgun	2010
Losses Analysis and Performance Improvement of a Rectenna for RFID Systems	2.45 GHz	15 dBm	HSMS 2860	Single Diode	-	300 Ω	-	0.793	N/A - 50 Ohm Power Source	Rectenna	Douyere	2008
Design of a Compact Planar Rectenna for Wireless Power Transfer in the ISM Band	2.45 GHz	8 dBm	HSMS 8101	Single Diode	115.461-j260.633	100 Ω	2.0 V	0.729	Two Element Rectangular Patch Array	Rectenna	Zhang	2014
Low-profile circularly polarized rectifying antenna for wireless power transmission at 5.8 GHz	5.8 GHz	-5dBm, 0 dBm	HSMS 2862	Voltage Doubler	-	8.2 kΩ	0.6 V, 1.3 V	17%, 23%	Shorted Annular Ring-slot Structure	Rectenna	Heikkinen	2004
Harvesting RF Energy with Rectenna Arrays	2.4 GHz to 6.6 Ghz	3 dBm (source power)	SMS7621-079F	Single Diode	-	-	140 mV	TBD	Circle Dipole Antenna	Rectenna	Zhang	2011
Prototype of 5.8 GHz Wireless Power Transmission System for Electric Vehicle System	5.8 GHz	0 dBm	HSMS 8202	Single Diode	-	50Ω	230 mV	49% (200 mm), 75%(400mm)	4 x 4 Rectangular Patch Array	Rectenna	Ahn	2011
5.8 GHz Circularly Polarized Dual-diode Rectenna and Rectenna Array for Microwave Power Transmission	5.8 GHz	0 mW to 30 mW	MA4E1317	Dual-diode	-	150Ω	2 V to 20 V	49% to 74%	4 Patch Rectangular Array	Rectenna	Ren	2006
Ambient RF Energy Harvesting	1 GHz to 3 GHz	-40 dBm	HSMS 2850	Voltage Doubler	-	18 kΩΩ	-83 dBm and -80 dBm (DC power)	0.6%	Spiral	Rectenna	Bouchouicha	2010
[illegible] microwave energy with broad-band rectenna arrays	2 GHz to 18 GHz	0.01 mW/cm2	SMS7630-079	Single Diode	-	600 Ω	[illegible] dBm, -40dBm (DC power)	20%	64 Element Spiral Array	Rectenna	Hagerty	2004
A Wideband Circularly Polarized Rectenna for Wireless Power Transmission to Embedded Sensors	5.15 GHz to 5.35 GHz (communication) 5.5 GHz (rectenna)	-	MA4E1317	Single Diode	172Ω	280 Ω	2.8 V	-	Circularly Polarized Microstrip Patch Antenna	Communication Rectenna	Ali	2005
Approximate Antenna Ar	2.45 GHz	4.77 dBm	HSMS 2852	Voltage Doubler	-	-	0.7 V (at resonance), 1.2 V at 2.38 GHz	-	2 Element Rectangular Patch	Communication Rectenna	Visser	2009
Reconfigurable Stacked Patch Antenna for Wireless Power Transfer and Data Telemetry Sensors	5.8 GHz (rectenna), 2.45 GHz (Communication)	0 dBm	HSMS 2862	Voltage Doubler	-	200Ω	2.7 V	85%	Reconfigurable Stacked Patch Antenna	Communication Rectenna	Yang	2012

2.3 Benefits of Current Research Over Prior Art

The benefits of the Wireless Rectenna Communication System (WRCS) described in this dissertation over the art cited are several. For example, in addition to increased rectified voltage (1.7 V for single diode versus 1.2 V for a voltage double configuration), the benefit of the WRCS system over [12] is that the WRCS system does not require a forced-phase shift in order to rectify voltage. The WRCS system uses the difference in received power at the antenna input ports to rectify voltage. The addition of a microstrip line to force the phase shift in [12] increases the dimensions of the rectenna system which can lead to additional cost. The benefits of the proposed WRCS system over [10] is that the single rectenna WRCS system operates as an array when in communication mode. The system described in [10] utilizes only a single antenna and thus does not have the advantages of an array over a single antenna system. In [12] additional MEMS circuitry is added to the device in order to perform rectification. The additional MEMS circuitry increases cost and intricacy of the communication rectenna. Thus, compared to the WRCS system designed in this research, the added complexity and cost does not overcome the simplicity and utility of the WRCS system designed to rectify by simply using the power difference at each antenna port.

2.4 References

[1] S. Riviere, F. Alicalapa, A. Douyere, J-D. Lan Sun Suk, B. Grondinn-Perez, "An integrated model of a wireless power transportation for RFID and WSN applications", IEEE, 2009.

[2] U. Olgun, C. Chen, J. Volakis, "Low-Profile Planar Rectenna for Batteryless RFID Sensors", IEEE, 2010.

[3] A. Douyere, F. Alicalapa, J-D. Lan Sun Luk, A. Celeste, "Losses Analysis and Performance Improvement of a Rectenna for RFID Systems", IEEE 2008.

[4] J. Heikkinen, M. Kivikoski, "Low-Profile Circularly Polarized Rectifying Antenna for Wireless Power Transmission at 5.8 GHz", IEEE Microwave and Wireless Components Letters, vol. 14, no. 4, pp. 162-164, April 2004.

[5] C. Ahn, T. Kamio, H. Fujisaka, K. Hawiewa, "Prototype of 5.8 GHz Wireless Power Transmission System for Electric Vehicle System", 2011 2nd International Conference on Environmental Science and Technology, 2011.

[6] Y. Ren, K. Chang, "5.8-GHz circularly polarized dual-diode rectenna and rectenna array for microwave power transmission", IEEE Transaction on Microwave Theory and Techniques, Vol. 54, No. 4, April 2006.

[7] J. Zhang, Y. Huang, P., "Harvesting RF Energy with Rectenna Arrays", 6th European Conference on Antennas, 2011.

[8] D. Bouchouicha, F. Dupont, M. Latrach, L. Ventura, "Ambient RF Energy Harvesting", International Conference on Renewable Energies and Power Quality, Granada, 2010.

[9] J.A. Hagerty, W. H. McCalpin, R. Zane, Z. B. Popovic, "Recycling Ambient Microwave Energy With Broad-Band Arrays", IEEE Transactions On Microwave Theory and Techniques, 2004, Vol. 52.

[10] M. Yang, R. Dougal, “A Wideband Circularly Polarized Rectenna for Wireless Power Transmission to Embedded Sensors”,

[11] H.J. Visser, *Approximate Antenna Analysis for CAD*, John Wiley & Sons, Chichester, 2009.

[12] G. Yang, M. Islam, R. Dougal, M. Ali, “A Reconfigurable Stacked Patch Antenna for Wireless Power Transfer and Data Telemetry in Sensors”, Progress in Electromagnetics Research C, Vol. 29, 67-81, 2012.

3 WILKINSON RECTENNA COMMUNICATION SYSTEM

3.1 Introduction

The Wilkinson Rectenna Communication System (WRCS) is a communication system that combines both a rectenna and combiner into a simple communication system capable of both power and data transfer. A second spiral rectenna can be added to the system to function as an always-on rectenna. The WRCS is based on the Wilkinson power combiner and functions as part of the rectenna communication system.

The figure below exemplifies the harvesting and communication structure of the Wilkinson Rectenna Communication System. Amplitude modulation can be used for data transfer on a 5.8 GHz carrier signal. The spiral rectenna is capable of rectifying energy between 8 GHz to 12 GHz.

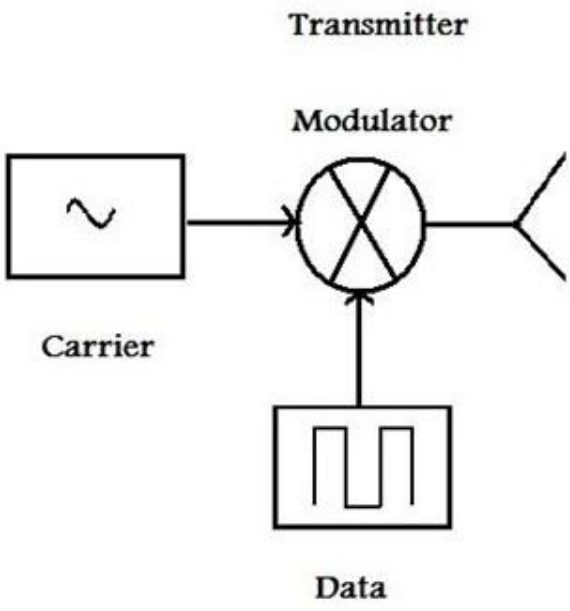

Figure 26: WRCS Transmitter

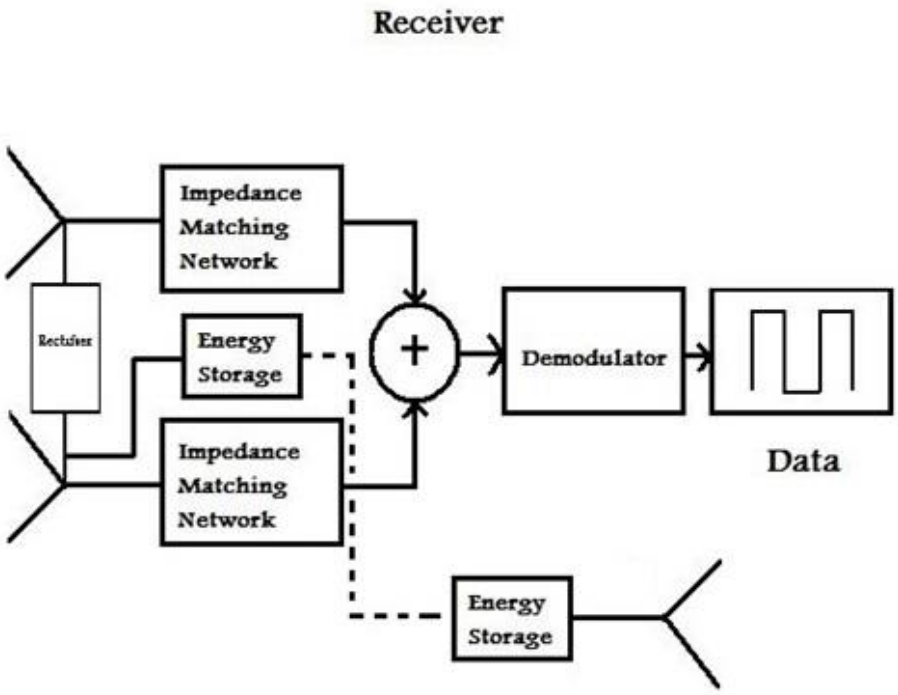

Figure 27: WRCS Receiver

The two-element array connected to the Wilkinson rectenna consists of mictrostrip rectangular patch antennas operating at a narrowband frequency of 5.8 GHz. The rectangular patch antennas toggle from communication system to rectenna based on the differences in power received at the antenna input ports. When the power levels received at the antennas are relatively equal, the WRCS works as communication system, transferring data to the remainder of the system. When the power received at the antennas is not equal, the WRCS works as a wireless power transfer rectenna.

A Wilkinson power combiner is modified for both data transfer and DC conversion. The resistor normally used in the Wilkinson power combiner is replaced by a rectifier. When the rectangular patch antennas receive signals and there is a power difference between the received signals, a voltage difference develops across the rectifier. This causes a current to flow through

the rectifier. The rectifier then converts the current to DC which can then be provided for power storage. When the rectangular patch antennas receive signals that have the same power, there is no or minimal voltage difference across the rectifier and the rectifier provides minimal DC to the load. The received signals flow through the WRCS system as data to the demodulator, which then demodulates the signal.

The always-on spiral rectenna is a broadband rectenna operating between 8 GHz to 12 GHz. When the spiral rectenna receives energy within this frequency range, it immediately rectifies the energy for power storage. The spiral rectenna can be coupled to its own energy storage unit or be coupled to the energy storage device that is connected to the Wilkinson rectenna. The energy collected from both the Wilkinson Rectenna and the spiral rectenna can be combined to provide the energy required to power low power devices.

3.2 Wilkinson Combiner

The Wilkinson power divider is a matched three port system that receives power at port 1 and divides the power evenly between ports 2 and ports 3 using arms 1 and 2 and a resistor [2]. In addition to dividing power between ports 2 and 3, a primary benefit is that the Wilkinson power divider provides isolation between ports 2 and 3 by way of the resistor [2]. To accomplish isolation, ports 1, 2, and 3 each have impedances of 50 ohms, arms 1 and 2 each have impedance of 70.71 ohms and a length of $\frac{\lambda}{4}$, and the resistor has a resistance of 100 ohms. Ideally, the isolation provided by the resistor allows the combiner to be reciprocal, lossless, and matched [4]. A Wilkinson power divider is shown in the figure below. The figure shows a power divider with a receiving port and two arms separated by a resistor where the power is equally split.

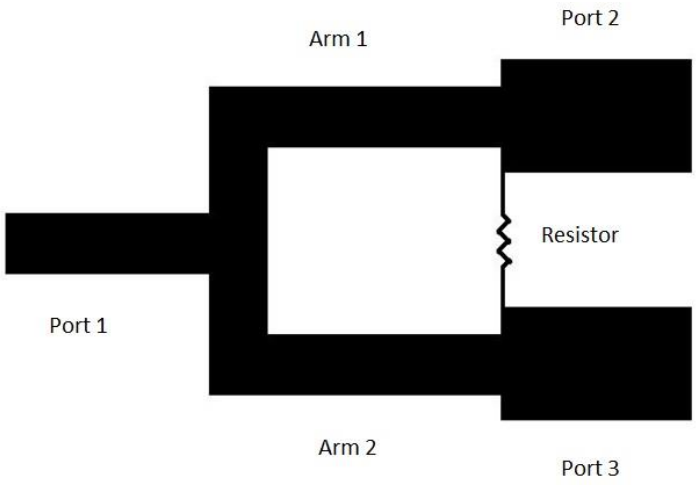

Figure 28: Wilkinson Power Divider

As stated previously, the Wilkinson power combiner is simply the Wilkinson power divider operating to combine power instead of dividing power. The Wilkinson power combiner receives power at ports 1 and 2 and combines the power at port 3 and provides isolation between ports 1 and 2 [1]. A typical microstrip Wilkinson power combiner is shown in the figure below.

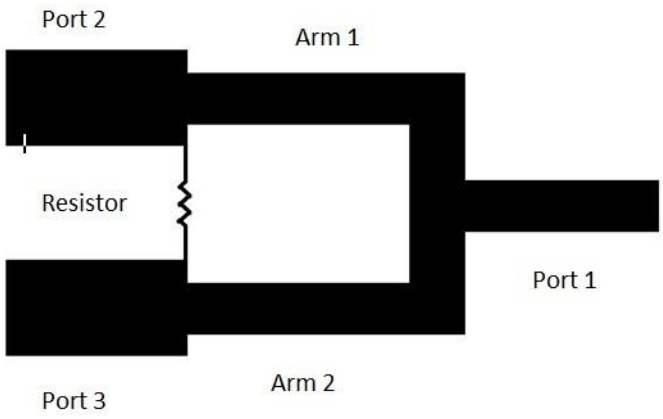

Figure 29: Wilkinson Power Combiner

To analyze the Wilkinson power combiner, an Even mode – Odd mode analysis has been developed [1, 2, 3, 4]. The equivalent transmission line circuit of the above Wilkinson power combiner is shown in the figure below. As is the case with a typical power combiner, the characteristic impedance of each arm is: $\sqrt{2}Z_0$. The length of each arm is $\frac{\lambda}{4}$. The resistance of the resistor is then: $2Z_0$.

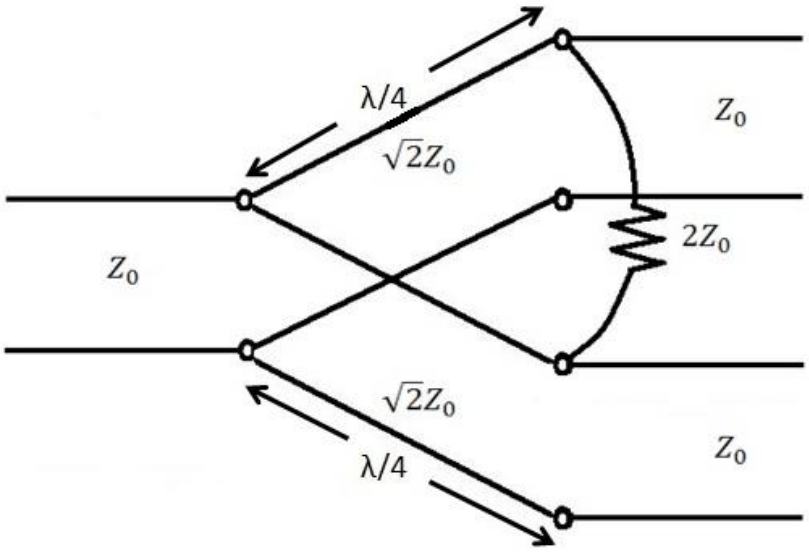

Figure 30: Equivalent Transmission Line Circuit of the Wilkinson Power Divider

To analyze the Wilkinson combiner, two separate modes of excitation are defined, the even mode and the odd mode. From [1], the Even-Odd Mode analysis uses the symmetrical equivalent of the transmission line circuit shown in the figure below. As can be seen from the figure, in order to perform the even mode – odd mode analysis, voltage generators with voltages V_{g2} and V_{g3} are placed at the output ports [2]. The output arms each have an associated resistance of 1. The arms connecting port 1 to ports 2 and 3 are each a quarter-wave in length and have an impedance $\sqrt{2}Z_o$. Coupled at port 1 are two resistors each having a value of 2. From this symmetric equivalent line circuit, the operation of the Wilkinson power combiner is described using two modes: even mode and odd mode.

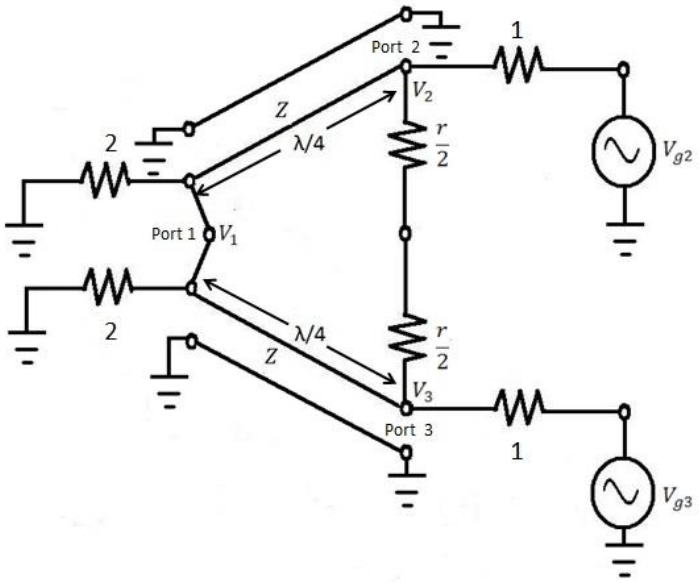

Figure 31: Symmetric Equivalent Transmission Line Circuit

By definition, during the even mode [2],

$$V_{g2} = V_{g3} = 2V$$

Because the voltages are equivalent, current does not flow between the transmission line inputs nor the r/2 resistors [2]. As a result, a "line of symmetry" [3] or bisection [2] can be used to describe the operation of each mode. The bisected network is shown below.

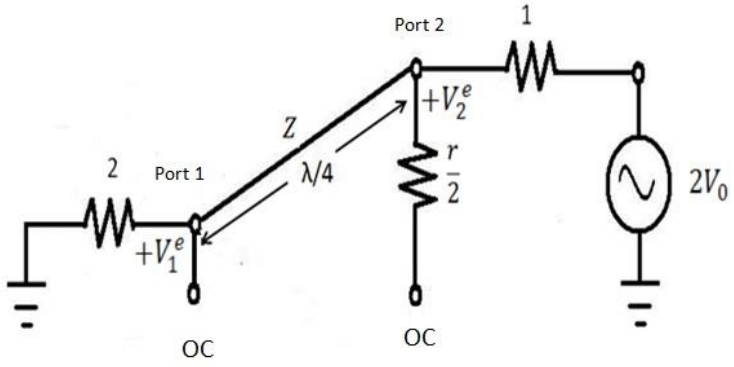

Figure 32: Bisected Circuit - Even Mode Excitation

The even mode excitation is shown in the figure. During the even mode of operation, the voltages at the input ports 1 and 2 are in phase, current is not flowing between the transmission lines at port 1 or through the resistor as "all points along the symmetrical line are open" [3]. Using the bisected circuit, it is now necessary to compute the input impedance looking towards port 1 from port 2. The input impedance is shown in the bisected circuit below.

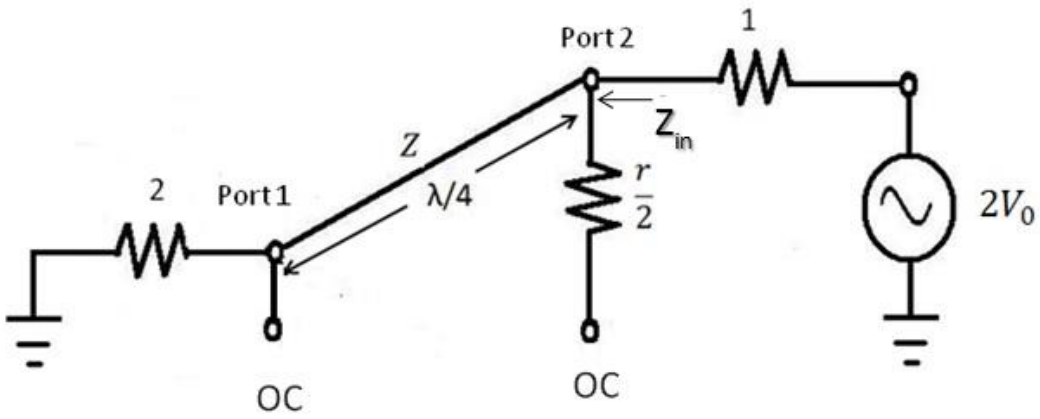

Figure 33: Bisected Circuit - Even Mode Excitation - Input Impedance

As adapted from [2] and [4] and the figure above, the input impedance can be written as:

$$Z_{in} = \frac{Z^2}{2}$$

In order to have Z_{in} matched at port 2

$$Z = \sqrt{2}$$

and

$$V_2^e = V_0$$

because

$$Z_{in} = 1$$

From transmission line theory [2], the voltage on the transmission line can be determined using:

$$V(x) = V^{+}(e^{-j\beta x} + \Gamma e^{-j\beta x})$$

Thus, at a quarter-wave length on the line, i.e., $x = (-\frac{\lambda}{4})$,

$$V_2^e = V(-\frac{\lambda}{4})$$

and

$$V_2^e = V^{+}(e^{-j\beta(-\frac{\lambda}{4})} + \Gamma e^{-j\beta(-\frac{\lambda}{4})})$$

When

$$\beta = \frac{2\pi}{\lambda}$$

then

$$V_2^e = V^{+}(e^{-j\frac{2\pi}{\lambda}(-\frac{\lambda}{4})} + \Gamma e^{-j\frac{2\pi}{\lambda}(-\frac{\lambda}{4})})$$

which yields

$$V_2^e = V^{+}(e^{j\frac{\pi}{2}} + \Gamma e^{-j\frac{\pi}{2}})$$

Using trigonometric identities yields

$$V_2^e = V^{+}\,[(\cos\frac{\pi}{2} + j\sin\frac{\pi}{2}) + \Gamma\,(\cos -\frac{\pi}{2} + j\sin\frac{\pi}{2})]$$

Breaking it down to

$$V_2^e = V^{+}(j - j\Gamma)$$

Extracting j yields

$$V_2^e = jV^+(1-\Gamma)$$

Thus

$$V_2^e = jV^+(1-\Gamma) = V_0$$

Solving for V^+in terms of V_2^e yields

$$V^+ = \frac{V_2^e}{j(1-\Gamma)}$$

and further

$$V^+ = \frac{jV_2^e}{(-1+\Gamma)}$$

Now solving for V_1^e in terms of V_0

$$V_1^e = V(0)$$

$$V_1^e = V^+(e^{-j\beta(0)} + \Gamma e^{-j\beta(0)})$$

which yields

$$V_1^e = V^+(1+\Gamma)$$

Plugging in V^+ yields

$$V_1^e = \frac{jV_2^e}{(\Gamma-1)}(\Gamma+1)$$

Γ can then be found using the reflection at port 1

$$\Gamma = \frac{2-\sqrt{2}}{2+\sqrt{2}}$$

Solving for V_1^e plugging in the value for Γ yields

$$V_1^e = \frac{jV_2^e}{\left(\frac{2-\sqrt{2}}{2+\sqrt{2}} - 1\right)}(\frac{2-\sqrt{2}}{2+\sqrt{2}} + 1)$$

which yields

$$V_1^e = -jV_2^e\sqrt{2}$$

and finally, recalling that $V_2^e = V_0$

$$V_1^e = -jV_0\sqrt{2}$$

By definition, during the odd mode [2],

$$V_{g2} = -V_{g3} = 2V$$

Because the voltages are opposite, the middle of the circuit has a voltage null [2]. As a result, the circuit can be bisected, i.e., it is grounded the two points on the midplane, resulting in the bisected circuit below [2].

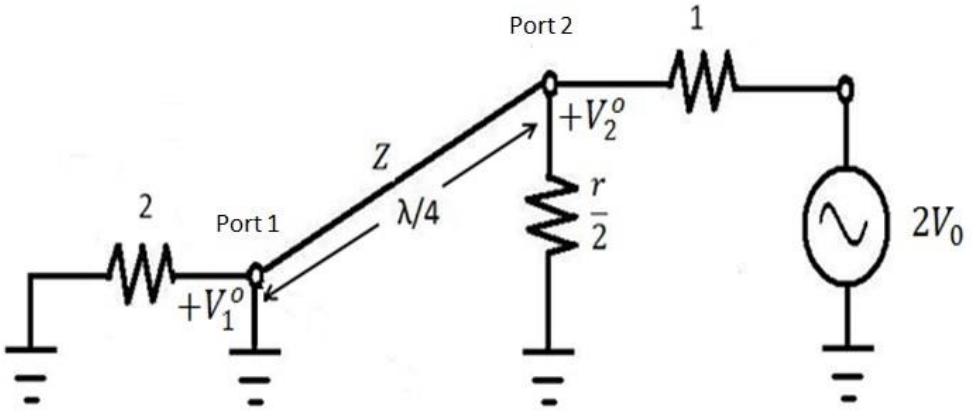

Figure 34: Bisected Circuit - Odd Mode Excitation

The odd mode excitation is shown in the figure. During the odd mode of operation, the voltages at the input ports 2 and 3 are out of phase, transmission lines at port 1 are shorted and current flows through the resistor [3].

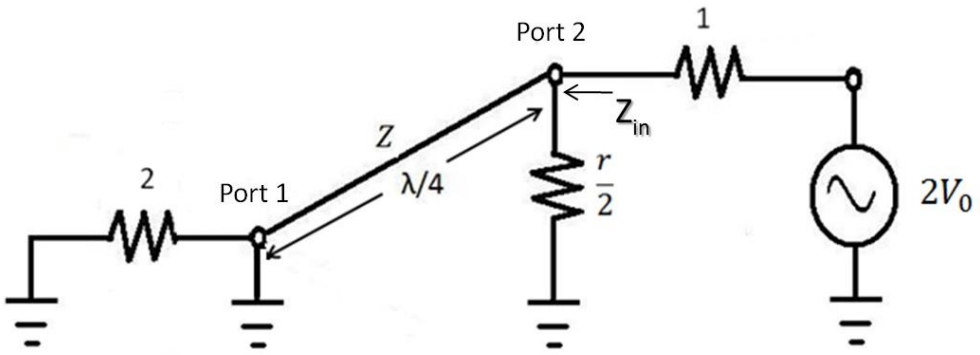

Figure 35: : Bisected Circuit - Odd Mode Excitation - Input Impedance

The input impedance at port 2 is $\frac{r}{2}$.

To match the input impedance to the remainder of the circuit

$$r = 2.$$

In addition,

$$V_2^o = V_0$$

and

$$V_1^o = 0$$

When matched loads terminate ports 2 and 3 the input impedance can be determined. The terminated Wilkinson power divider is shown in the figure below.

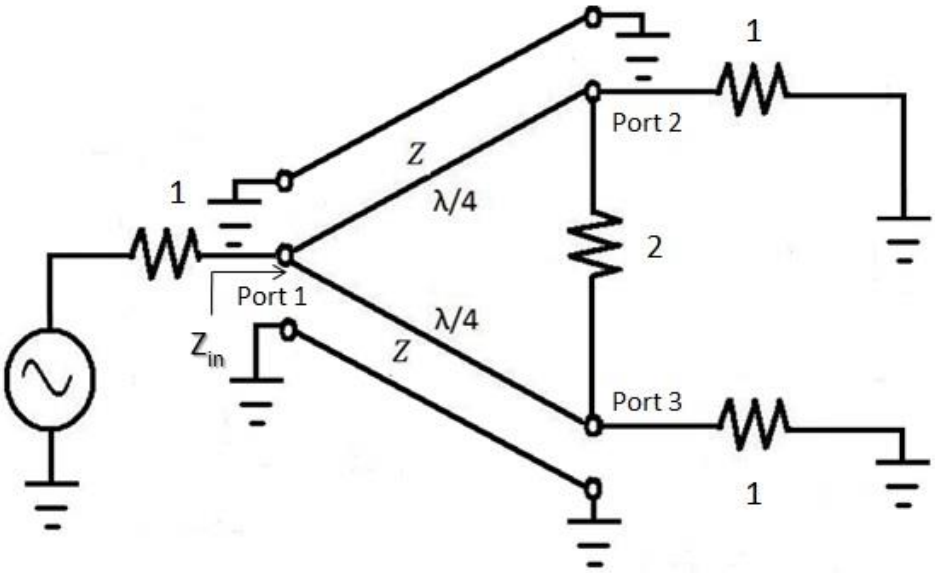

Figure 36: Wilkinson Power Divider with Terminated Matched Loads

Because $V_2 = V_3$ current does not flow through the center resistor and the equivalent circuit can be represented by the figure below ignoring the resistor.

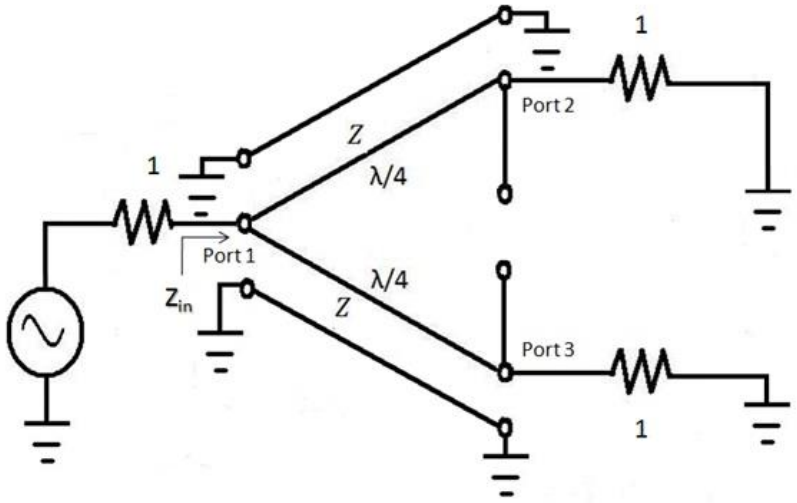

Figure 37: Wilkinson Power Divider with Terminated Matched Loads - Bisection

With the center resistor ignored, Z being equal to $Z = \sqrt{2}$, the input impedance is computed using

$$Z_{in} = \frac{1}{2}(\sqrt{2})^2 = 1$$

Using the Even-Mode and Odd-Mode analysis, a generic version of the bisected Circuit can be generated [1]. Both the Even-Mode and Odd-Mode bisected circuits are shown in the figures below. Notice that the resistive element is now replaced with a generalized circuit G_{ckt} whose purpose is to allow the capacitive element to be considered in the design of the overall system.

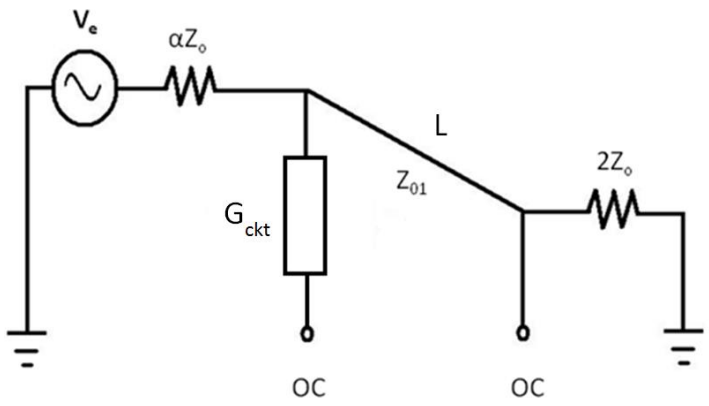

Figure 38: Bisected Circuit - Even Mode Excitation with Generalized Circuit

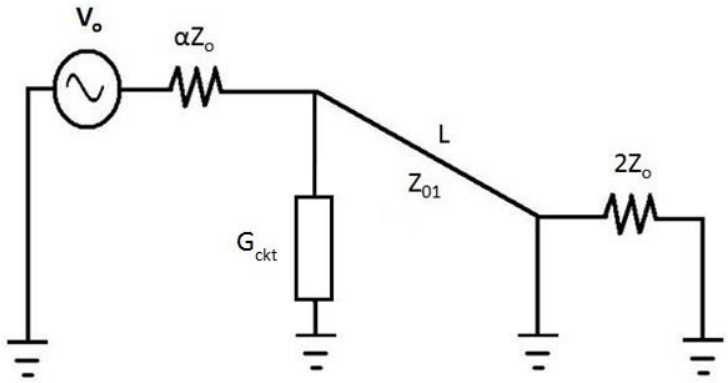

Figure 39: Bisected Circuit - Odd Mode Excitation with Generalized Circuit

From both the bisected even-mode and odd-mode excitation circuits it can be seen that there are several variables of interest:

α, Z_{01} , G_{ckt}, and L,

where

α is a constant;

G_{ckt} is a variable that includes the resistance R and capacitance C of the rectifying circuit

L is the length of a transmission line; and

Z_{01} is the impedance of a microstrip transmission line of length L.

Each variable of interest can be used in the design of the Wireless Rectenna Communication System. The bisection of the power combiner of the Wilkinson Rectenna Communication System is similar to that of the Wilkinson power combiner except the resistor is replaced with the diode and the length of the three arms of the power combiner are now

dependent upon the diode's impedance. During the even mode of operation, the rectifying portion of the Wilkinson Rectenna Communication System is treated as an open circuit. Thus, the system is able to function as a communication device. The equal power mode of the WRCS system is shown in the figure below [1]. The circuit replaces the open circuit resistor with both a resistor and a capacitor [1].

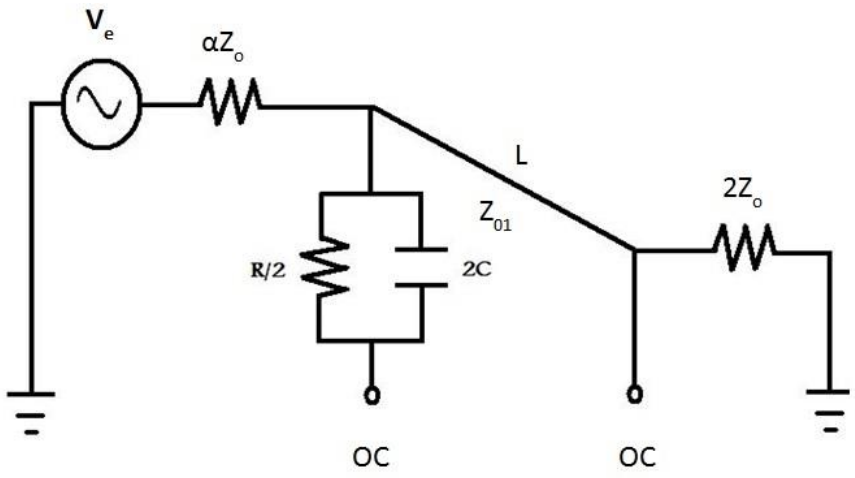

Figure 40: Even-Mode Circuit

The goal is to develop a generic system for a diode that allows for the determination of the length L that corresponds to both the resistance and capacitance of the diode that allows the rectifier circuit to be matched to the power combiner [1].

From [1], the length of L can be represented generically as L:

$$L = \frac{1}{\beta}\tan^{-1}\left(\frac{1}{\omega RC}\right)$$

For the case when C = 0 (the capacitance for the generic circuit is 0) and $\beta = \frac{2\pi}{\lambda}$ the length of the combining arm is $\frac{\lambda}{4}$. That is,

$$L = \frac{1}{\frac{2\pi}{\lambda}} \tan^{-1}(\frac{1}{0})$$

$$L = \frac{\lambda}{2\pi}(\frac{\pi}{2})$$

$$L = \frac{\lambda}{4}$$

This shows that for a generic circuit having no capacitance and where R is Z_0, α is 1, Z_{01} is$\sqrt{2}Z_0$, the power combiner is a basic quarter-wave power combiner shown above.

As stated in [1], when the bisected circuit is in even-mode,

$$\alpha = 2$$

and

$$Z_{01} = 2Z_0$$

As stated previously, the process of bisecting the power combiner of the Wilkinson Rectenna Communication System is similar to that of the Wilkinson power combiner except the resistor is replaced with the diode and the length of the three arms of the power combiner are now dependent upon the diode's impedance.

During the odd mode of operation, the rectifying portion of the Wilkinson Rectenna Communication System is treated as a short. Thus, the system is able to function as an energy harvesting device. The odd phase mode of the WRCS system is shown in the figure below.

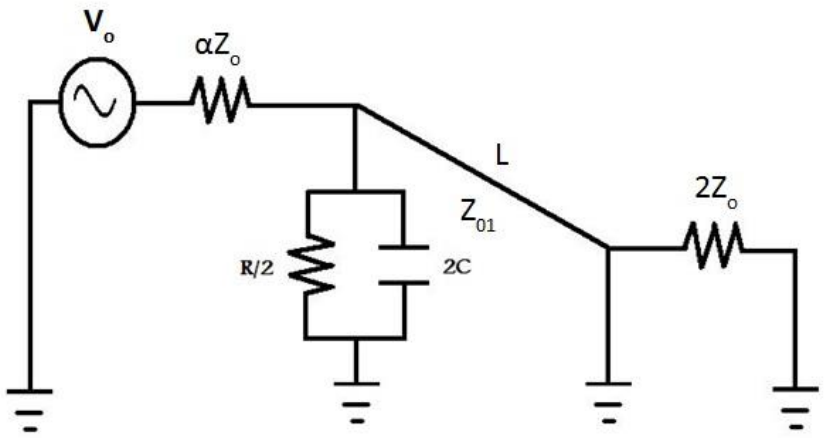

Figure 41: Even-Mode Excitation Generic Circuit

As stated in [1], when the bisected circuit is in odd mode,

$$Z_0 = \frac{R}{4}$$

and

$$L = \frac{1}{\beta}\tan^{-1}\left(\frac{1}{\omega RC}\right)$$

When the capacitance is not equal to 0, as is the case with a diode rectifying circuit, then

$$C \neq 0$$

and

$$L \neq \frac{\lambda}{4} + n\lambda$$

where

$$n = 0,1,2, \ldots$$

Thus, when the generalized circuit has a capacitance not equal to 0, then the length of the arms to make the power combiner matched to the generalized circuit, which in this case is a rectifying circuit, is determined using

$$L = \frac{1}{\beta}\tan^{-1}\left(\frac{1}{\omega RC}\right)$$

In the actual design the Wilkinson combiner in RF communications, the input arms of the combiner are made of microstrip transmission line and the dimensions can be calculated using LineCalc as shown below.

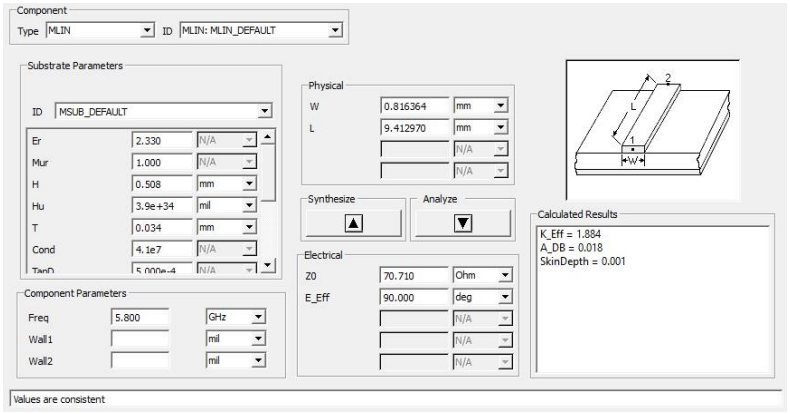

Figure 42: Calculation of length and width of microstrip arms of Wilkinson Rectenna using LineCalc

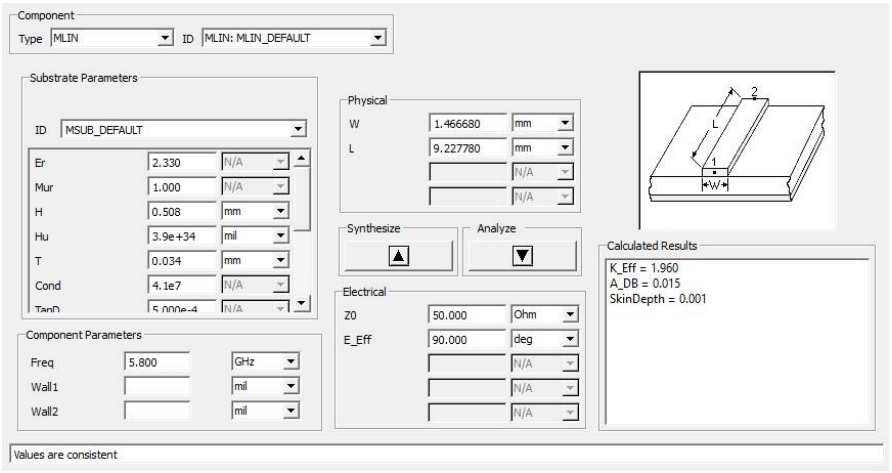

Figure 43: Calculation of length and width of 50 ohm microstrip arm of Wilkinson Rectenna using LineCalc

The lengths and widths can be determined using the impedance of the Schottky diode and the characteristics of the microstrip [1].

From [1], the impedance Z_D of the rectifying circuit is represented by:

$$Z_D = X + Yi$$

where

X is the real portion of the measured value of the impedance; and

Y is the imaginary portion of the measured value of the impedance.

From [1], [2], and [6], the length of input arms 1 and 2 are found using the following equations:

$$L_{arm1} = \frac{1}{\beta_{arm1}} \arctan\left(\frac{1}{\omega RC}\right)$$

$$R = X\left(1 + \left(\frac{Y}{X}\right)^2\right)$$

$$C = \frac{\frac{Y}{X}}{\omega X\left(1 + \left(\frac{Y}{X}\right)^2\right)}$$

$$\beta_{arm1} = k_o\sqrt{\epsilon_{effarm1}}$$

and

$$\omega = 2\pi f$$

where

β_{arm1} is the wave number of the microstrip transmission line;

ω is the angular frequency;

R is the resistance of the rectifying circuit;

X is the real portion of the measured value of the impedance;

Y is the imaginary portion of the measured value of the impedance;

C is the capacitance of the rectifying circuit; and

f is the operating frequency

With an approximation of the effective dielectric constant given as:

$$\epsilon_{effarm1} = \left(\frac{\epsilon_r + 1}{2}\right) + \left(\frac{\epsilon_r - 1}{2}\right)(1 + \frac{10h}{W_{arm1}})^{\frac{-1}{2}}$$

where

h is the height of the substrate;

ϵ_r is the dielectric constant of the substrate; and

$\epsilon_{effarm1}$ is the effective dielectric constant of the microstrip line.

Due to the symmetry of the power combiner, the length of the first arm and the second arm are equivalent [1]. Thus, the length of the arm 2 is:

$$L_{arm2} = L_{arm1}$$

With the lengths of arm 1 and arm 2 having been calculated, the widths of arm one and arm two can now be calculated.

From [2], the width of the arm can be calculated using:

$$W_{arm1} = h\frac{2}{\pi}(E_{arm1} - 1 - \ln(2E_{arm1} - 1) + \frac{\epsilon_r - 1}{2\epsilon_r}\left(\ln(E_{arm1} - 1) + 0.39 - \frac{0.61}{\epsilon_r}\right))$$

$$E_{arm1} = \frac{377\pi}{2Z_{o1}\sqrt{\epsilon_r}}$$

From Visser [1], in order to match the power combiner to the rectifying circuit the formula for the characteristic impedance of the arm is:

$$Z_{o1} = \frac{R}{2}$$

Due to the symmetry of the power combiner, the width of the first arm and second arm are equivalent [1].

$$W_{arm2} = W_{arm1}$$

From [2], the width of the arm 3 can be calculated using:

$$W_{arm3} = h\frac{2}{\pi}(E_{arm3} - 1 - \ln(2E_{arm3} - 1) + \frac{\epsilon_r - 1}{2\epsilon_r}\left(\ln(E_{arm3} - 1) + 0.39 - \frac{0.61}{\epsilon_r}\right))$$

$$E_{arm3} = \frac{377\pi}{2Z_{arm3}\sqrt{\epsilon_r}}$$

From [1], the characteristic impedance of arm 3 can be calculated using:

$$Z_{arm3} = 2Z_o$$

where

$$Z_o = \frac{R}{4}$$

From [2], the length of the arm 3 can be calculated using:

$$L_{arm3} = \frac{90(\frac{\pi}{180})}{k_o\sqrt{\epsilon_{effarm3}}}$$

$$\epsilon_{effarm3} = \left(\frac{\epsilon_r + 1}{2}\right) + \left(\frac{\epsilon_r - 1}{2}\right)(1 + \frac{10h}{W_{arm3}})^{\frac{-1}{2}}$$

The lengths and widths of arms 1, 2, and 3 can be calculated based on the impedance of the rectifying circuit and the characteristics of the microstrip line and substrate. The inherent characteristics of the power combiner allow for the formulation of the of the design parameters based on the phase of the input power and the The formulas were ascertained based on [1], [2],

and [6] (Visser, Pozar, and Bolanis respectively) and show that it is possible to design the Wilkinson Rectenna Communication System that works both for wireless power transmission and data communication.

3.2.1 References

[1] H.J. Visser, *Approximate Antenna Analysis for CAD*, John Wiley & Sons, Chichester, 2009.

[2] D.M. Pozar, Microwave Engineering, 3rd Edition, Wiley, New York, 2005.

[3] A.D. Pham, "Outphase Power Amplifiers in OFDM Systems," Ph.D. dissertation, MIT, Sept. 2005.

[4] R.H. Chatim, Modified Wilkinson Power Combiner for Applications in the Millimeter-Wave Range, Masters Thesis, University of Kassel, 2005.

[5] D. Harty, "Novel Design of a Wideband Ribcage-Dipole Array and its Feeding Network", Thesis, Worcestor Polytechnic Institute, Dec. 2010.

[6] C.A. Balanis, Antenna Theory: Analysis and Design, Third Edition, Wiley, New York, 2005.

3.3 Rectification Circuit

A rectifier is used to convert alternating current (AC) to direct current (DC). For low power wireless power transmission, the Schottky diode is the heart of a rectenna, as the conversion of AC to DC in a rectenna generally requires the use of a diode that utilizes minimal energy to operate. The electrical parameters of the Schottky diode affect the size of both the antenna and the rectifying circuit. For a Wilkinson rectenna, the design of the antenna and circuit are based on the electrical parameters of the Schottky diode. For the spiral rectenna, in addition to the electrical parameters, the design of the antenna is based on the physical parameters of the Schottky diode.

The diode is used for rectification purposes in the rectenna. The equivalent circuit of the diode is shown below.

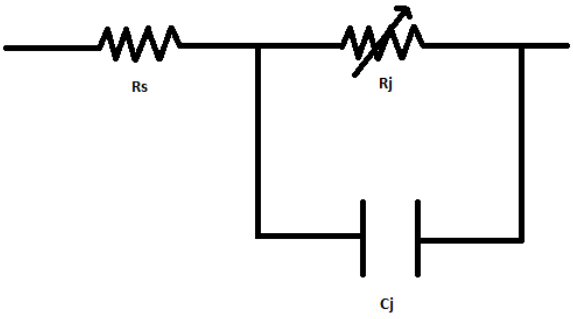

Figure 44: Diode Equivalent Circuit

R_s is the series resistance;

R_j is the junction resistance of the diode; and

C_j is the parasitic junction capacitance.

The voltage-current characteristic of a diode is expressed as:

$$I_D(V_D) = I_S\left(e^{\left(\frac{q}{nkT}\right)V_D} - 1\right)$$

where

I_D is the current through the diode;

V_D is the diode voltage;

I_S is the saturation current;

q is the charge of an electron;

n is the ideality factor;

k is Boltzmann's constant; and

T is the temperature in kelvin [10], [11].

The junction resistance is:

$$Rj = \frac{8.33x10^{-5}nT}{I_b + I_s}$$

where

I_b is the externally bias current in amps [5].

The current-voltage equation above does not include the packaging effects of the Schottky diode. The packaged Schottky diode includes a parasitic inductance L_p and a parasitic capacitance C_p, which are shown in the equivalent circuit for a packaged Schottky diode shown in the section below.

The Schottky diode is the type of diode generally selected for low power wireless power transmission because it has a fast switching time, does not require a separate bias current, and utilizes minimal power to perform rectification. Due to the Schottky diode's relatively low junction capacitance, it is more suitable for high frequency applications (unlike the pn junction diode which is not suitable for high frequency applications because of its high junction

capacitance) [9,10]. Compared to standard diode, the Schottky diode has a higher switching speed due to its low voltage drop (0.15 – 0.45 volts compared to 0.6 – 1.7 volts for the standard silicon diode) [17]. The switching speed of the diode for systems requiring high frequency, low power consumption and AC to DC conversion is best described in [1].

Generally, there are two types of Schottky diodes that are used for rectification purposes:

(1) zero biased diode; or

(2) externally biased diode [1].

The n-type silicon is used for externally biased diodes and requires an external bias for small signal operation. Zero bias diodes use p-type silicon and do not require external bias for operation [1]. In addition, the p-type Schottky diode is relatively inexpensive and has a reduced size [1]. The externally biased diode is generally not used in energy harvesting applications because it requires an external bias that reduces the amount of energy harvested by the system. There are other advantages to utilizing the zero bias Schottky diode in rectenna design, including reduced flicker noise. However, it is not necessary to discuss the theory of flicker noise in great detail for this application. For further information regarding flicker noise the reader can refer to [2].

In order to properly assess the Schottky diode for appropriate selection, the equivalent circuit of the diode including packaging parasitic inductance and capacitance must be described in detail. The equivalent circuit of a Schottky Diode can be represented by the circuit shown below.

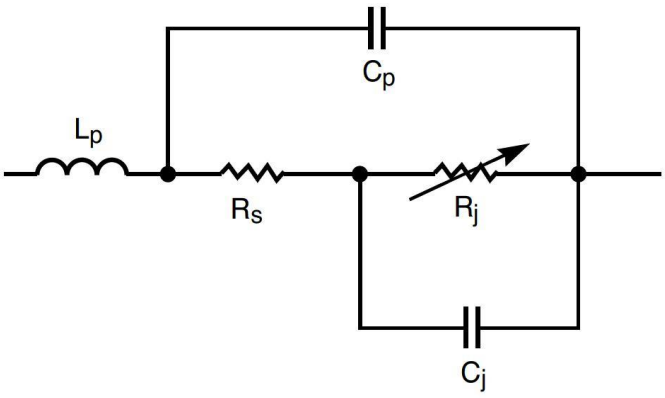

Figure 45: Schottky Diode Equivalent Circuit [3]

For the Schottky diode equivalent circuit,

L_p is the package parasitic inductance;

C_p is the package parasitic capacitance;

R_s is the parasitic series resistance;

R_j is the junction resistance of the diode; and

C_j is the parasitic junction capacitance.

The junction resistance equation for Rj is

$$R_j = \frac{(8.33 \times 10^{-5}) \times n \times T}{I_b + I_s}$$

where, as stated previously,

T is the temperature in Kelvin;

I_s is the saturation current;

I_b is the external bias current, and

n is the ideality factor [3].

The above equivalent circuit is also used as the Schottky model in ADS as shown below [4].

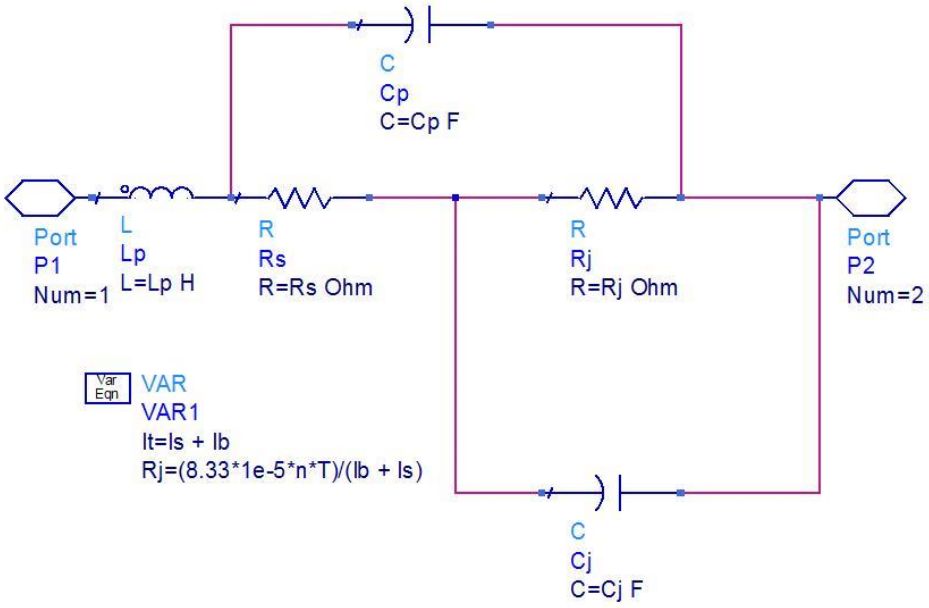

Figure 46: Schottky Diode Model in ADS

Although not necessary for implementation of the current rectenna system, the impedance of the Schottky diode can be calculated using closed form formulas from [6]-[7]. Confirmation of the mathematical procedure is evidenced in [8].

$$Z_d = \frac{\pi R_s}{cos\theta_{on}\left(\frac{\theta_{on}}{cos\theta_{on}} - sin\theta_{on}\right) + j\omega R_s C_j\left(\frac{\pi - \theta_{on}}{cos\theta_{on}} + sin\theta_{on}\right)}$$

and

$$tan\theta_{on} - \theta_{on} = \frac{\pi R_s}{R_L\left(1 + \frac{V_{bi}}{V_o}\right)}$$

where

R_s is the series resistance;

C_j is the junction capacitance;

θ_{on} is called a dynamic variable that is dependent on the diode's input power;

V_{bi} is the built in voltage of the diode in the forward bias region;

V_o is the output voltage at the load resistance; and

R_L is the load resistance.

From [8], to determine the output voltage V_o and the output power P_{out}, the breakdown voltage V_{br} is used, that is,

$$V_o = \frac{V_{br}}{2}$$

and

$$P_{out} = \frac{V_o^2}{R_L}$$

Using iteration, θ_{on} can be determined and the impedance Z_d of the diode calculated mathematically.

ADS can also be used to determine the impedance of the diode. In ADS, for small signal applications, an S-Probe is placed in series with the Schottky Diode terminated with 50 ohm ports. As described previously, the parameters used to model the Schottky diode in ADS are the package parasitic inductance ($L_{p)}$, package parasitic capacitance (C_p), parasitic series resistance (R_s), and the parasitic junction capacitance (C_j). R_j is the junction resistance of the diode and is calculated by ADS using T, I_s, I_b, n, defined as the temperature in Kelvin, saturation current, external bias current, and ideality factor, respectively. Below is a schematic used to calculate the impedance in ADS.

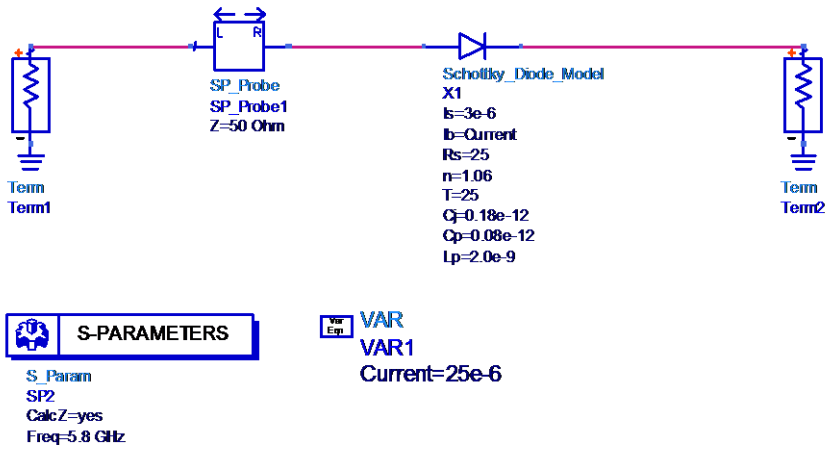

Figure 47: Schematic in ADS used to calculate Diode Impedance.

For non-linear, large signal applications, the LSSP simulation is used utilizing the harmonic balance method in ADS [16], [19]. An example of the impedance calculation using LSSP for the HSMS 2820 diode at 5.8 GHz with 0 dBm input power is shown in the figure below.

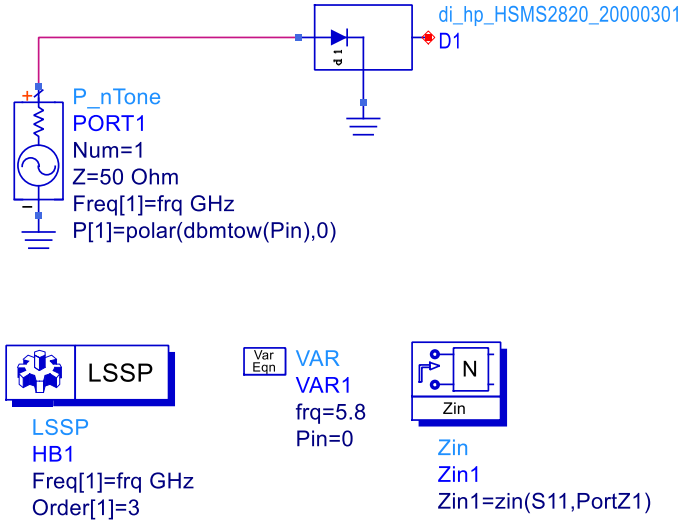

Figure 48: Calculating Diode Impedance using LSSP in ADS.

Due to the minimal amount of power received by the rectenna, the rectifier must be relatively efficient in order to store enough energy worthy of wireless power transmission. According to [18], the efficiency of the rectenna should typically be greater than 60%. Thus, depending on overall system requirements, the Schottky diode with the highest conversion efficiency is generally the diode that should be selected for rectification purposes.

The efficiency of a rectenna with a load attached is:

$$\eta = \frac{P_{DC}}{P_{RF}}$$

where P_{RF} is incident power received at the diode, P_{DC} is the dc power output by the diode, which can be calculated using V_{load} (the voltage across the load); and R_{load} (the resistance of the load).

Examples of efficiency calculations for various diodes have been calculated in the literature. For example, the efficiencies of the HSMS 2820, HSMS 2850, and HSMS 2860 have been compared and contrasted showing the importance of diode parameters on rectification efficiency [12]. In [13], a summarized comparison table was generated using the results in [12]. The table shows the critical parameters of the diodes that have a major effect on performance and efficiency of the rectenna.

Table 2: Critical Parameters for Schottky Diodes (adapted from [13])

Parameter	Description	Units	HSMS 2820	HSMS 2850	HSMS 2860
Cj	Junction Capacitance	pF	0.7	0.18	0.18
Rs	Series Resistance	Ohm	6	25	5

For the given diodes, as demonstrated by Merabet in [12], the HSMS 2860 is has the highest conversion efficiency compared to the HSMS 2820 and HSMS 2850. However, selection of the appropriate diode for rectification is application based. According to Avago

Technologies (manufacture of the HSMS 2820, HSMS 2850, and HSMS 2860), the HSMS 282x series is likely the appropriate choice for most rectification applications, because it features low series resistance, low forward voltage at all current levels, and good RF characteristics [15]. The efficiencies of the diodes are calculated in Chapter 4.

3.3.1 References

[1] Avago Technologies, “Designing Detectors for RF/ID Tags – Application Note 1089”, October 8, 2008.

[2] Avago Technologies, “Flicker Noise in Schottky Diodes – Application Note 956 – 3”, July 13, 2010.

[3] Avago Technologies, “Designing the Virtual Battery – Application Note 1088”, July 22, 2010.

[4] Agilent Design Systems Software, Schottky Diode Model.

[5] Avago Technologies, “HSMS 285x Series – Surface Mount Zero Bias Schottky Detector Diodes”, Datasheet, May 29, 2009.

[6] J.O. McSpadden, L. Fan, and K. Chang, “Design and Experiments of A High-Conversion-Efficiency 5.8 GHz Rectenna,” *IEEE Trans. Microwave Theory Tech*, vol. 46, No. 12, Dec. 1998.

[7] Y-H. Suh and K. Chang, “A High-Efficiency Dual-Frequency Rectenna for 2.45- and 5.8-GHz Wireless Power Transmission,” *IEEE Trans. Microwave Theory Tech*, Vol. 50, pp. 1784-1789, July 2002.

[8] L. H. Toh, “A Follow-up Study on Wireless Power Transmission for Unmanned Air Vehicles,” Naval Postgraduate School, Dec. 2007.

[9] C. Mikeka, H. Arai, Y. K. Tan, *Design Issues in Radio Frequency Energy Harvesting System - Sustainable Energy Harvesting Technologies - Past, Present and Future*, InTech, Available from: http://www.intechopen.com/books/sustainable-energy-harvestingtechnologies-past-present-and-future/design-issues-in-radio-frequency-energy-harvesting-system, 2011.

[10] D.M. Pozar, *Microwave Engineering*, 3rd Edition, Wiley, New York, 2005.

[11] H.J. Visser, *Approximate Antenna Analysis for CAD*, John Wiley & Sons, Chichester, 2009.

[12] B. Merabet, H. Takhedmit, B. Allard, L. Cirio, F. Costa, O. Picon, and C. Vollaire, "Low-cost converter for harvesting of microwave electromagnetic energy," *IEEE Energy Conversion Congress and Exposition*, (ECCE 2009), September 2009.

[13] S. Hong, R. Ibrahim, M. Khir, H. Daud, M. Zakariya, "Rectenna Architecture Based Energy Harvester for Low Power RFID Application," *2012 4th International Conference on Intelligent and Advanced Systems* (ICIAS2012), 2012.

[14] R. Waugh, "Choosing the Right Diode for Your AGC Detector," Diode Applications, Wireless Semiconductor Division, Hewlett Packard Company, July 6, 1999.

[15] Avago Technologies, "HSMS 282x Series – Surface Mount RF Schottky Barrier Diodes", Datasheet, May 28, 2009.

[16] T. Weller, RF/Microwave Circuits I Laboratory #5 – Diode Matching Circuit, Baylor University,http://web.ecs.baylor.edu/faculty/baylis/EEL4421/EEL4421_6935SoftwareLaboratory5Fall2007.pdf.

[17] H. Visser, V. Pop, B. Veld, R. Vullers, "Remote RF Battery Charging," http://cap.ee.ic.ac.uk/~pdm97/powermems/2010/poster-pdfs/037_Visser_61.pdf.

[18] J.L. Volakis, C. Chen, K. Fujimoto, *Small Antennas: Miniaturization Techniques & Applications*, McGraw Hill, New York, 2010.

[19] F. Zhang, J. Lee, "5.8 GHz Simple Compact Folded Dipole Rectenna without Chip Capacitor", *The 2009 International Symposium on Antennas and Propogation (ISAP 2009)*, October 20-23, 2009, Bangkok, Thailand.

3.4 Microstrip Antenna Array

The Wilkinson Rectenna Communication System (WRCS) uses an array of two antennas for power reception and data transfer. Microstrip rectangular patch antennas have been selected due to the ease of fabrication, limited size requirements, and minimal costs. Industrial, Scientific, and Medical bands (ISM bands) allow for the operation of these antennas at 5.8 GHz, which is the operating frequency selected for this work. In one instance, the patch antennas for the WRCS system can be designed based on the impedance of the rectifying circuit. In another instance, the impedance characteristics of the Wilkinson combiner itself can be used to design WRCS. Due to the symmetric nature of the power combiner, when designing the WRCS, the design parameters for both antennas are equivalent.

IEEE defines a microstrip antenna as a "a thin metallic conductor bonded to a thin grounded dielectric substrate" and is the "part of a transmitting or receiving system that is designed to radiate or to receive electromagnetic waves."[6] Microstrip antennas are designed in many different shapes and used in communication systems primarily because they are relatively inexpensive, easy to manufacture, and have decent propagation characteristics. Microstrip antennas are generally designed to be narrow band [2] operating at a specific frequency, but some microstrip antennas may be designed to be broadband allowing use of the antenna at multiple frequencies [4]. In addition, microstrip antennas can be easily embedded onto the surfaces of different objects (such as packages and vehicles) [8].

The physical structure of a microstrip antenna consists of a radiation patch, feedline, a substrate, and a ground plane [5]. The grounded dielectric substrate has a relative permittivity ϵ_r, permeability μ_r , and thickness h [7]. Analysis of microstrip antennas can be accomplished by using several models, including the:

Transmission Line Model;

Cavity Model; and

Full-wave Model.

Each model has its own benefits. The full-wave model uses the Moment Method and integrals for analysis and is considered the most accurate and most complex of the models [2]. The cavity model treats the antenna as a resonant cavity, with the patch being the top of the cavity, the ground plane being the bottom of the cavity, and the patch edges serving as the sides of the cavity [7]. The cavity model is beneficial because it takes into account the field variations along the patch's edges. The transmission line model represents the microstrip patch antenna using two slots separated by a transmission line. Compared to the full-wave model and the cavity model, the transmission line model is a simpler form of analysis but is less accurate then the cavity model and full-wave model [2].

The transmission line model can be used to describe the radiation characteristics of the rectangular patch antenna [15]. Two parallel radiating slots are separated by a transmission line and are used to represent to the microstrip patch antenna. Both the rectangular patch and its transmission line model equivalent are shown in the figures below.

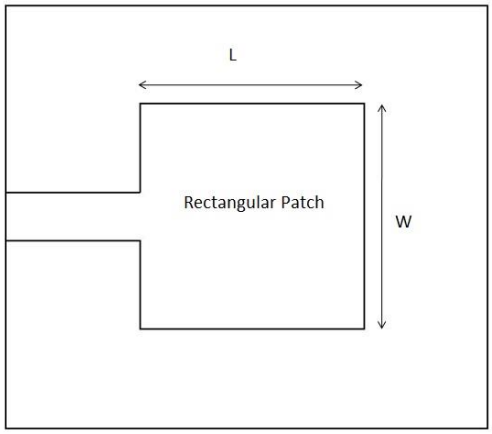

Figure 49: Rectangular Microstrip Patch

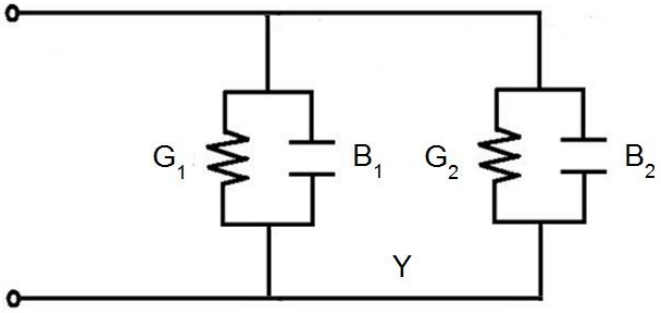

Figure 50: Transmission Line Model Equivalent Circuit of Rectangular Microstrip Patch

Using the transmission line model, the equivalent admittances of slot 1 and slot 2 are:

$$Y_1 = G_1 + jB_1$$

and

$$Y_2 = G_2 + jB_2$$

where

$$G_1 = \frac{W}{120\lambda_0}\left(1 - \frac{1}{24}(k_0 h)^2\right)$$

$$B_1 = \frac{W}{120\lambda_0}\left(1 - 0.636ln(k_0 h)\right)$$

$$G_2 = \frac{W}{120\lambda_0}\left(1 - \frac{1}{24}(k_0 h)^2\right)$$

$$B_2 = \frac{W}{120\lambda_0}\left(1 - 0.636 ln(k_0 h)\right)$$

and

$$Y_1 = Y_2.$$

Thus, for a given value of G, the width W of the rectangular patch can be determined.

The far-field electric field for the microstrip antenna is determined by treating both slots as a two-element array and adding the fields of each. An array factor can be used since the slots are the same [2]. As stated previously, the rectangular patch antenna can be represented by two radiating slots separated by a distance L.

From [2], the radiated fields (total electric field for slots 1 and 2) are:

For the principal E-plane:

$$E_\varphi^t = +j\frac{k_0 W V_0 e^{-jk_0 r}}{\pi r}\left\{\frac{\sin\left(\frac{k_0 h}{2}\cos\phi\right)}{\frac{k_0 h}{2}\cos\phi}\right\}\cos\left(\frac{k_0 L_e}{2}\sin\phi\right)$$

for the x-y plane with $\theta = 90°$, $0° \le \phi \le 90°$, and $270° \le \phi \le 360°$

For the principal H-plane:

$$E_\varphi^t \cong +j\frac{k_0 W V_0 e^{-jk_0 r}}{\pi r}\left\{\sin\theta\,\frac{\sin\left(\frac{k_0 h}{2}\sin\theta\right)}{\frac{k_0 h}{2}\sin\theta}\,\frac{\sin\left(\frac{k_0 W}{2}\cos\theta\right)}{\frac{k_0 W}{2}\cos\theta}\right\}$$

for the x-z plane with $\phi = 0°$, and $0° \le \theta \le 180°$

where

V_0 is the voltage across the slot;

L_e is the separation distance; and

W is the width of the microstrip patch.

The directivity of a microstrip antenna is [2]:

$$D = \begin{cases} 6.6 \text{ or } 8.2\ dB & for\ W \ll \lambda_0 \\ 8\left(\frac{W}{\lambda_0}\right) & for\ W \gg \lambda_0 \end{cases}$$

The extended length caused by the fringing fields is ΔL. From [2], the extended length can then be approximated as:

$$\Delta L = 0.412h\left(\frac{(\epsilon_{reff} + 0.3)(\frac{W}{h} + 0.264)}{(\epsilon_{reff} + 0.258)(\frac{W}{h} + 0.8)}\right)$$

Where the effective dielectric constant

$$\epsilon_{reff} = \frac{\epsilon_r + 1}{2} + \frac{\epsilon_r - 1}{2}\left(1 + 12\frac{h}{W}\right)^{-\frac{1}{2}}$$

The effective length of the patch including the extended length is then:

$$L_{eff} = L + 2\Delta L$$

The width of the microstrip patch antenna is determined using [2]:

$$W = \frac{1}{2f_r\sqrt{\mu_o\epsilon_o}}\sqrt{\frac{2}{\epsilon_r + 1}}$$

which can be rewritten as:

$$W = \frac{v_o}{2f_r}\sqrt{\frac{2}{\epsilon_r + 1}}$$

where

ϵ_r is the dielectric constant of the substrate;

f_r is the resonant frequency; and

$v_o$is the free-space velocity of light.

Feed lines are used to feed the microstrip antenna [5]. The most common feed lines are the coaxial probe, microstrip feed line, aperture and proximity coupling [2]. For the microstrip patch antenna, the feed line is typically a microstrip feed line or coaxial probe. Due to the inherent design of the microstrip Wilkinson combiner, the microstrip feed line is used to feed the two rectangular patch antennas. Examples of the microstrip patch antenna with the microstrip feed line are shown in the figure below.

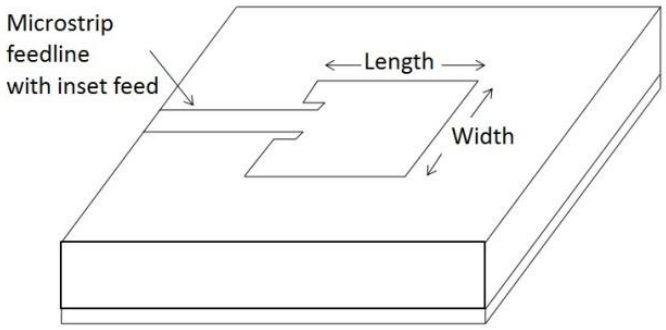

Figure 51: Microstrip Patch Antenna With Microstrip Feed Line

Determination of the resistance of the rectangular patch antenna at its edge is important in designing the Wilkinson rectenna and is described in detail in [2]. This is because, once the resistance of the rectangular patch antenna is known, the feedline can be designed to be matched to the antenna. In addition, the inset feed can be designed based on the antenna's resistance to yield a specific impedance at the antenna's input.

The resonant input resistance of the patch antenna can be represented as:

$$R_{in} = \frac{1}{2(G_1 \pm G_{12})}$$

where + is for odd mode resonant voltage distribution and – is for even mode resonant voltage distribution.

The conductance G1is:

$$G_1 = \frac{I_1}{120\pi^2}$$

where

$$I_1 = -2 + \cos(X) + XS_i(X) + \frac{\sin(X)}{X}$$

and

$$X = k_o W$$

Asympotically the conductance can be obtained using:

$$G_1 = \begin{cases} \frac{1}{90}\left(\frac{W}{\lambda_0}\right)^2 & W \ll \lambda_0 \\ \frac{1}{120}\left(\frac{W}{\lambda_0}\right) & W \gg \lambda_0 \end{cases}$$

The mutual conductance is:

$$G_{12} = \frac{1}{120\pi^2}\int_0^{\pi}\left(\frac{\sin\left(\frac{k_o W}{2}\cos\theta\right)}{\cos\theta}\right)^2 J_o(k_o L\sin\theta)sin^3\theta d\theta$$

The input resistance taking into account mutual effects is:

$$R_{in}(y=0) = \frac{1}{2(G_1 \pm G_{12})}cos^2\left(\frac{\pi}{L}y_o\right)$$

where

y_o is the length of the inset feed, shown in the rectangular patch with inset feed below. Once $R_{in}(y = 0)$, $G_1$and $G_{12}$are known, the length of the inset feed y_o can be determined.

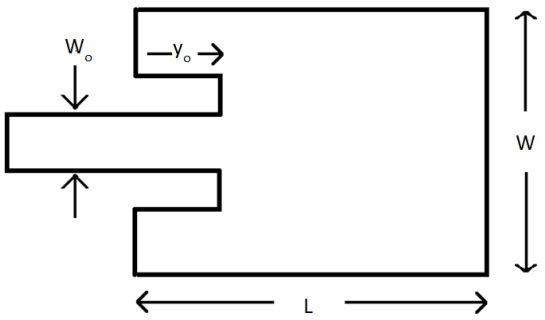

Figure 52: Rectangular Patch with Inset Feed.

The Wilkinson Rectenna Communication System uses a two element microstrip array for both communication and wireless power transfer. The two element microstrip array essentially works as a natural switch toggling from communication to power rectification. When a device, such as an RFID, is not in communication mode, it can be used to store energy for present or later use. It is important that the microstrip antenna array be designed to work cohesively with the communication system, otherwise the device will not be able to function for both data transfer and energy storage.

For a two-element array the total field can be represented by [2]:

$$E_{total} = E_1 + E_2$$

$$E_{total} = \hat{a}_\theta j\eta \frac{kI_o l}{4\pi}\left\{\frac{e^{-j[kr_1-\left(\frac{\beta}{2}\right)}}{r_1}\cos\theta_1 + \frac{e^{-j[kr_2-\left(\frac{\beta}{2}\right)}}{r_2}\cos\theta_2\right\}$$

For the far-field:

$$\theta_1 \cong \theta_2 \cong \theta$$

$$r_1 \cong r - \frac{d}{2}\cos\theta$$

and

$$r_2 \cong r + \frac{d}{2}\cos\theta$$

for phase variations and

$$r_1 \cong r_2 \cong r$$

for amplitude variations.

Employing substitution yields a total electric field of :

$$E_{total} = \hat{a}_\theta j\eta \frac{kI_o le^{-jkr}}{4\pi r}\cos\theta\left\{2\cos\left[\frac{1}{2}(kd\cos\theta + \beta)\right]\right\}$$

Thus, the electric field in the far zone of a uniform two element array is determined by multiplying the field of a single element times the array factor of the array [2] and is shown below.

$$E_{total} = E_{single\ element} \times Array\ Factor$$

The array factor for a two-element array of constant amplitude is:

$$AF = 2\cos\left[\frac{1}{2}(kd\cos\theta + \beta)\right]$$

Thus, the total radiated field for a two-element array can be written as [2]:

$$E_{total} = \hat{a}_\theta j\eta \frac{kI_o le^{-jkr}}{4\pi r}\cos\theta\left\{2\cos\left[\frac{1}{2}(kd\cos\theta + \beta)\right]\right\}$$

The microstrip antenna array is simply an array of microstrip patch antennas. The microstrip antenna array for the Wilkinson rectenna communication system is a broadside linear

array with maximum radiation normal to the axis of the array [2]. The array is designed by designing each patch according to general microstrip patch design principles described above and ensuring that the spacing between the elements does not produce unwanted grating lobes (principal maximums at unwanted directions)[2]. In order to avoid grating lobes, the maximum spacing between the two microstrip patch antennas should be less than a wavelength. That is,

$$d_{max} < \lambda$$

Microstrip patch antennas are vital to the design of Wilkinson Rectenna Communication Systems. The ability to design the microstrip antennas to be of limited size and weight allows for the antennas to be fit easily in RFID systems as an array. For such a system, the means of determining the length and width of two rectangular patch microstrip antennas for the Wilkinson Rectenna Communication System has been provided.

3.4.1 References

[1] H.J. Visser, *Approximate Antenna Analysis for CAD*, John Wiley & Sons, Chichester, 2009.

[2] C.A. Balanis, Antenna Theory: Analysis and Design, Third Edition, Wiley, New York, 2005.

[3] T.A. Milligan, Modern Antenna Design, Second Edition, New Jersey, 2005.

[4] G. Kumar, K.P. Ray, Broadband Microstrip Antennas, Artech House, Massachussets, 2003.

[5] Y. Huang, K. Boyle, Antennas From Theory to Practice, Wiley, West Sussex, 2008.

[6] Antenna Standards Committee of the IEEE Antennas and Propagation Society, IEEE Standard Definitions of Terms for Antennas, IEEE, New York, 1993.

[7] R. Bansal, Fundamentals of Engineering Electromagnetics, CRC Press, Boca Raton, 2006.

[8] R.A. Sainati, CAD of Microstrip Antennas for Wireless Applications, Artech House, Massachusetts, 1996.

[9] Y.T. Lo, S.W. Lee, Antenna Handbook – Theory, Applications, and Design, Van Nostrand Reinhold Company, New York, 1988.

[10] S. Jensen, Microstrip Patch Antenna, Northern Arizona University, December 14, 2010.

[11] P. J. Bevelacqua, Microstrip Antennas: The Patch Antenna, http://www.antenna-theory.com/antennas/patches/antenna.php#introduction, antenna-theory.com, 2011.

[12] C. Reddy, R. Rana, "Design of Linearly Polarized Rectangular Microstrip Patch Antenna Using IE3D/PSO", Thesis, National Institute of Technology Rourkela, 2009.

[13] A. Hashim, "Development of Microstrip Patch Array Antenna for Wireless Local Area Network (WLAN)", Thesis, Universiti Malaysia Perlis Malaysia, 2007.

[14] A. Alsager, “Design and Analysis of Microstrip Patch Antenna Arrays”, Thesis, University College of Boras, 2011.

[15] Y. Singh, S. Ghosh, K. Prathyush. S. Ranjun, S. Suthram, A. Chakrabarty, S. Sanyal, “Design of a Microstrip Patch Antenna Array Using IE3D Software”, Indian Institute of Technology.

[16] A. Akhtar, H. Alahi, M. Sehnan, Simulation of Phased Arrays with Rectangular Microstrip Patches on Phontonic Crystal Substrates, Masters Thesis, Linnaeus University, 2012.

4 DESIGN OF THE WILKINSON RECTENNA COMMUNICATION CIRCUIT

The Wilkinson Rectenna Communication System includes three microstrip arms, two of which are connected to two transmit-receive antennas and the rectifying circuit. The third microstrip arm is coupled to the communication portion of the circuit. When there is a threshold power differential in the received signals from the two antennas, the rectifying circuit can be essentially ignored and the two input arms receive the signals and combine the signals into the third arm. The output of the combiner is then provided to the communication portion of the circuit. When there is a limited power differential in the received signals, the combiner portion of the combination circuit is essentially inactive and the received signals are rectified and can be stored in an energy storage device.

4.1 Microstrip Rectangular Patch – Design and Simulations

The microstrip rectangular patch antennas were designed to operate at 5.8 GHz. The width of the rectangular patches were determined using :

$$W = \frac{v_o}{2f_r}\sqrt{\frac{2}{\epsilon_r + 1}}$$

where the dielectric constant of the substrate ϵ_r is 2.33, the resonant frequency f_r is 5.8 GHz, and the free-space velocity of light $v_o$is 2.998 x $10^{8,}$ which yielded W = 0.020029 m.

The lengths of the antennas were determined using

$$L_{eff} = L + 2\Delta L$$

and

$$\Delta L = 0.412h\left(\frac{\left(\in_{reff} + 0.3\right)\left(\frac{W}{h} + 0.264\right)}{\left(\in_{reff} + 0.258\right)\left(\frac{W}{h} + 0.8\right)}\right.$$

and the effective dielectric constant

$$\epsilon_{reff} = \frac{\epsilon_r + 1}{2} + \frac{\epsilon_r - 1}{2}(1 + 12\frac{h}{W})^{-\frac{1}{2}}$$

With the height of the substrate h = 0.00508 and the width of the antenna W = 0.020029 m, the length was determined to be L = 0.016526 m.

The length of the inset feed y_o was determined using

$$R_{in}(y = 0) = \frac{1}{2(G_1 \pm G_{12})} cos^2\left(\frac{\pi}{L} y_o\right)$$

which, for R_{in} = 249.234283 yielded y_o equaling 0.010707 m. The length and width of the microstrip feed line (calculated using ADS's linecalc) with E_{eff} = 90° and Z_o = 50 is 9.21 mm and 1.48 mm, respectively.

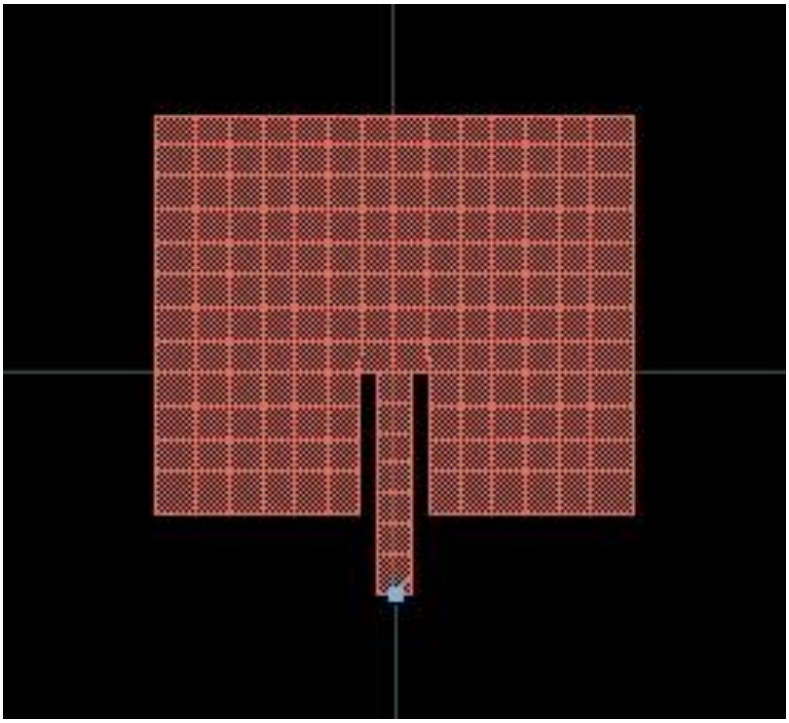

Figure 53: Rectangular patch antenna operational at 5.8 GHz designed in ADS Momentum

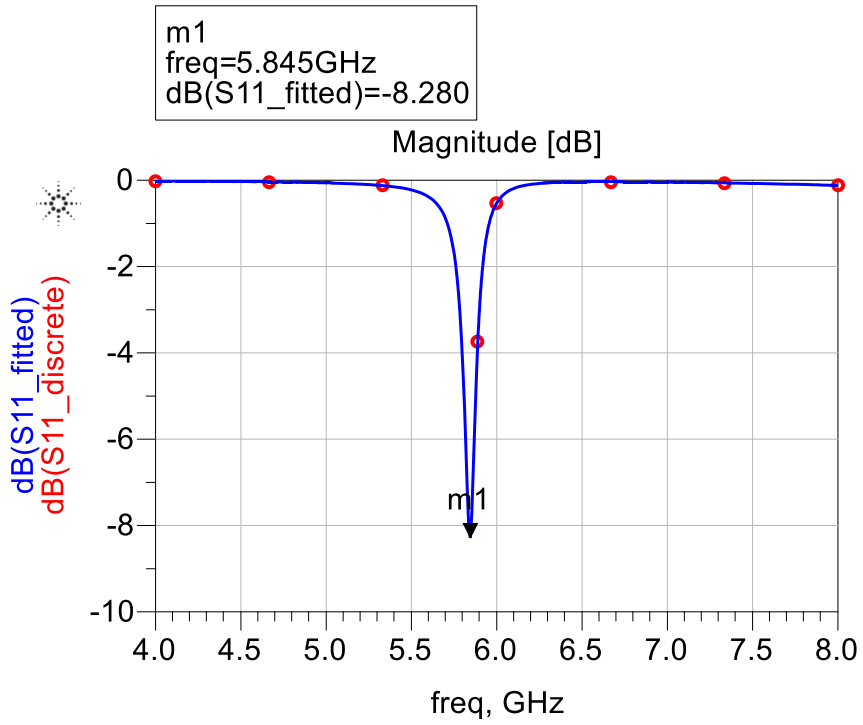

Figure 54: Simulation results for microstrip rectangular patch antenna operating at 5.8 GHz

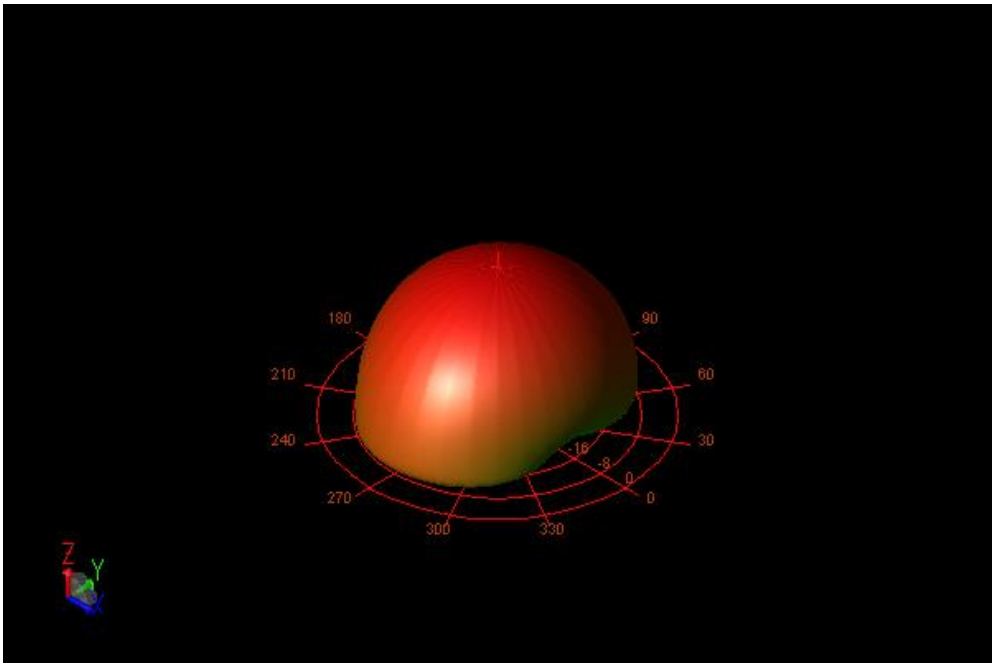

Figure 55: Radiation pattern for the 5.8 GHz microstrip rectangular patch antenna

To minimize grating lobes in the design, the distance between the rectangular patch antennas was designed using:

$$\frac{d}{\lambda} = \frac{1}{1 + |\sin \theta_o|}$$

For the microstrip rectangular patch antenna $\theta_o = 90^o$. Thus, $\sin 90 = 1$ and

$$\frac{d}{\lambda} < \frac{1}{1 + |1|}$$

$$d < \frac{\lambda}{2}$$

For c = 2.998 x 10^8 and f = 5.8 x 10^9 ,

$$d < 25.88\, mm$$

To satisfy this requirement, the distance between the microstrip antennas in the array was selected to be

$$d = 9\, mm$$

The 3D radiation pattern of the designed microstrip antenna array is shown in the figure below.

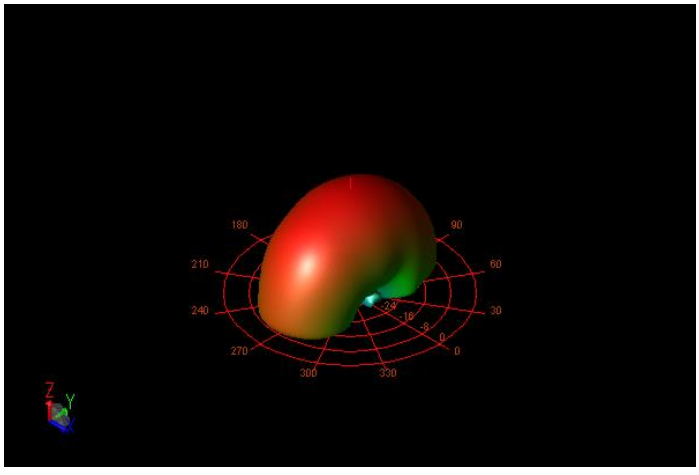

Figure 56: 3D radiation pattern for the microstrip antenna array coupled to the Wilkinson Rectenna Communication System

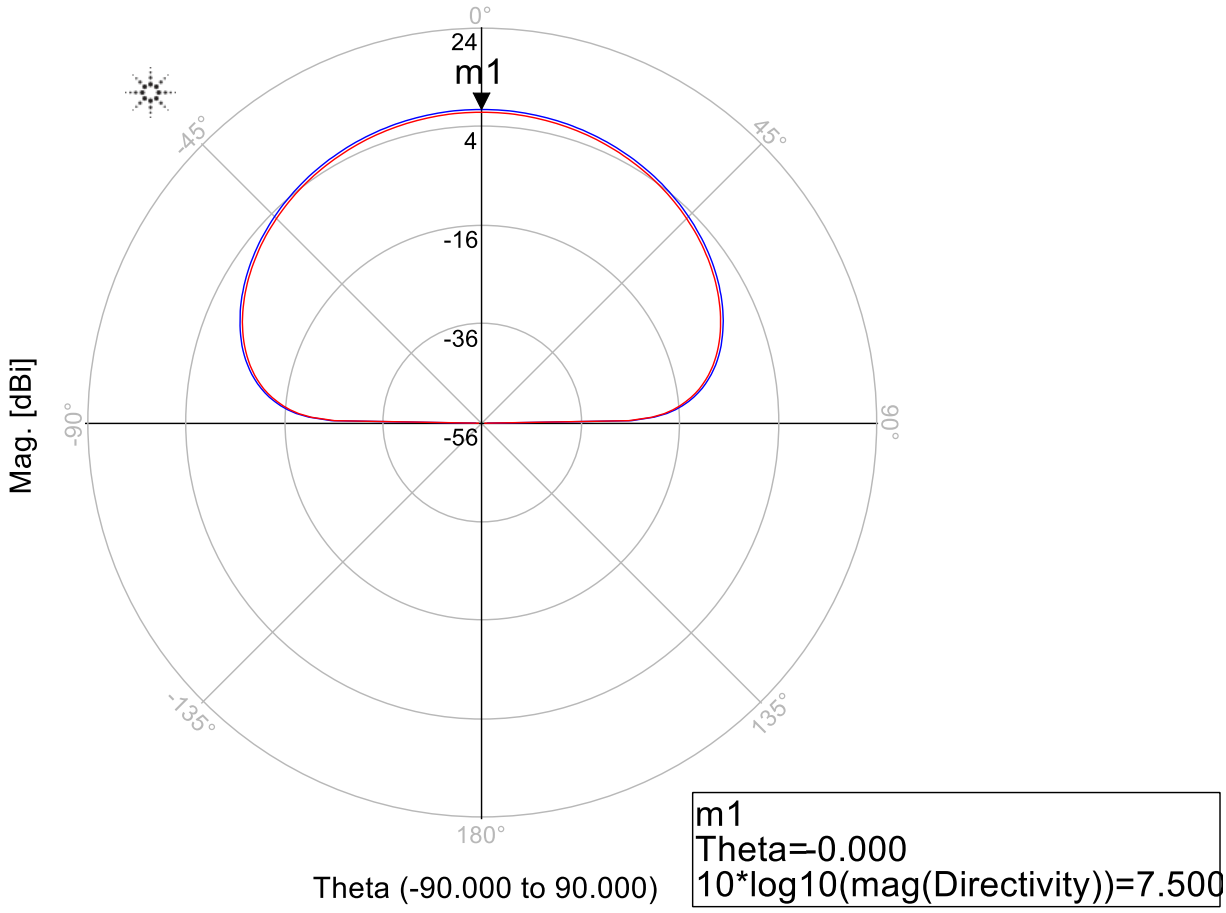

4.2 Design and Simulation of the Wilkinson Combiner

The Wilkinson Combiner was designed to operate at 5.8 GHz. Initially, a 100 ohm resistor was placed between arms 1 and 2 to provide isolation. Arms 1, 2, and 3 were designed to be resonant at 5.8 GHz. Fifty ohm terminals were placed at the antenna inputs/outputs to simulate the impedance of the microstrip patch antennas and at the communication port to simulate the communication portion of the transmitter/receiver. The techniques describe above in the Wilkinson Combiner portion were used to design the combiner in ADS. The Wilkinson power combiner is simulated in ADS and shown in the figure below.

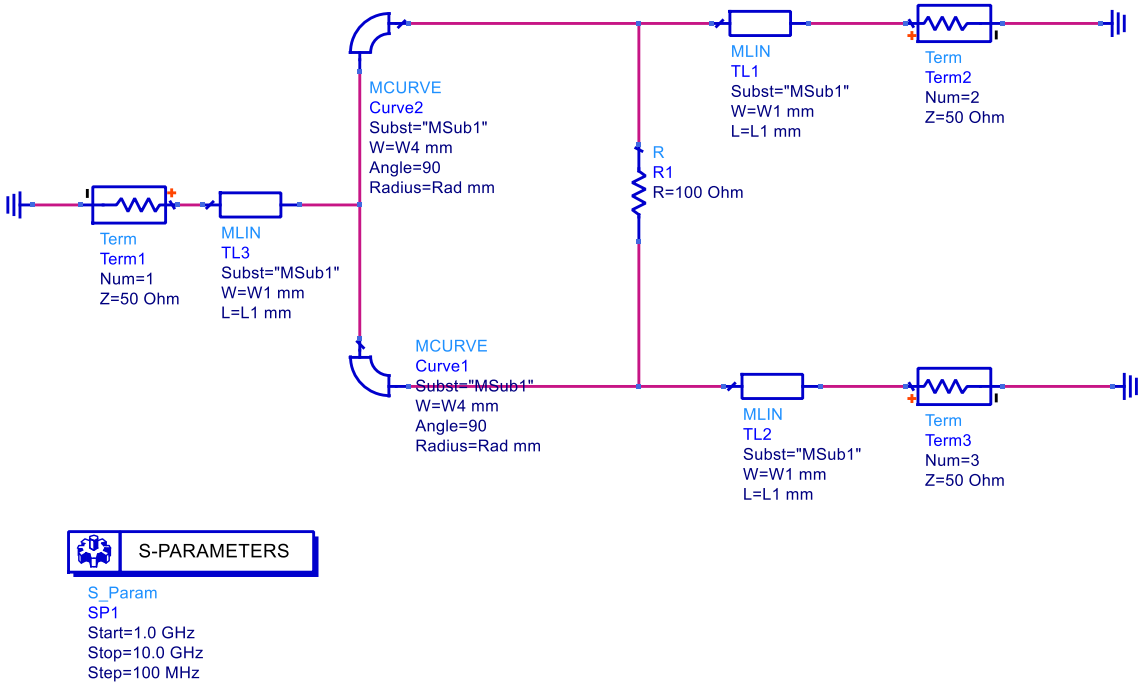

The frequency response of a Wilkinson combiner is shown in the figure below. The resulting simulation shows that the return loss S11is approximately -36 dB, the isolation S23 is approximately -40 dB, and insertion loss (S21) is -3.4 dB.

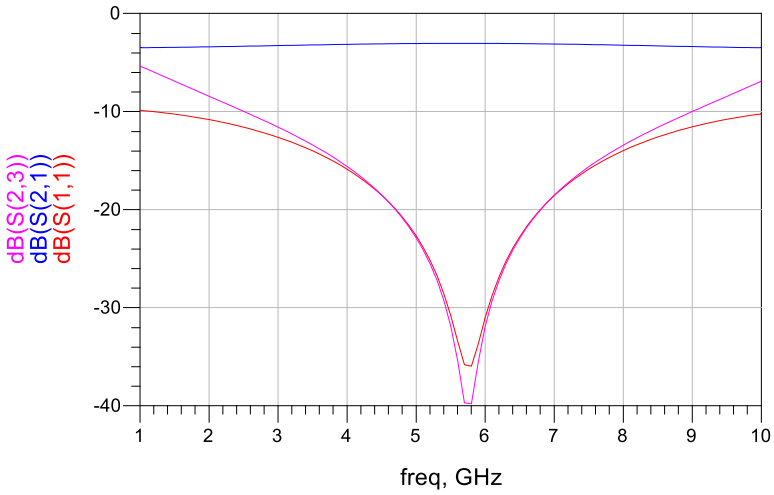

Figure 57: Frequency response of a Wilkinson power combiner operating at 5.8 GHz

4.3 Rectification Circuit Design and Simulations

The rectification circuit was designed in ADS. Numerous diodes were tested to attain a minimal reactance. As diodes could not be manufactured in the UNM lab to have the desired reactance (approximately zero), off the shelf high frequency diodes had to be tested to determine the amount of reactance. Various manufacturers provide off the shelf diodes for immediate use in rectenna systems. The impedance of numerous high frequency Schottky diodes has been determined and are shown in the table below.

Diode Manufacturer	Component Name	Type of Schottky Diode	Impedance
Siemens	di_sms_bav99_199930908	Voltage Doubler	0.410 + j96.445
Siemens	di_sms_bas70_199930908	Single Diode	30.928+j2.591
Siemens	di_sms_bas70_04_199930908	Voltage Doubler	16.231+j34.827
Siemens	di_sms_bas40_19930908	Single Diode	7.822+j76.864
Siemens	di_sms_bas125_19930908	Single Diode	11.909+j69.066
Motorola	di_mot_mmbd353lt1_19930908	Voltage Doubler	5.766+j47.687
Motorola	di_mot_mmbd352l_19930908	Voltage Doubler	4.698-j18.128
Motorola	di_mot_mmbd101l_19930908	Single Diode	8.832+j38.597
Hitachi	di_hit_hsr276_19930908	Single Diode	3.244-j31.541
Hitachi	di_hit_hsr276s_19930908	Voltage Doubler	1.390+j4.644
Hitachi	di_hit_hsm88as_19930908	Voltage Doubler	5.986-j7.337
Agilent	di_hp_hsms282B_20000301	Single Diode	8.102+j43.791
Agilent	di_hp_hsms2860_20000301	Single Diode	2.815-j50.276
Agilent	di_hp_hsms2862_20000301	Voltage Doubler	37.519-j17.405
Agilent	di_hp_hsms2820_20000301	Single Diode	7.538+j30.533
Agilent	di_hp_hsms282c_20000301	Voltage Doubler	3.860+j36.350
Agilent	di_hp_hsms2852_20000301	Voltage Doubler	7.669-j16.640

Table 3: Impedance values of high frequency Schottky Diodes at 5.8 GHz

The circuit used to determine the impedance in ADS is shown in the figure.

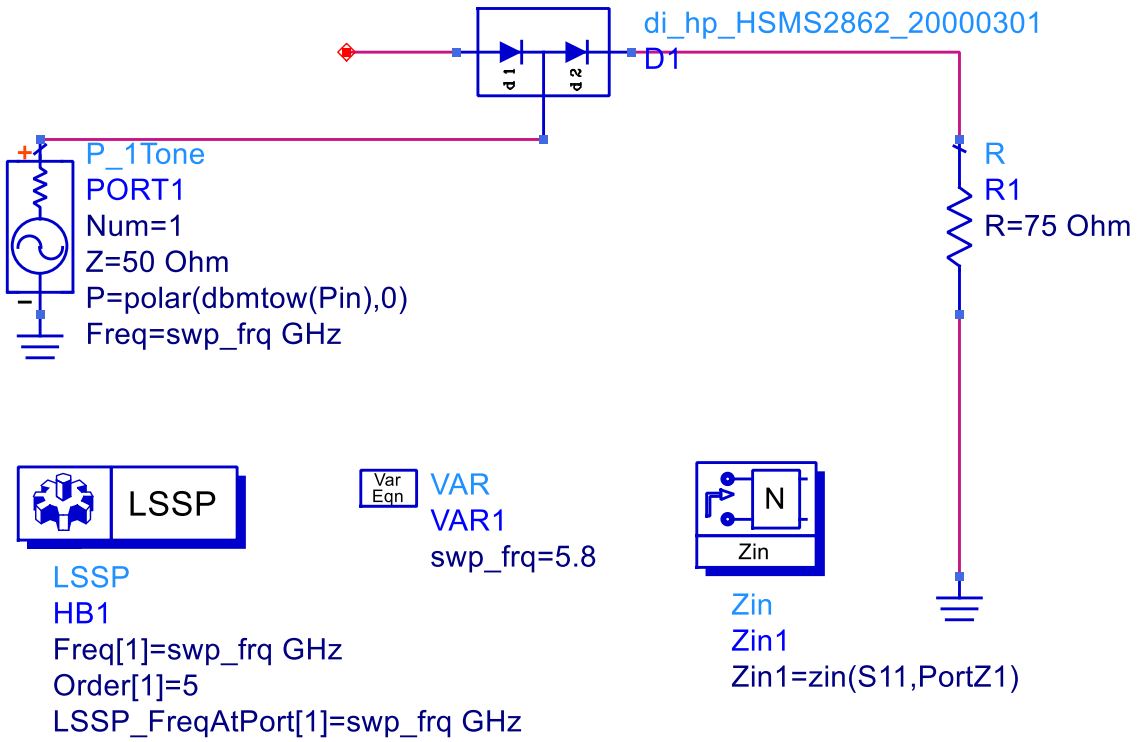

Figure 58: Impedance calculation of high frequency diode using ADS for Wilkinson Rectenna Communication System design at 0 dBm.

After numerous calculations, the HSMS 2862 diode was selected because of its minimal reactance. The resistance value was then calculated using the equation below:

$$R = X(1 + (\frac{Y}{X})^2)$$

with X = 93.71 and Y = -34.945. A 75 ohm Vishay high frequency surface mount resistor was selected as the load, which resulted in a total resistance across the rectifier circuit of 106.62 ohms at 0 dBm.

4.4 Simulation and Fabrication of the Wilkinson Rectenna Communication System

Initial design of the WRCS required designing the Wilkinson combiner based on the operational frequency, antenna selection, the physical parameters of the selected diode, and the physical parameters of the load. The resonant frequency of the WRCS system is 5.8 GHz Since the HSMS-2862 was selected as the rectification diode, the SOT-23 physical parameters shown below were used in the design.

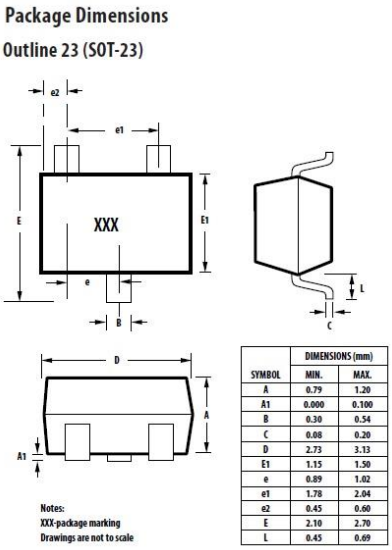

SYMBOL	DIMENSIONS (mm) MIN.	MAX.
A	0.79	1.20
A1	0.000	0.100
B	0.30	0.54
C	0.08	0.20
D	2.73	3.13
E1	1.15	1.50
e	0.89	1.02
e1	1.78	2.04
e2	0.45	0.60
E	2.10	2.70
L	0.45	0.69

Figure 59: Package dimensions of the HSMS-2862 used in the combiner design.

DIMENSIONS in inches (millimeters)

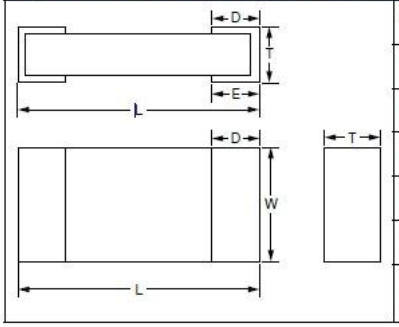

CASE SIZE	LENGTH	WIDTH W (± 0.005)	THICKNESS TYPICAL	TOP PAD D (± 0.005)	BOTTOM PAD E (± 0.005)
0402	0.042 ± 0.008 (1.067 ± 0.203)	0.022 (0.559)	0.015 (0.381)	0.010 (0.254)	0.010 (0.254)
0505	0.055 ± 0.006 (1.397 ± 0.152)	0.050 (1.270)	0.015 (0.381)	0.010 (0.254)	0.015 (0.381)
0603	0.064 ± 0.006 (1.626 ± 0.152)	0.032 (0.813)	0.015 (0.381)	0.012 (0.305)	0.015 (0.381)
0805	0.080 ± 0.006 (2.032 ± 0.152)	0.050 (1.270)	0.015 (0.381)	0.016 ± 0.008 (0.406 ± 0.203)	0.015 (0.381)
1005	0.105 ± 0.008 (2.667 ± 0.203)	0.050 (1.270)	0.015 (0.381)	0.015 (0.381)	0.015 (0.381)
1206	0.126 ± 0.008 (3.200 ± 0.203)	0.063 (1.600)	0.015 (0.381)	0.020 + 0.005/- 0.010 (0.508 + 0.127/- 0.254)	

Figure 60: Physical parameters of the Vishay surface mount resistor used in the design of the WRCS system.

The resulting WRCS was designed using ADS and Momentum is shown in the figures below.

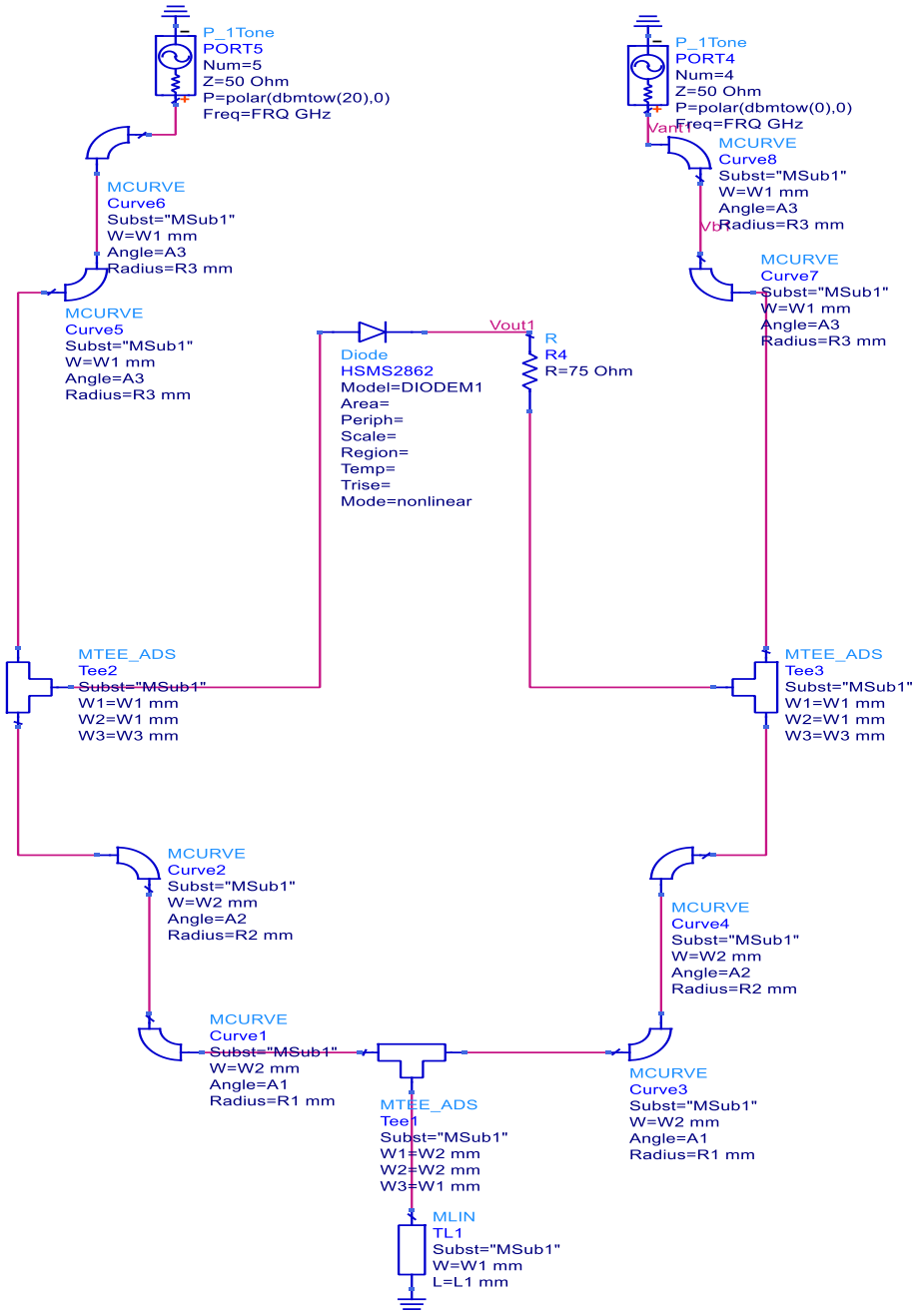

Figure 61: WRCS Rectenna operating at 5.8 GHz with an HSMS 2862 diode

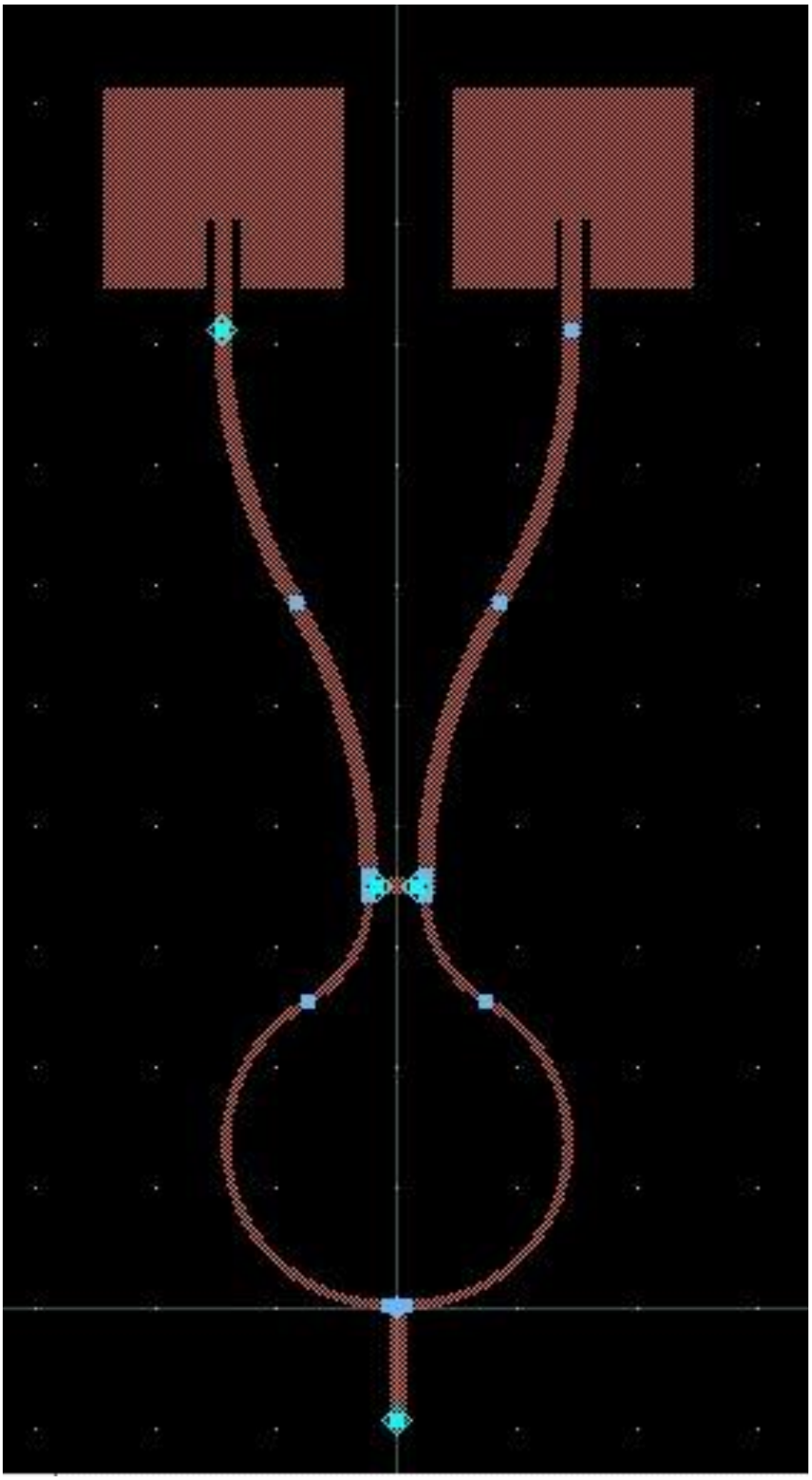

Figure 62: Wilkinson Rectenna Communication System design in Momentum provided for fabrication.

The Wilkinson Rectenna Communication System is simulated using ADS. HFSS was used to generate the radiation pattern. The WRCS system was simulated in both communication and rectification mode. The frequency response of a WRCS system is shown in the figure below. The resulting simulation shows that the return loss S11is approximately -55 dB, the isolation S23 is approximately -36.759 dB, and insertion loss (S21) is -3.4 dB, comparable to the values attained for an ideal Wilkinson Combiner.

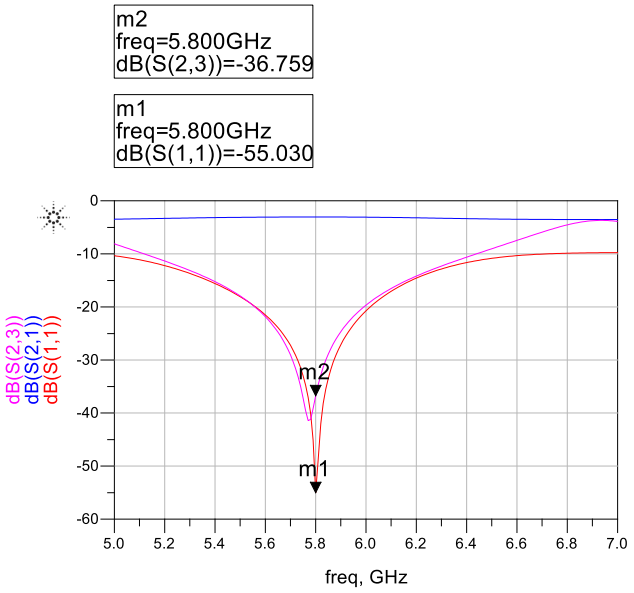

Figure 63: Wilkinson Rectenna Communication System operating at 5.8 GHz.

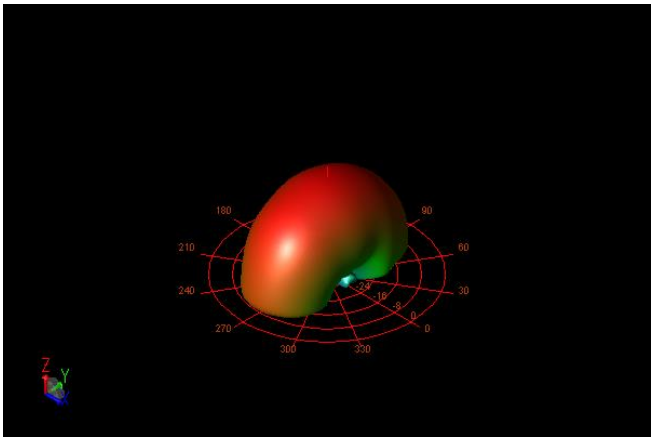

Figure 64: 3D radiation pattern for Wilkinson Rectenna Communication System in HFSS

As can be seen from the results below, the DC voltage output by the WRCS at resonance is 0.64 V with a 20 dBm power differential. The DC voltage output is negligible (approximately 0 Voltas) when the WRCS is in communication mode. This shows that the designed WRCS is operational as expected.

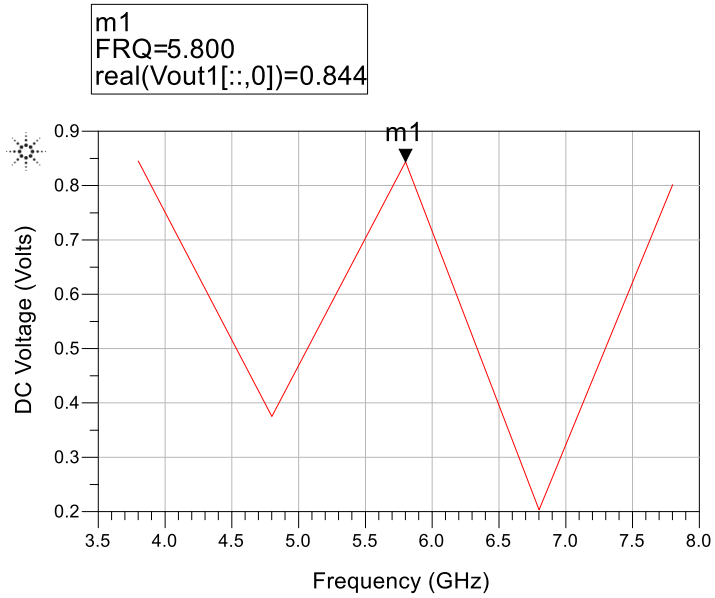

Figure 65: Output Voltage WRCS Rectenna with a 20 dBm power differential

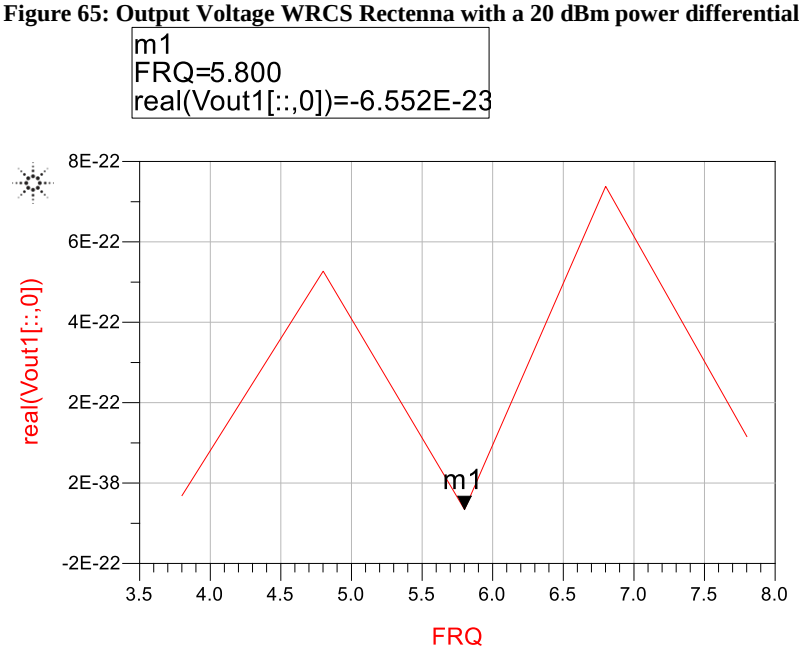

Figure 66: Output voltage of the WRCS at 5.8 GHz with zero power differential at the antenna inputs

Comparing the results shown above to Figure 22 of the prior art referenced in Chapter 2 of the Literature Review, we can see that a minimal voltage (approximately 0 volts) is provided to the communication portion of the WRCS when it is is operating as a rectification device. To increase the amount of voltage provided to the load, the WRCS rectenna array was designed and simulated using ADS. A 1 kOhm was attached to the array as the load. Each element rectifer has a 1 pF capacitor attached at the output. The WRCS rectenna arrays were simulated in both power differential and zero power differential modes. The array of rectennas can be used to increase the amount of voltage rectified, however, due to the non-linear nature of the device, the amount of voltage rectified does not necessarily double for each rectenna added to the scheme . For an array of WRCS rectennas, power combiners can be used to combiner the received RF

signals, whereas DC combiners can be used to combine the DC voltage. The WRCS circuits as well as the DC voltages are shown in the figures below.

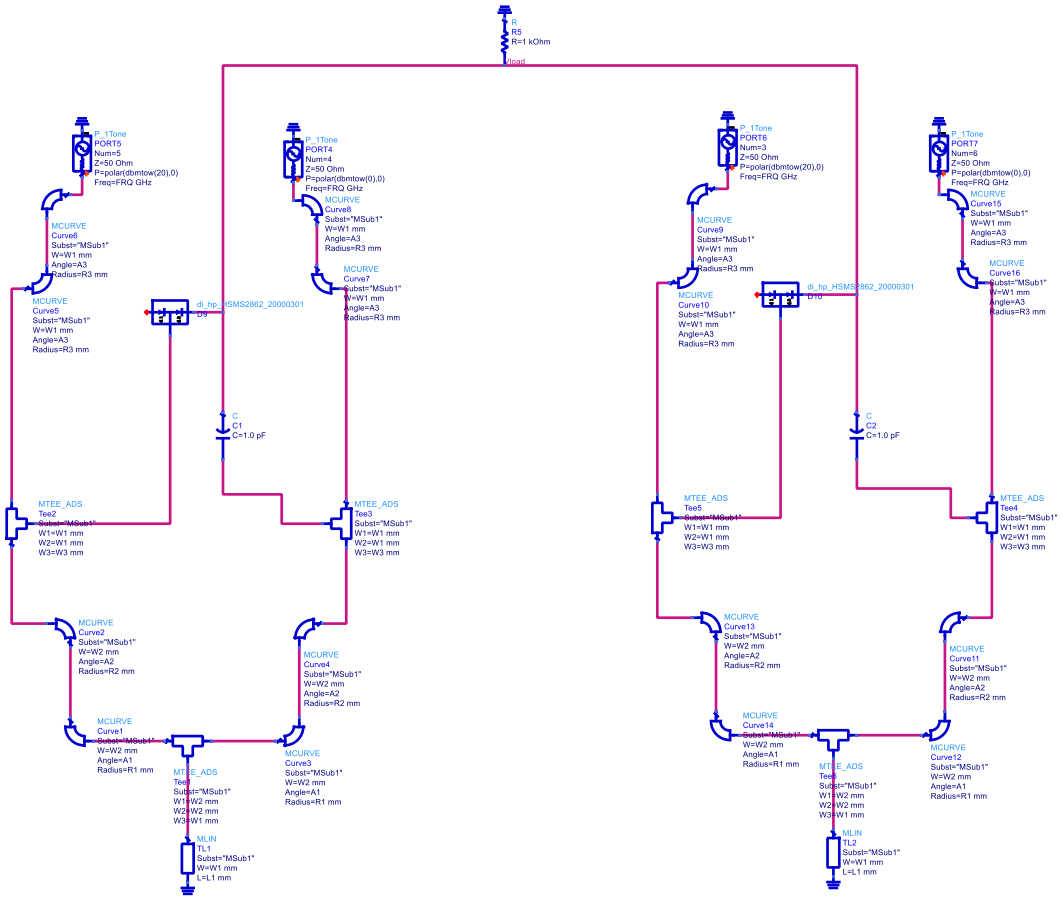

Figure 67: WRCS Rectenna Array with a 20 dBm difference at the antenna ports.

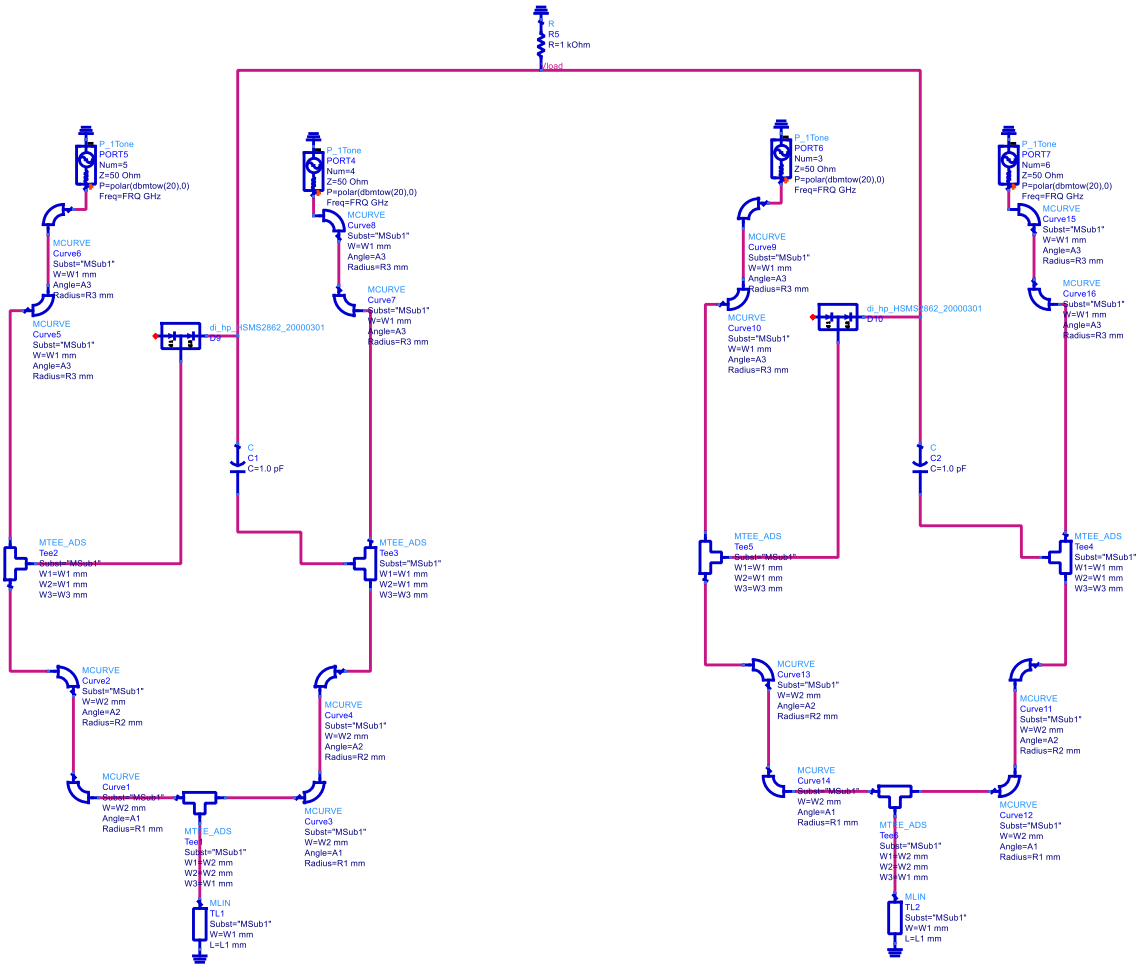

Figure 68: WRCS rectenna array with input powers equivalent at the antenna input ports.

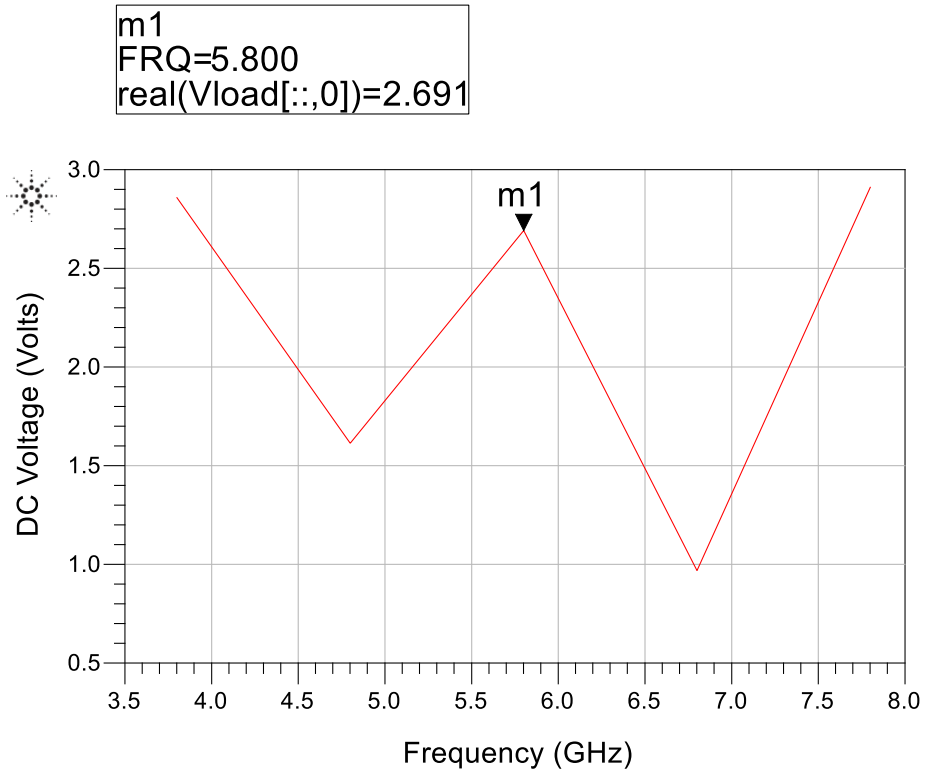

Figure 69: WRCS Rectenna Array Output DC Voltage with a 20 dBm power differential at the input ports.

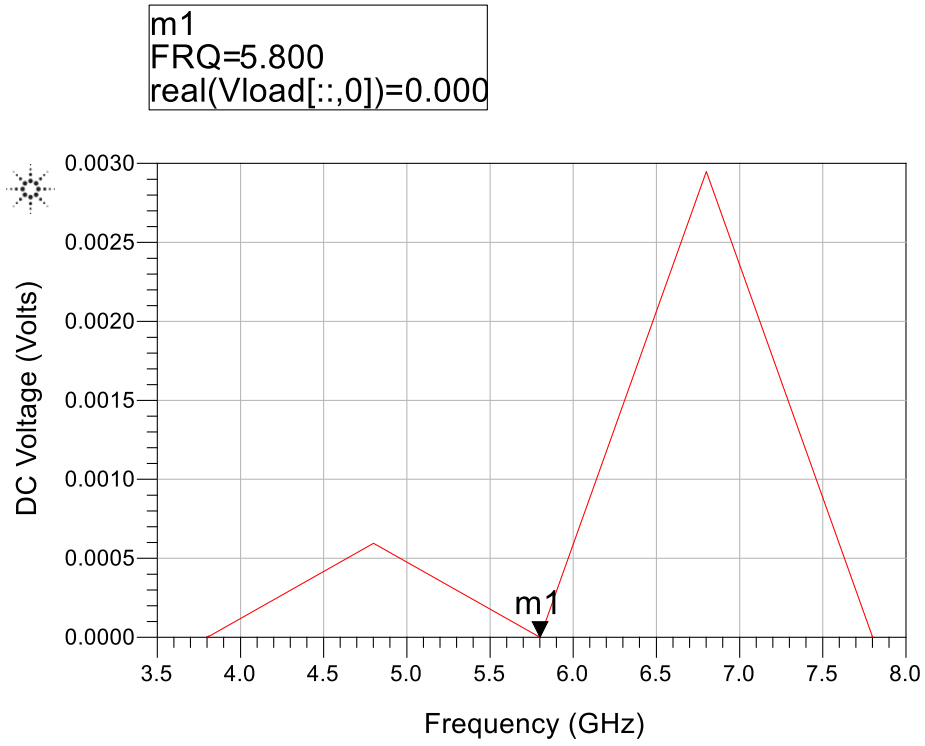

Figure 70: Rectified voltage at 5.8 GHz when the input powers at the antenna terminals are equivalent.

The fabrication process for both the Wilkinson rectenna and spiral rectenna took place in the Antennas Lab at UNM and require the use of the LPKF milling machine to mill the RT/duroid substrate for fabrication as shown in the figure below.

Figure 71: LPKF Milling Machine

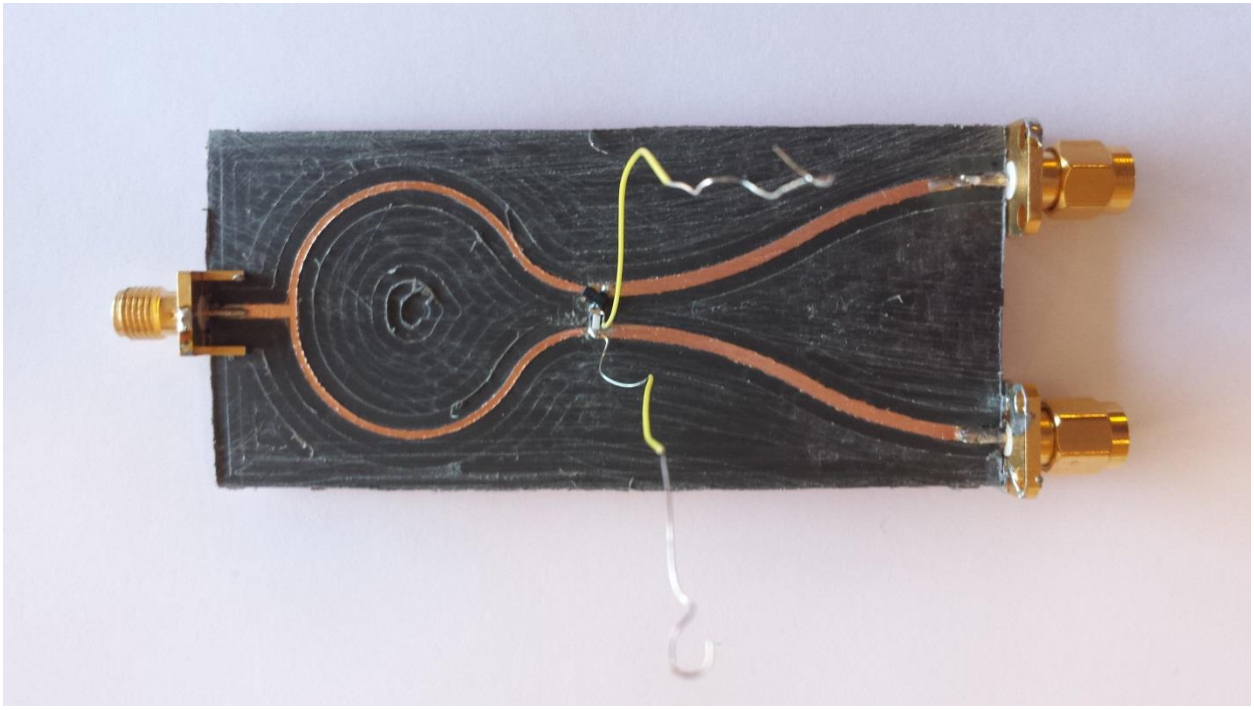

Figure 72: Mobile WRCS System for DC verification and wireless testing.

The fabricated WRCS system with 2 element rectangular patch array is shown in the figure below.

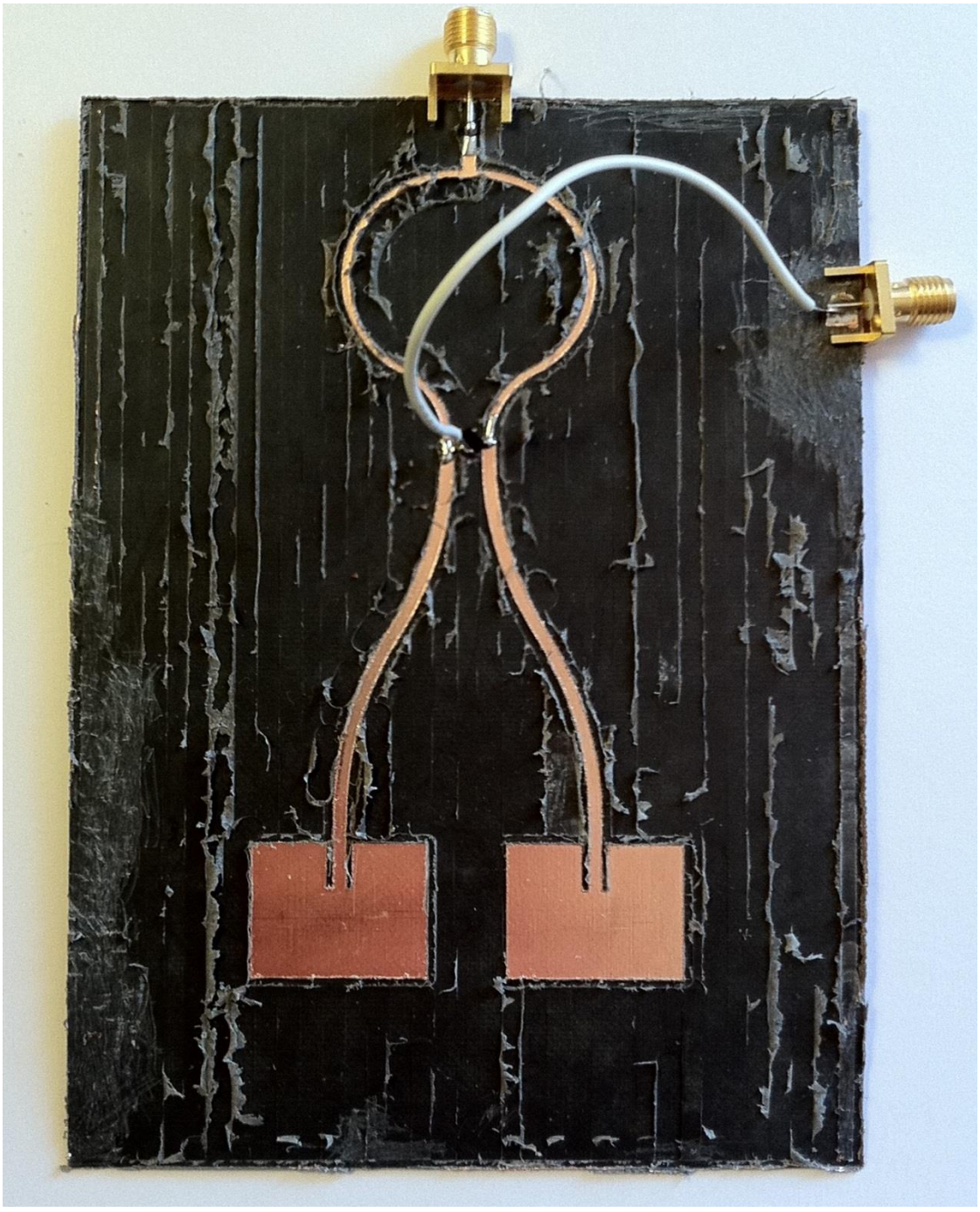

Figure 73: Fabricated Wilkinson Rectenna Communication System

To test the Wilkinson Rectenna Communication System, the following components were used: a high frequency signal generator (HP83752B - 0.01 – 20 GHz Synthesized Sweeper), the HP 8517B vector network analyzer (used to test the communication port of the WRCS system), and the BK Tool Kit voltage meter was used to measure the rectified voltage across the load. To test the communication portion of the WRCS system for basic functionality, the WRCS system was coupled to the VNA and the S11 parameters were measured as shown in the set-up below.

For testing purposes, the transmit power at antenna terminal 1 was 18 dBm. 20 dBm could not be used as the output power of the transmitter because the transmitter had a maximum transmit power of 18 dBm. The transmit power at antenna terminal 2 was -2 dBm to allow for the 20 dBM power differential. Losses in the cables were measured in the lab and the input powers to the terminals were adjusted accordingly. With losses in the channel (i.e., cable in this case), the received power was measured at approximately 14 dBM.

DC rectification occurred as expected. The average of the rectified voltage is 1.96 V. Several iterations of voltage rectification to confirm functionality. The difference in measured voltage versus simulated voltage in ADS can be attributed to the natural constant phase difference in received signals at antenna ports 1 and 2. The phase difference also causes an increase in rectified voltage. Over time the rectified voltage can be stored in a capacitor or battery and used for powering the wireless communication system. RFID sensors requiring 1.4 V to 2 V would be able to use the WRCS system to recharge their batteries or store energy in a capacitor. Because the measured voltage meets the requirements of the RFID system, no additional array configuration or spiral configuration is required generate enough voltage to power the sensors. The results of the rectification tests are shown in the figure and table below.

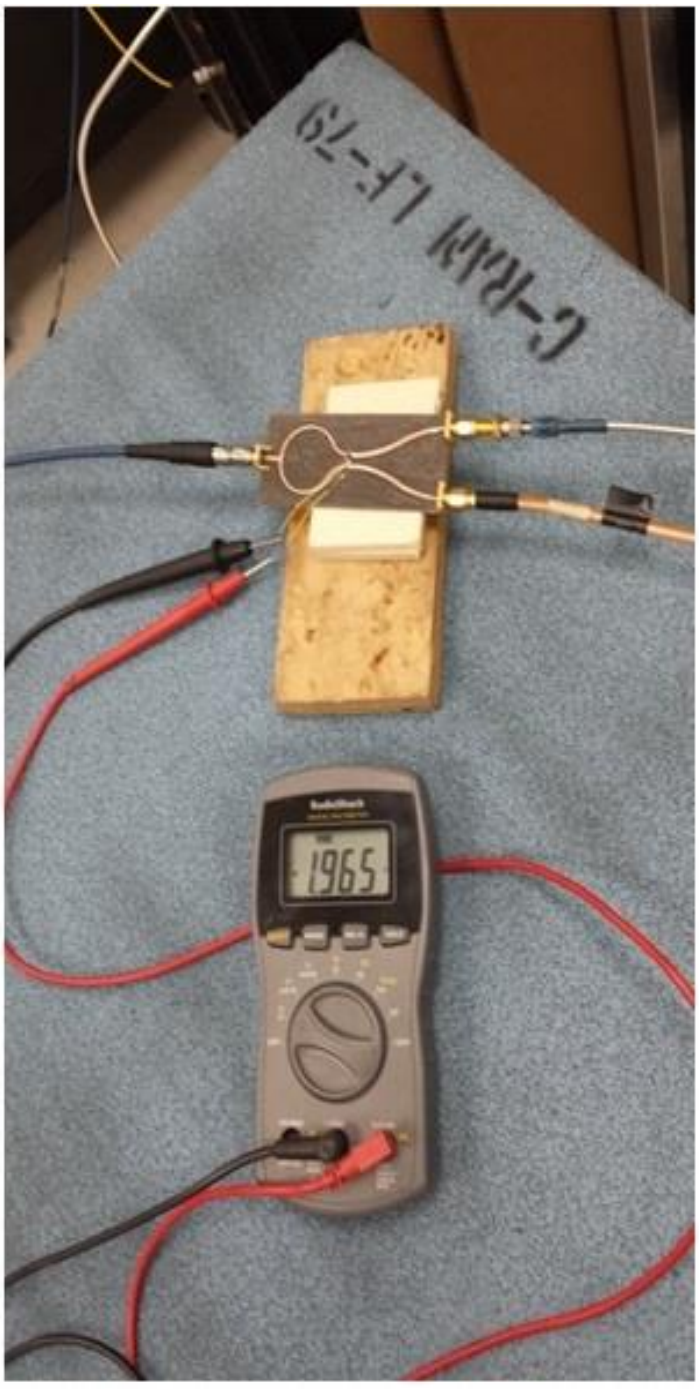

Measured DC Voltage (Volts)
1.967
1.965
1.963
1.964
1.962
1.964
1.963
1.964
1.964
1.962
1.963
1.962
1.962
1.942

Figure 74: Verification of rectified voltage at 1.96 V.

To determine whether the rectification circuit was primarily rectifying or communicating at zero power differential, the input powers for each antenna port were both set to 5 dBm. As can be seen from the measured DC voltages below, the amount of rectified voltage was negligible, around 76 mV when the antenna input powers were equivalent.

Table 4: Measured DC voltage when WRCS is in communication mode

DC Voltage (Volts)
0.076
0.0763
0.076
0.0763
0.0762
0.0763
0.0762
0.0762
0.0763
0.0762
0.0763
0.0762
0.0761
0.076

A VNA was used to test whether the communication portion of the WRCS system was operable at 5.8GHz. To determine whether the communication portion of the receiver operated effectively, the communication port was connected to a VNA to check the S11 parameters as shown in the figure below. The S11 measured using the VNA at the digital communication port was approximately -15 dB.

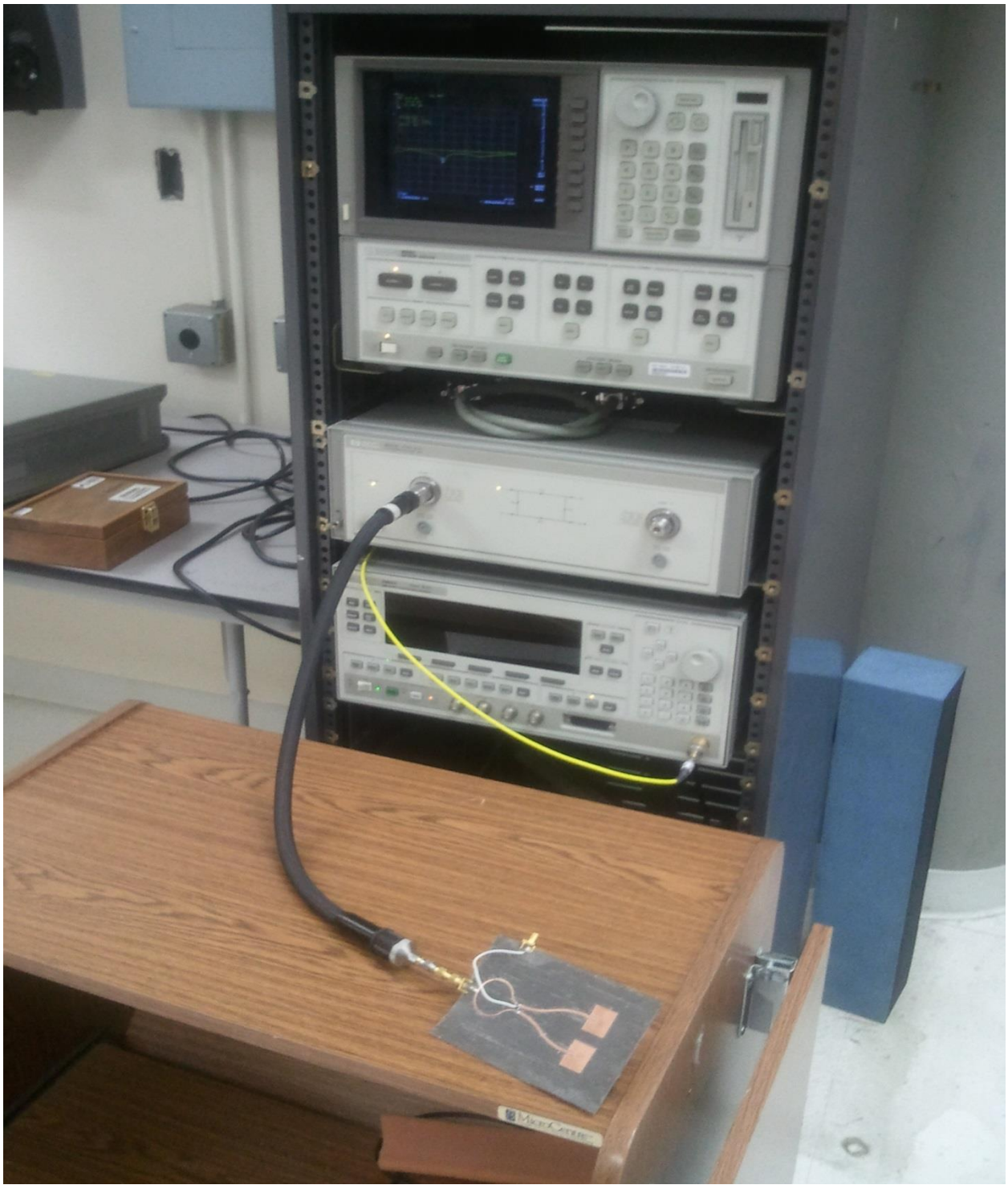

Figure 75: Wireless Rectenna Communication System test with VNA to ensure the communication system is functional.

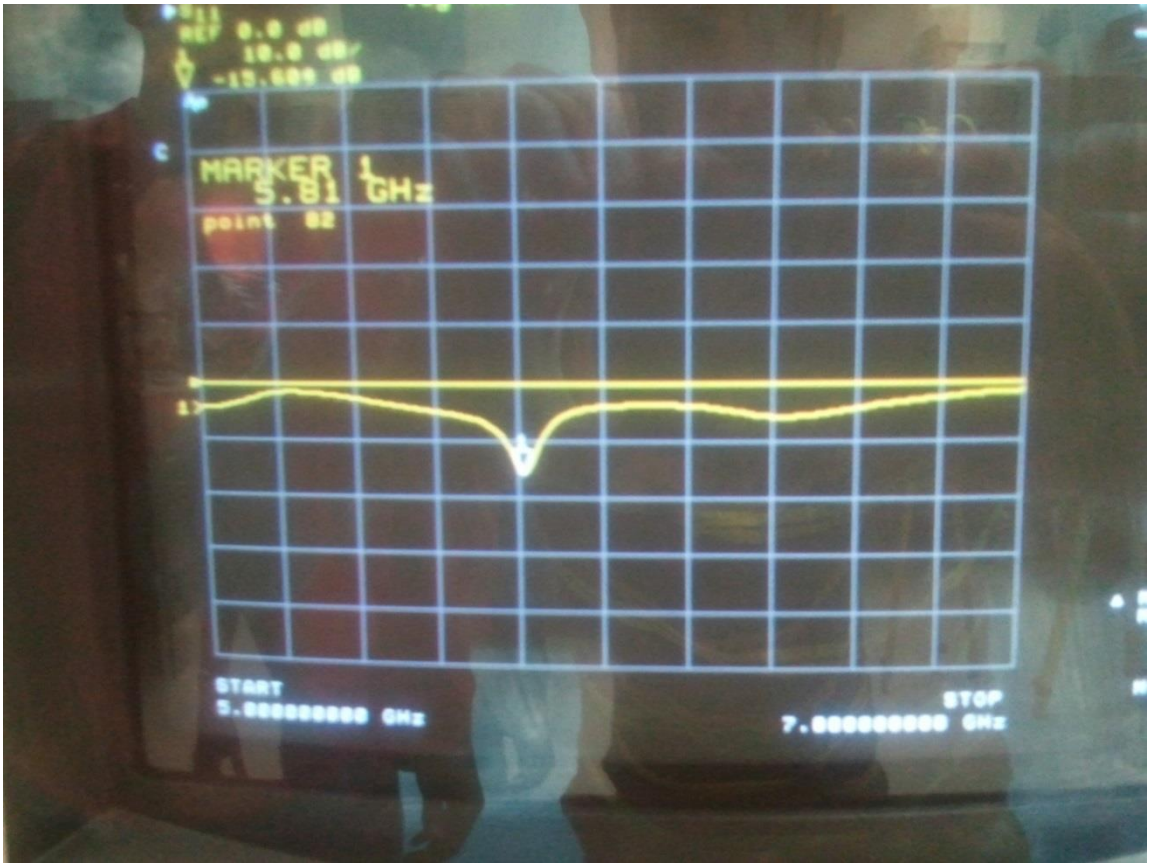

Figure 76: Wireless Rectenna Communication System test with VNA to ensure the communication system is functional.

The Agilent Spectrum Analyzer was also used to test the functionality of the communication portion of the WRCS system. As shown in the figure below, the communication port of the WRCS system is operational at 5.8 GHz. The power received at the communication port is 5.17 dBm in this instance. For the communication port, input powers of 10 dBm were used for each antenna, with a peak measurement of 6 dBm and a minimum of -10 dBm. The peak voltage occuring when both the phase of both input powers are closest to being in phase. Similar tests were conducted to measure viability of the communication for equivalent input powers of 5 dBm. For these equivalent powers, the combiner output had a minimum value of -12 dBm and a maximum value of -4 dBm. The peak power reading likely occuring when the

input powers are most in phase. The received values verify the functionality of the communication port of the WRCS system.

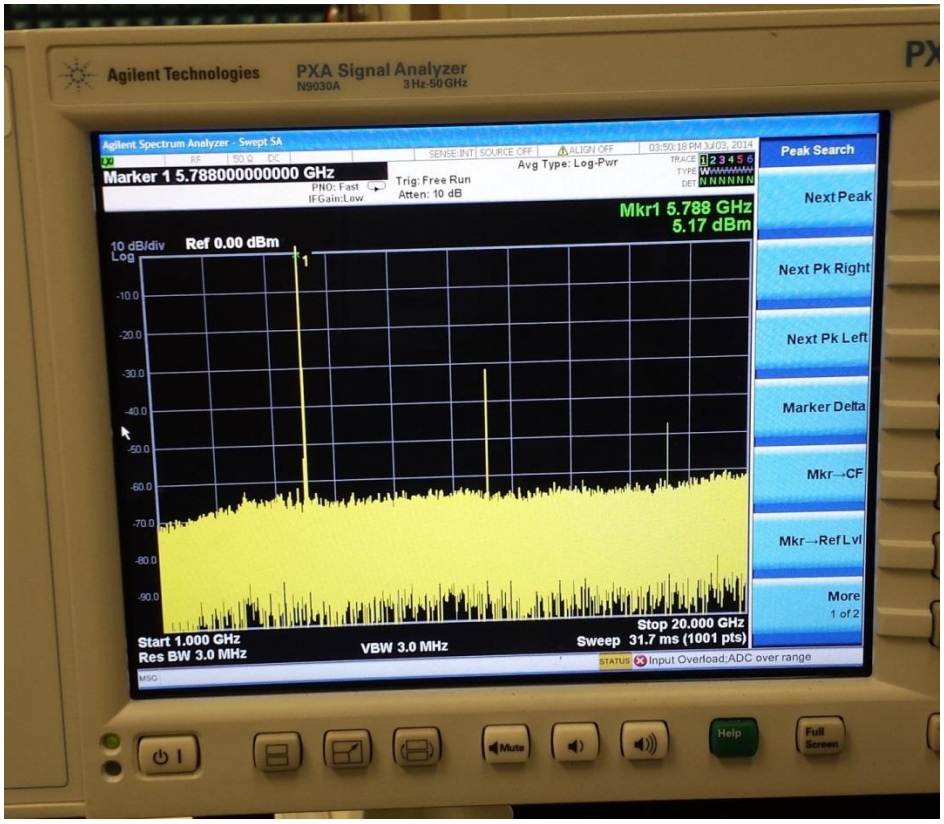

Figure 77: WRCS System working as a receiver (minimal rectification) with a 5.17 dBm receive signal

Rectenna performance is generally determined using the RF-to-DC conversion efficiency. The efficiency of the rectenna portion of the WRCS using the power input into the diode and the power output from the diode. Rectenna efficiency with an attached load is:

$$\eta = \frac{P_{DC}}{P_{RF}}$$

Because of the design of the WRCS, the tools present in the lab do not allow us to calculate the exact power at the input of the diode. However, based on the transmit power and

the cable loss, an assumption can be made that the received power was between 17.9 dBm and 17.3 dBm. The efficiency of the WRCS can be calculated and is shown in the figure below.

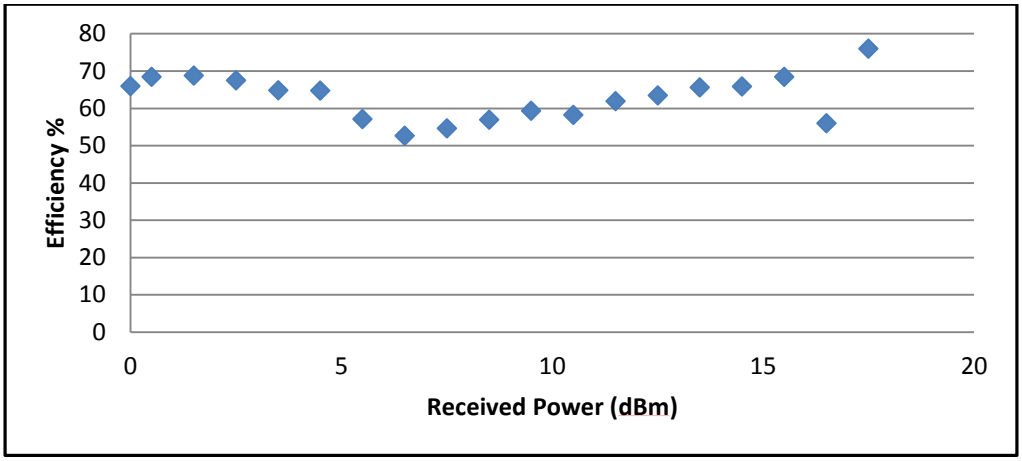

Figure 78: Efficiency calculation for the WRCS communication rectenna.

Efficiency is used as the primary tool in measuring the performance of a rectifying system. (See [1]-[13] of the Literature Review.) In rectification systems, efficiency is defined as the power rectified by the system divided by the power received by the system. It is not atypical for rectification systems, especially those using patch based antennas, to have efficiencies above 70%. For example, in *A Reconfigurable Stacked Patch Antenna for Wireless Power Transfer and Data Telemetry In Sensors* published in Progress In Electromagnetics Research C in 2012 (See [12] in Literature Review), the rectification system achieved an efficiency of 85.5%. In *Losses Analysis and Performance Improvement of a Rectenna for RFID Systems* published by IEEE in 2008 (See [4] in Literature Review), the rectification system achieved an efficiency of 79.3%. In *5.8-GHz Circularly Polarized Dual-Diode Rectenna and Rectenna Array for Microwave Power Transmission* published by IEEE Transactions on Microwave Theory and Techniques in 2006, the rectification system achieved a conversion efficiency of 76%. (See [7] in Literature Review) In *Prototype of 5.8 GHz Wireless Power Transmission System for Electric*

Vehicle System from the 2011 2nd International Conference on Environmental Science and Technology, the rectification system was able to achieve up to 75% efficiency. Similar to the rectification systems cited above, the WRCS was able to yield efficiencies up to 77% (between 50% and 77%), well in line with the efficiency calculations cited in the literature (See Table 1) and the published works cited above.

As stated previously, the difference in power between antenna ports 1 and 2 dictates the functionality of the WRCS system. When the difference between the power is maximum, the WRCS functions primarily as a rectenna. When the difference in power is at its minimum, the WRCS operates primarily as a communication device. In order to further prove this concept, the power differential versus DC Voltage was measured in the lab and is shown in the table below.

Table 5: DC voltage versus power differential at 5.8 GHz.

Pt1 (dBm)	Pt2 (dBm)	Power Differential (dBm)	DC Voltage (Volts)
18	-2	20	1.79
17	-2	19	1.37
16	-2	18	1.35
15	-2	17	1.18
14	-2	16	1.05
13	-2	15	0.92
12	-2	14	0.81
11	-2	13	0.7
10	-2	12	0.63
9	-2	11	0.55
8	-2	10	0.48
7	-2	9	0.42
6	-2	8	0.39
5	-2	7	0.37
4	-2	6	0.33
3	-2	5	0.3
2	-2	4	0.27
1	-2	3	0.24
0	-2	2	0.21
-1	-2	1	0.19
-2	-2	0	0.17

Under this test, the transmit power was decreased 1 dBm and the resulting DC voltage was measured. As can be seen from the data, there is a smooth transition in DC voltage for a 1 dBm reduction from antenna input port 1 and antenna input port 2. However, there is a significant change in voltage (and thus communication) for a substantial drop in transmit power at antenna input port 1. For example, for a drop of 10 dBm, the amount of DC voltage drops from 1.79 V to 0.4 V rectification. At this point, the WRCS functions more as a communication device then a rectification device.

In order to determine whether the proposed WRCS is functional in both communication and rectification modes with antennas connected, a second WRCS functionality test was conducted in the antennas lab at UNM. Two sets of antennas were connected to the antenna input ports, with one set simulating two antennas receiving the equivalent power (communication mode), and the second set simulating two antennas receiving different power (rectification mode).

For the rectification mode functionality test, a two element horn antenna array was connected at the input ports of the WRCS system. The two-element horn antenna array was selected as the array because it was easier to control the power differential due to the size of the horns, i.e., the wireless power transmitter could be placed directly in from of antenna 1 to achieve a maximum power differential between antennas 1 and 2. The set-up of the rectification functionality tests are shown in the figures below.

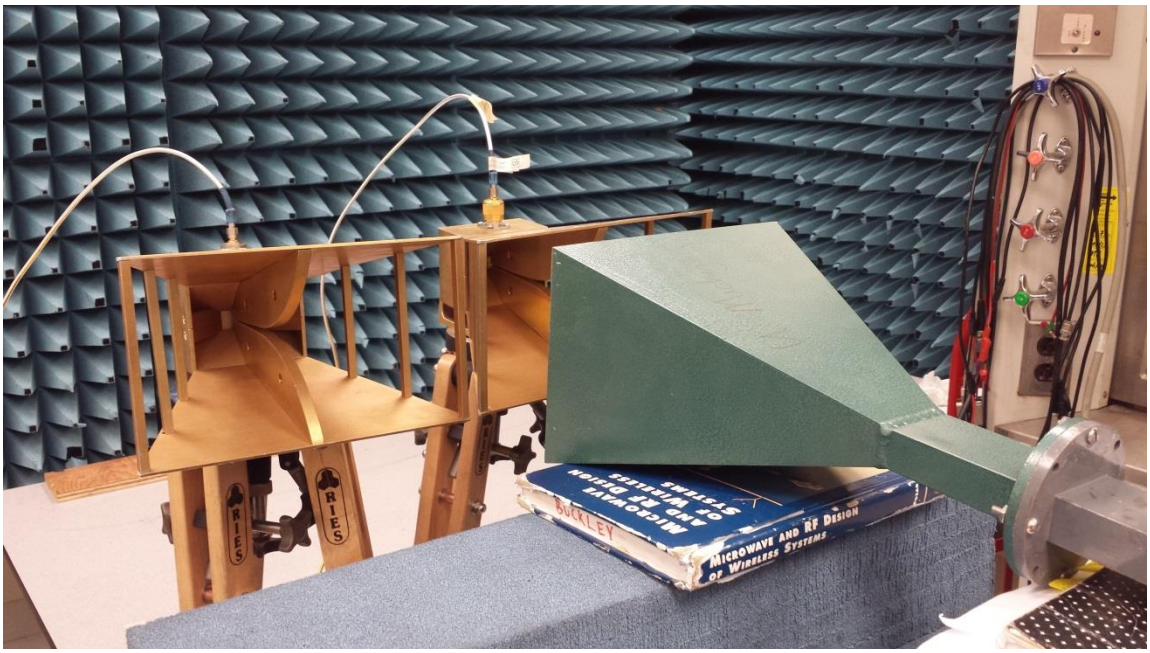

Figure 79: Rectification test set-up of the WRCS system (near field).

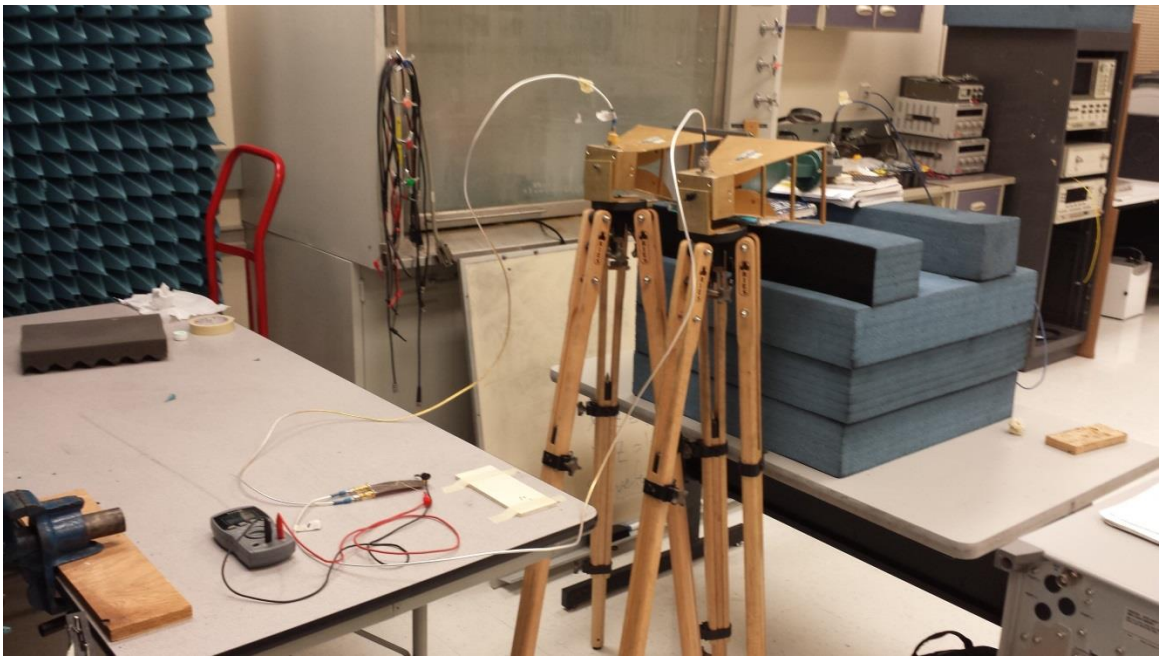

Figure 80: Rectification test set-up of the WRCS system (near field).

As with the functionality tests conducted with the high frequency signal generators as direct sources, the power of the wireless power transmitter was selected to be between 18 dBm and – 2 dBm. Tests were conducted in 1 dBm increments. Unlike the 17.5 dBm power received by the WRCS system in previous functionality test, due to limitations in the transmitter and transmission channel losses, the maximum power capable of being received by the WRCS system antennas at the input ports was 3 dBm. Thus, for functionality and efficiency calculations, 3 dBm is the maximum received power for, instead of 17.5 dBm. The measurement results for the WRCS system rectification test is shown in the table below.

Table 6: Rectified DC voltage for WRCS system coupled to antennas.

Transmit Power (dBm)	Received Power Ant 1 (dBm)	Received Power Ant 2 (dBm)	DC Voltage (Volts)
18	-33.49	3	0.34
17	-33.52	2.12	0.2956
16	-34.6	1.65	0.256
15	-35.69	0.61	0.227
14	-36.51	-0.58	0.1965
13	-38.15	-1.38	0.1694
12	-40.47	-2.54	0.145
11	-40.56	-3.53	0.1259
10	-41.38	-4.53	0.1052
9	-41.85	-5.49	0.0915
8	-42.51	-6.66	0.0776
7	-43.6	-7.96	0.0658
6	-44.75	-8.81	0.0569
5	-45.27	-9.52	0.0472
4	-46.9	-10.49	0.0396
3	-47.45	-11.75	0.0329
2	-48.3	-12.72	0.0274
1	-49.99	-13.76	0.0227
0	-50.16	-14.71	0.0185
-1	-51.75	-15.97	0.0152
-2	-52.32	-16.62	0.0124

Efficiency calculations were also conducted for the WRCS system and are shown in the table below.

Table 7: Efficiency calculations for the WRCS system.

Received Power (dBm)	DC Voltage (Volts)	Efficiency (%)
3	0.34	77.249659
2.12	0.2956	71.506842
1.65	0.256	59.761112
0.61	0.227	59.702216
-0.58	0.1965	58.838805
-1.38	0.1694	52.573338
-2.54	0.145	50.312366

As can be seen from the measured results, the efficiency of the WRCS system for power levels comparable to the receive power calculations (minimum receive power of -2 dBm) is from 50% to 80%. This is comparable to the efficiency calculations generated for the previous WRCS system. (See Figure 78)

For the communication mode functionality test, a two element microstrip antenna array was connected at the input ports of the WRCS system. Microstrip antennas were selected as the array because it was easier to minimize the power differential in the lab setting because of the smaller size of the microstrip antennas, i.e., the wireless power transmitter could be placed directly in front of antenna 1 and antenna 2 achieve equivalent powers. The set-up of the communication functionality tests are shown in the figures below.

Figure 81: Communication test set-up of the WRCS system.

Figure 82: Communication test set-up for the WRCS system (near field).

In order to test the communication portion of the WRCS system, the microstrip antenna array was placed directly in front of the wireless power transmitter. Because the received power for the WRCS was too low in the far-field, the received power at the WRCS system was measured placing the transmit antenna as close as possible to the WRCS to emulate the actual power that a WPT system is capable of generating to recharge the WRCS system. This allowed the WRCS system to have a relatively equivalent power differential (+- 2dBm) at the input ports. (See table 6 below) A table of the power received by the WRCS system for communication mode is shown in the table below.

Table 8: Table of verification of communication power level.

Transmit Power (dBm)	Received Power Ant 1 (dBm)	Received Power Ant 2 (dBm)	Received Power Ant 1 (Watts)	Received Power Ant 2 (Watts)	Pcom (dBm)
18	-6.49	-7.94	0.000224	0.000161	1.66
17	-7.72	-9.53	0.000169	0.000111	0.58
16	-8.58	-10.48	0.000139	8.95E-05	-0.57
15	-10.15	-11.12	9.66E-05	7.73E-05	-1.26
14	-11.06	-12.26	7.83E-05	5.94E-05	-2.95
13	-12.78	-13.75	5.27E-05	4.22E-05	-3.54
12	-13.11	-14.88	4.89E-05	3.25E-05	-4.39
11	-14.14	-15.39	3.85E-05	2.89E-05	-5.38
10	-15.93	-16.43	2.55E-05	2.28E-05	-6.75
9	-16.94	-17.11	2.02E-05	1.95E-05	-7.93
8	-17.82	-18.32	1.65E-05	1.47E-05	-8.53
7	-18.55	-19.35	1.4E-05	1.16E-05	-9.47
6	-20.29	-20.72	9.35E-06	8.47E-06	-10.65
5	-21.32	-21.53	7.38E-06	7.03E-06	-11.93
4	-22.21	-22.67	6.01E-06	5.41E-06	-12.94
3	-22.93	-23.74	5.09E-06	4.23E-06	-14.11
2	-24.08	-24.24	3.91E-06	3.77E-06	-14.98
1	-25.22	-25.75	3.01E-06	2.66E-06	-16.34
0	-26.42	-26.21	2.28E-06	2.39E-06	-17.97
-1	-27.4	-27.33	1.82E-06	1.85E-06	-18.45
-2	-28.67	-28.76	1.36E-06	1.33E-06	-19.33

As can be seen from the communication measurements, for a receive power of approximately – 7 dBm, the power provided to the communication port is approximately 1.66 dBm. For approximately - 8 dBm, the power provided to the communication Since levels as lower than -10 dBm can be provided to the input of communication systems, the amount provided is an acceptable level for communication for the WRCS system.

Because a significant number of modern wireless power transfer systems are designed to operate in the near-field to improve the efficiency of the rectenna systems (See [1], [2], [3] and the figures below), measurements of the WRCS system were conducted in the near-field. It is

important to note that there are several applications where near-field wireless power transfer applications require the use of testing configurations similar those exemplified in this research [3], [4], [5]. For example, for electric autonomous vehicles requiring wireless power transmission and communication capability (RFID) (similar to those being developed by, for example, Tesla and Google), the wireless charging of these vehicles generally does NOT take place in far-field, but rather in the near-field (See figures below).

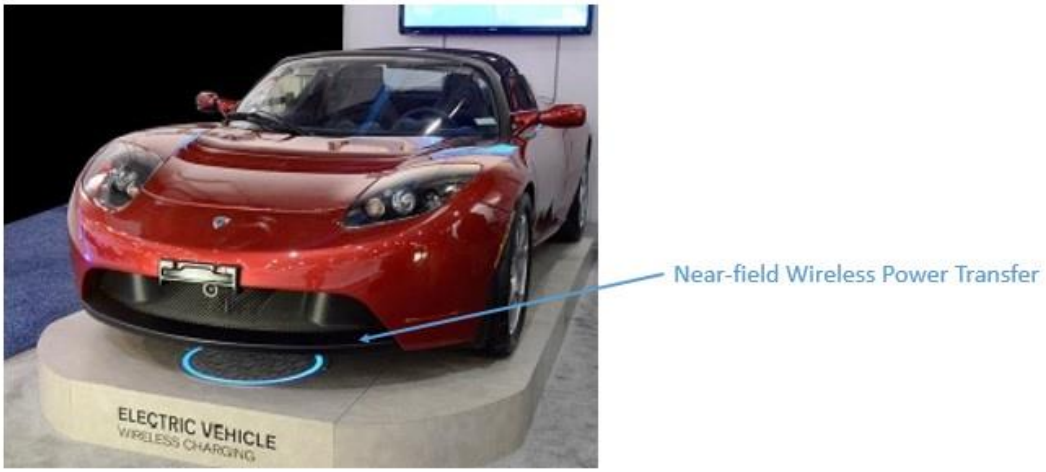

Figure 83: Near-field wireless power transfer - electric vehicle using wireless charging in the near field [4].

These wireless autonomous vehicles would be able to use the WRCS system described in this research to avoid having different sets of antennas for wireless charging and communication. In addition, the same sets of antenna arrays in the WRCS system would still be able to operate as communication devices in the far-field, thus making them operable for autonomous vehicle functionality. These near-field systems have greater efficiencies than those in the far-field because of the proximity of the wireless power transmitter to the rectification system (See figure below).

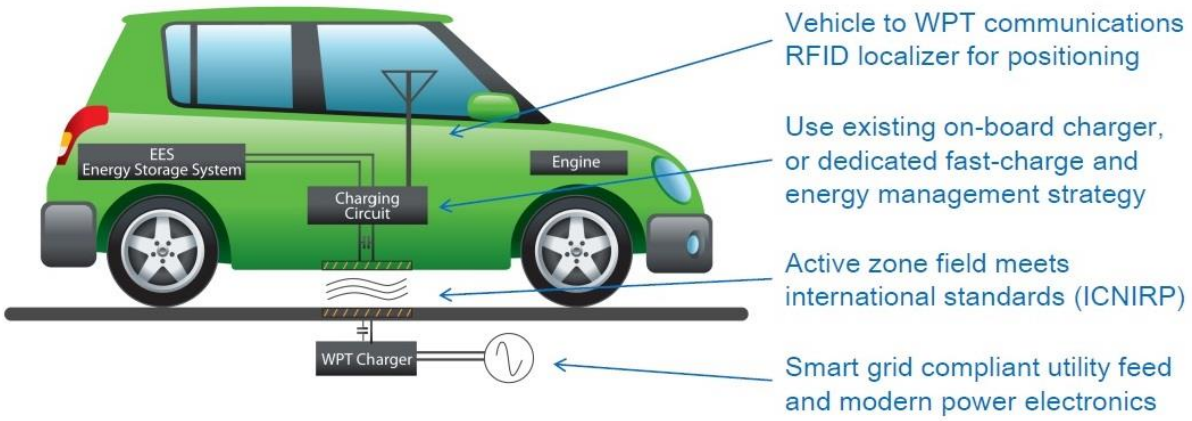

Figure 84: Near-field Power transfer method in an Autonomous Electrical Vehicle (Source: Oak Ridge National Laboratory – Department of Energy)[5]

As compared to efficiency calculations in the far-field, the near-field wireless power transmission efficiency calculations generally result in greater efficiency values than those taken in the far-field (greater than 40% for varying receive powers). This is in line with efficiency values calculated for other rectennas placed in the near-field (between 40% and 70%) [3] (See figure below).

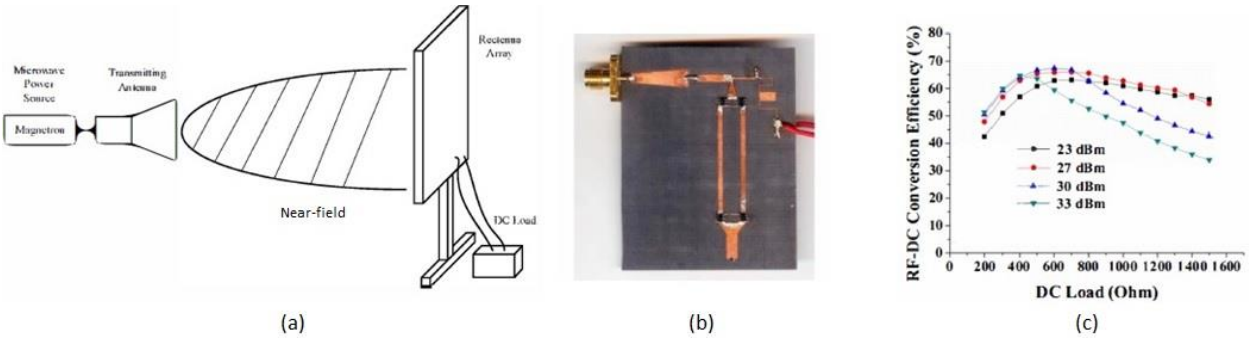

Figure 85: Near-Field Wireless Power Transmission System with 2.45 GHz Rectenna (a) Lab Test Set-up (b) Rectifying Circuit Unit (c) Calculated Efficiencies [3]

Thus, for an absolute efficiency calculation in the near-field (calculating the efficiency based on using the actual power measurements of power received at the receive antennas), the formula to calculate efficiency remains the same because the rectifier is only concerned with the actual

power that is receiving, not how the power actually was derived (whether in the far-field or the near-field such as is the case here) [3].

The fabricated proof-of-concept measurements for the WRCS system were conducted following procedures similar to those conducted in [3]. In [3], a 2.45 GHz rectification system was placed in the near-field of a wireless power transmitter and the voltage rectified by the system was measured. Rectified voltage calculations were taken with efficiencies similar to those conducted for the WRCS rectification system. The lab set-up is shown in the figure below.

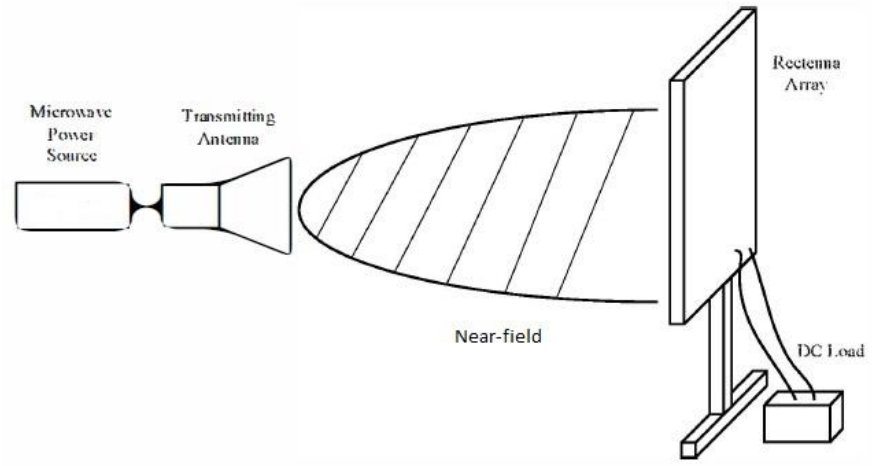

Figure 86: Lab-set up for near-field Wireless Power Transmission [3].

To extend the measurements to the far-field, the near-field values were mapped to the far-field using both the Friis transmission formula and the absolute receive powers. These formulas can be used to describe the relationship between the power received by the WRCS system and the efficiency. Friis transmission formula is used to describe the free space power transmission through the atmosphere [6].

The gain of the transmit antenna can be formulated as:

$$G_t = \frac{4\pi}{\lambda^2} A_{et}$$

where A_{et} is the effective area of the transmit antenna. When the transmit antenna is not an isotropic antenna (such as the case here), the power density at a distance R from the transmit antenna is:

$$S = \frac{P_t G_t 4\pi}{4\pi R^2}$$

The power available at the receive antenna may then be calculated using:

$$P_r = S = \frac{P_t G_t 4\pi}{4\pi R^2} A_{er}$$

where A_{er} is the effective area of the receive antenna. The receive power can now be formulated as:

$$P_r = \frac{P_t G_t G_r \lambda^2}{(4\pi R)^2}$$

With the power efficiency of the WRCS system being defined as the total dc power (P_{DC}) measured at the output of the rectenna system divided by the time-average RF input power, the relationship between the power received by the WRCS system and the efficiency is

$$\eta = \frac{P_{DC}}{P_r}$$

Using this relationship for received power values between -6.66 dBm and – 12.72 dBm, the corresponding efficiency values are shown in the table below. As can be seen from the table, the efficiencies are significantly less than that of near-field, this is because the efficiency is directly

proportional to power received (P_{DC} / P_r) and in the far field less power is received by the WRCS then in the near-field.

Table 9: Efficiency values mapped to far-field for WRCS system.

Received Power (dBm)	DC Voltage (Volts)	Efficiency (%)
-6.66	0.078	37.21
-7.96	0.066	36.09
-8.81	0.057	32.82
-9.52	0.047	26.60
-10.49	0.040	23.41
-11.75	0.033	21.59
-12.72	0.027	18.73

4.5 Conclusion

The Wilkinson Rectenna Communication System was able to rectify energy as well as operate as a communication device. Overtime, the energy collected via wireless power transmission can be collected in a battery or capacitor and provided to a load, while still performing its fundamental requirement of transmitting data. Although less efficient in the far-field then in the near-field, only a microstrip Wilkinson rectenna circuit with a diode with minimum reactance need be added to existing circuitry and still allow for rectification, and thus less need for manually changing batteries in difficult to reach circuits, such as those embedded in concrete applications.

4.6 References

[1] A. Costanzo, M. Dionigi, D. Masotti, M. Mongiardo, G. Monti, L. Tarricone, R. Sorrento, *"Electromagnetic Energy Harvesting and Wireless Power Transmission: A Unified Approach"*, Proceedings of the IEEE, Vol. 102, No. 11, Nov. 2014.

[2] N. Carvalho, A. Georgiadis, A. Costanzo, H. Rogier, A. Collado, J. Garcia, S. Lucyszyn, P. Mezzanotte, J. Kracek, D. Masotti, A. Boaventura, M. Lavin, M. Pinuela, D. Yates, P.

Mitcheson, M. Mazanek, V. Pankrac, "*Wireless Power Transmission: R&D Activities Within Europe*", IEEE Transactions on Microwave Theory and Techniques. Vol. 62, No. 4, pp. 1031-1045, April 2014.

[3] W. Jiang, B. Zhang, L. Yan, C. Liu, "*A 2.45 GHz rectenna in a near-field wireless power transmission system on hundred-watt level*", Microwave Symposium (IMS), 2014 IEEE MTT-S International, June 2014.

[4] J. Lin, *"Wireless Power Transmission: From Far-field to Near-Field"*, Powerpoint Presentation.

[5] J. Miller, M. Scudiere, J. McKeever, C. White, "Wireless Power Transfer", Oak Ridge National Laboratory – U.S. Department of Energy, http://web.ornl.gov/adm/partnerships/events/power_electronics/presentations/T2-F-Wireless_Power_Transfer.pdf.

[6] C. Huang, "Design and Development of Wireless Power Transmission for Unmanned Air Vehicles", Naval Post Graduate School, Masters Thesis, September 2012.

5 X-BAND BROADBAND RECTENNA

5.1 Introduction

In its simplest form a spiral rectenna consists of a spiral antenna and a diode. IEEE defines a spiral antenna as an "antenna consisting of one or more conducting wires or tapes arranged as a spiral."[13] The spiral antenna is of specific importance in energy harvesting because of the nature of its frequency independency and its ability to receive power at a range of frequencies. Described first in the 1950's, Rumsey elaborated on the parameters of the spiral antenna noting its frequency independency due to its structure being defined by angles [14], [15].

Spiral antennas are known to operate efficiently over a broadband, in addition, spiral antennas can be designed to fit within a wireless communication device and function relatively well as part of a spiral rectenna [1], [2]. Ideally, the radiation pattern, polarization, and impedance of the spiral antenna change only minimally based on the frequency of operation within its prescribed bandwidth [30]. Spiral antennas have been used for energy harvesters [3], [4], wi-fi applications [5] , and even nantenna electromagnetic collectors [6]. Spiral antennas have been used in navigational applications for ultra-wideband car applications [7]. Some spiral antennas are even reconfigurable and can be used for MIMO communication systems [8]. Although each of the above uses of spiral antennas are desirable, this research focuses on the use of spiral antennas for broadband applications that require the reuse of power from the surrounding environment.

5.2 Analysis, Structure, and Design of the Spiral Antenna

An equiangular spiral antenna is a frequency independent antenna [10]. A frequency independent antenna is an antenna whose shape is determined solely by angles [11]. In order to design an equiangular spiral antenna, it is first necessary to describe an equiangular spiral. An equiangular spiral is shown in the figure below.

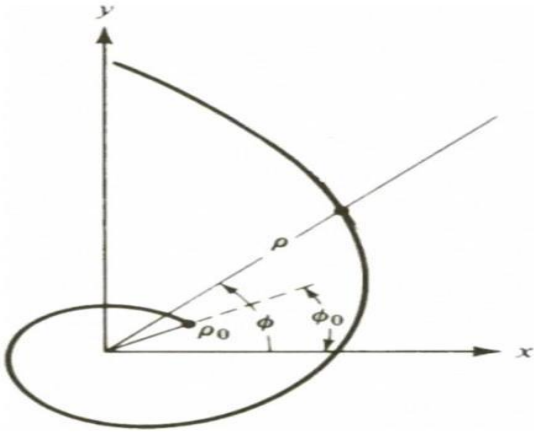

Figure 87 - Equiangular Spiral [23], [24]

The shape of the equiangular spiral can be described using the equation below [23], [24], [21]:

$$\rho = \rho_0 e^{a(\phi - \phi_0)}$$

where

ρ is the radius of the spiral at angle ϕ;

ρ_0 is the initial radius at an angle ϕ_0; and

a is the tightness of the spiral arm.

In practice, an equiangular spiral must be finite in length. The length corresponds to the angle at which the spiral can be truncated. The length of the spiral can be obtained using [23]:

$$L = (\rho - \rho_0)\sqrt{1 + \frac{1}{a^2}}$$

where

ρ_0 is the inner radius of the spiral;

ρ is the outer radius of the spiral.

The arm length is defined as "the spiral length along the center line of the arm."[32] Dyson stated that the length of the arm only has to be "comparable to one wavelength at the lowest frequency of operation to obtain performance essentially independent of frequency."[32] That is, according to [32], [25], in order for a spiral antenna to operate effectively as a frequency independent antenna, the length of the spiral antenna should be equal to a wavelength at the lowest frequency of operation [25]. Thus, if the lowest frequency of operation of a spiral antenna is known, the length of the spiral can automatically be determined.

The structure of a two arm equiangular spiral antenna is shown in the figure below.

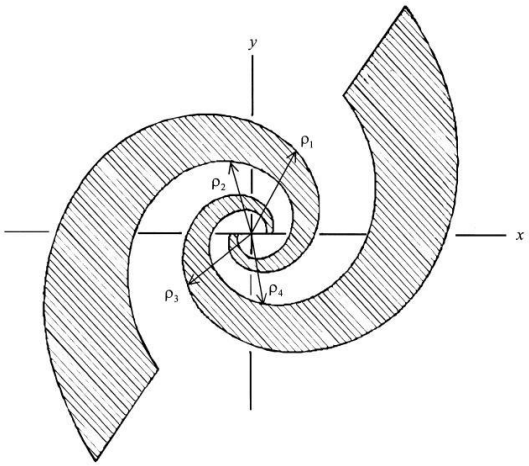

Figure 88: Equiangular Spiral Antenna(from [9])

In order to design the spiral antenna, the radii corresponding to each arm must be ascertained and are shown in the equations below [23], [31]

For the first arm,

$$\rho_1 = \rho_0 e^{a(\phi)}$$

and

$$\rho_2 = \rho_0 e^{a(\phi-\delta)}$$

where

ρ_0 is the terminal size; and

δ is the rotation angle.

For the second arm, the radii are:

$$\rho_3 = \rho_0 e^{a(\phi-\pi)}$$

and

$$\rho_4 = \rho_0 e^{a(\phi-\pi-\delta)}$$

Note that for the second arm, the first arm is simply shifted 180 degrees [11].

The arm width K of the spiral can then be determined using [23, 25]

$$K = \frac{\rho_2}{\rho_1}$$

which yields

$$K = e^{-a\delta}$$

Dyson is generally considered the father of truncation as he developed the Truncation Principle [19]. The truncation principal basically relies on the fact that after a certain distance along the spiral, current decreases to a point where truncating the spiral does not dramatically affect the active region of the spiral antenna [19]. That is, according to McFadden citing the Truncation Principle proposed by Rumsey, "In order to truncate the antenna properly, at any particular frequency, the majority of the radiation from the infinite antenna must be concentrated in a finite region."[19] After this distance, the spiral can be truncated and still allow for the antenna to be classified as a frequency independent antenna.

An ideal frequency independent spiral antenna would be infinite in length [27]. However, as stated previously, practical spiral antennas require finite dimensions to operate effectively. The equiangular spiral antenna can be truncated or tapered at a point along the spiral at which the current becomes negligible [27], [18]. That is, after the "active region", where the current is negligible at approximately a wavelength from the feed point, the spiral can be truncated or tapered [18]. This truncation sets the low frequency of the spiral antenna [33]. Below is a figure generated by McFadden [18] showing the active region of a spiral antenna.

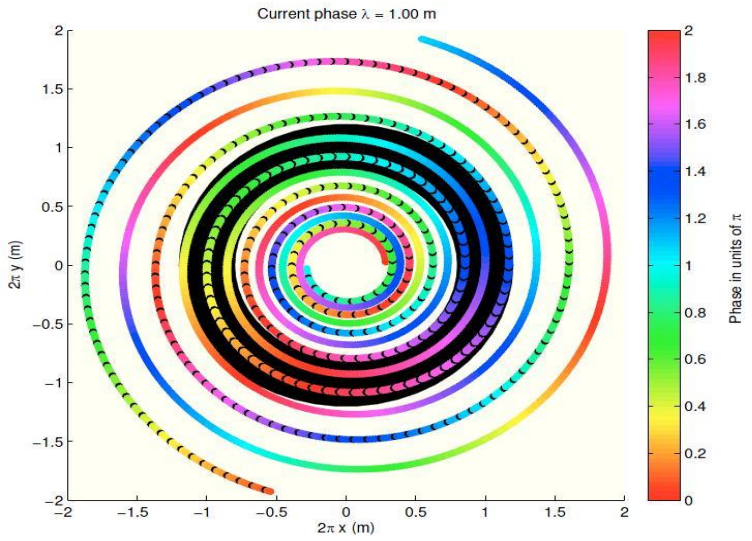

Figure 89: Active Region of Spiral Antenna [20]

The darkened region indicates the Active Region of the spiral antenna where the currents are in phase and thus do not cancel each other out [20]. The non-black regions represent the locations where the currents are out of phase and thus the region is not considered the active region [20].

Tapering is also a means used to limit the length of the spiral. Tapering allows the lower limit of frequency independent performance to be minimized [18]. A circle defined by the diameter at the large end of the spiral is generally used to taper the spiral [18]. Below is a sample of a figure spiral being tapered as opposed to truncated, after the active region of the spiral.

Figure 90: Truncated Spiral Antenna (Source: [34])

The main lobes radiated by the equiangular spiral are broadside lobes on both sides of the antenna and are perpendicular to the spiral antenna [32]. That is, a spiral antenna in free space radiates on both sides of the antenna. Radiation can be eliminated on a side of the spiral by mounting the spiral over a cavity. That is, to eliminate radiation on a specific side of the spiral, place a cavity on that side of the spiral [11].

Good radiation patterns (those that are consistent and display broadband properties) occur when the number of turns is 1.25 or 1.5 turns [32]. That is, in order to have a pattern that is reasonable, the minimum length of the spiral antenna should be 1.25 to 1.5 turns [11]. Radiation of the spiral antenna is caused primarily by the current in the active region of the spiral antenna [17]. At a distance of $r \cong \frac{1}{2}\lambda$ the current is considered at a maximum [12]. The active region is finite region of the spiral antenna [11].

The microstrip spiral antennas used in this research are planar spiral antennas. Microstrip planar spiral antennas are circularly polarized and radiate on the front side, since the backside has a conducting ground plane [9].

Bandwidth with regards to the equiangular spiral antenna is defined as the "band of frequencies over which the antenna radiates a field such that the axial ratio of the polarization, recorded on the axis of the antenna, is less than 2 to 1."[32]

The bandwidth of the equiangular spiral antenna can be written as [28]:

$$BW = \frac{f_{max}}{f_{min}}$$

The upper cutoff frequency is dictated by the feed size of the antenna [32]. The lower cutoff frequency of the spiral antenna is dictated by the length of the spiral antenna, respectively [24].

The arm length of each spiral controls the polarization of the spiral antenna [23]. When the lengths of the arms are a wavelength or greater, the antenna is circularly polarized [30]. Thus, for general applications, the equiangular spiral antenna radiates both right hand circular polarization and left hand circular polarization (RHC on the RHC side and LHC on the LHC side) [29]. The radiated field rotates in the same direction as the current [29].

The electric field of a two arm equiangular spiral antenna in the far field [26] is:

$$E_{\phi} \approx E_0 \beta^3 A(\theta) e^{j\left(n\left(\phi+\frac{\pi}{2}\right)-\psi(\theta)\right)} \frac{e^{-j\beta r}}{r}$$

where

$$A(\theta) = \frac{\cos\theta \left(\tan\frac{\theta}{2}\right)^n e^{\left(\frac{n}{a}\right)\tan^{-1}(a\cos\theta)}}{\sin\theta\sqrt{1+a^2(\cos\theta)^2}}$$

and

$$\psi(\theta) = \frac{n}{2a} ln|1+a^2(\cos\theta)^2| + \tan^{-1}(a\cos\theta)$$

For the far-field electric field in the above equation:

E_0 is an excitation strength related constant; and

n is an integer that indicates the order of the Bessel function of the first kind.

For the "most common spiral antenna mode" n = 1. Under the n = 1 mode, a broadside single side lobe is generated[26].

Radiation patterns for several different modes [9] are shown in the figure below.

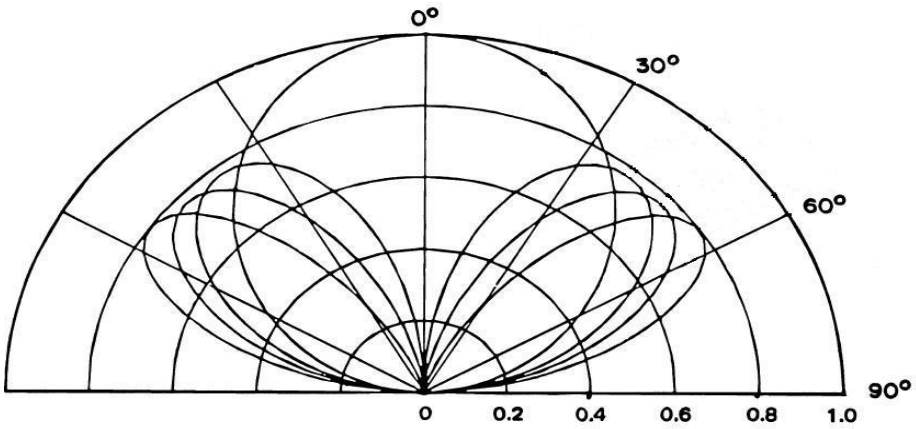

Figure 91: Radiation patterns of a spiral antenna for various modes (Adapted from [9])

The input impedance of the spiral antenna is extremely important in designing a spiral rectenna. When spiral antennas are being designed for use in a rectenna, the antennas are designed based on the impedance of the diode. Thus, diode selection is extremely important in designing the spiral antenna for a rectenna. That is, for a given impedance of the diode, the width, spacing, and length of arms must be calculated.

For a spiral antenna in free space, the input impedance using Babinet's principle [22] is

$$Z = \frac{\eta}{2}$$

which further reduces to

$$Z = \frac{1}{2}\sqrt{\frac{\mu}{\varepsilon}}$$

and

$$Z = \frac{1}{2}\sqrt{\frac{\mu_0}{\varepsilon_r \varepsilon_0}}$$

A spiral antenna's input impedance is a function of the antenna's mode of operation and the number of arms [16]. For a complementary arm spiral antenna in free space, the input impedance is 188.5 Ω.

The input impedance of an equiangular spiral antenna at the feed point with a substrate backing [19], [20] is given as:

$$Z_{in} = \frac{\eta_0}{2\sqrt{\varepsilon_{eff}}}$$

where

$$\varepsilon_{eff} = \frac{\varepsilon_r + 1}{2}$$

ε_r is the dielectric constant of the substrate.

From [21], this can be rewritten as:

$$Z_{in} = \frac{Z_{ant}}{\sqrt{\varepsilon_{eff}}}$$

where

Z_{ant} is the input impedance of the spiral antenna without the substrate

Thus, for a given input impedance:

$$Z_{in} = \frac{Z_{ant}}{\sqrt{\varepsilon_{eff}}}$$

where

$$\varepsilon_{eff} = \left(\frac{Z_{ant}}{Z_{in}}\right)^2$$

and

$$\frac{\varepsilon_r + 1}{2} = \left(\frac{Z_{ant}}{Z_{in}}\right)^2$$

$$\varepsilon_r = 2\left(\frac{Z_{ant}}{Z_{in}}\right)^2 - 1$$

Spiral rectennas provide a means of converting broadband energy to usable power. Hagerty was able to recycle ambient microwave energy by using an array of spiral rectennas [1,2]. Others have used single spiral rectennas to recycle energy [3,4]. This research focuses on utilizing a single spiral rectenna to harvest ambient microwave energy. As stated previously, a broadband spiral rectenna comprises a spiral antenna and a rectifier. The rectifier (diode) is placed at feed of the antenna at the center of the spiral. The general layout of a spiral rectenna [1] is shown in the figure below.

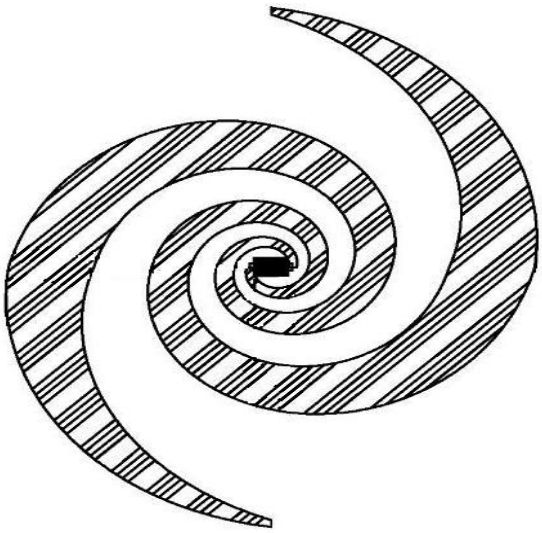

Figure 92: Spiral Rectenna (Adapted from [1])

The design parameters that are of specific concern are the size limitations and the efficiency required of efficiency required for conversion [35]. The conversion efficiency is a

function of the power incident on the antenna and the power output by the rectifier. Some rectennas add a matching network between the antenna and rectifier and are still considered rectennas. However, the additional matching network adds to the size of the rectenna and thus is not always considered practical when space considerations are of particular importance in the design.

A balanced spiral antenna, such as the equiangular spiral antenna, requires a balanced feed [36]. Note that the initial radius (and thus the diameter of the feed line) limits the upper frequency of the spiral antenna, and thus effects the bandwidth of the antenna [37]. The lower frequency is limited by the length of the spiral antenna. Normally, the design dimension of the feed line for the spiral antenna is flexible, meaning the diameter can be increased or decreased as needed for the specific application of the spiral antenna. However, when designing a spiral rectenna, the design of the feed and thus the design of the spiral rectenna is limited by the dimensions of the diode. Thus, when designing the spiral rectenna, the designer should determine the diameter of the diode, which will give the initial radius ρ_0 required for the design of the spiral.

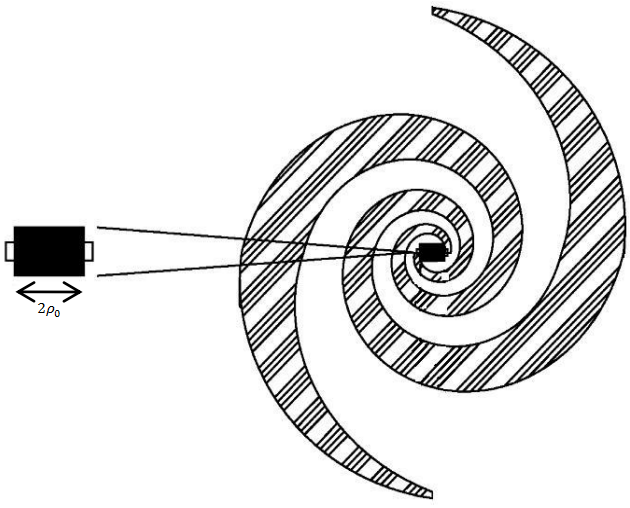

Figure 93: Spiral Rectenna Showing Initial Radius (Adapted from [1])

The DC power is given by the formula [3] below:

$$P_{dc} = \eta_{RF/DC} \, \mathrm{P_{RF}}$$

where

P_{dc} is the DC power;

P_{RF} is the available RF power; and

$\eta_{RF/DC}$ is the RF to DC power conversion efficiency.

Maximizing available RF power P_{RF} for energy harvesting is of critical importance in designing the spiral rectenna. Minimum and maximum frequencies should be selected that maximize the amount of power that will be available for AC-to-DC conversion.

5.3 Rectifier Design and Simulations

The diode selected for rectifier design is of particular importance because the diode is placed at the feed point of the spiral. As the diode is used for rectification, selection of the appropriate diode with a high conversion efficiency is of vital importance [38]. Recall that when designing a spiral rectenna, the feed size, and thus the diode package size, dictates the maximum frequency of the spiral rectenna [1].

The diode package type dictates the design of spiral rectenna. This is because the design of the spiral rectenna is based upon the length of the diode package, since it corresponds to the initial radius of the spiral and dictates the upper frequency of the spiral. Selecting the "smallest package" with no freestanding connectors is ideal because the amount of package parasitic are reduced [38]. The typical diode package used for the spiral antenna is illustrated in the above section concerning diodes.

There are generally two types of diode packages that can be used for high frequency Schottky diodes: SOT-23 and SC-79. The SOT-23 allows for the placement of two diodes in the package and is often used for voltage doubling. The SOT 23 package is generally not desirable for the spiral rectennas because of the third pin that can cause interference with rectification by basically acting as a freestanding antenna. The two types of packaging are shown below:

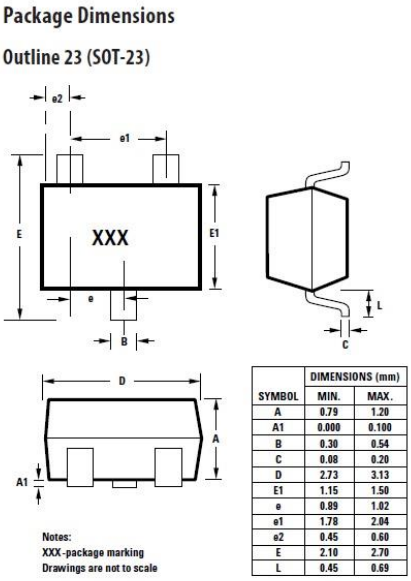

	DIMENSIONS (mm)	
SYMBOL	MIN.	MAX.
A	0.79	1.20
A1	0.000	0.100
B	0.30	0.54
C	0.08	0.20
D	2.73	3.13
E1	1.15	1.50
e	0.89	1.02
e1	1.78	2.04
e2	0.45	0.60
E	2.10	2.70
L	0.45	0.69

Figure 94: SOT-23 Schottky diode package type.

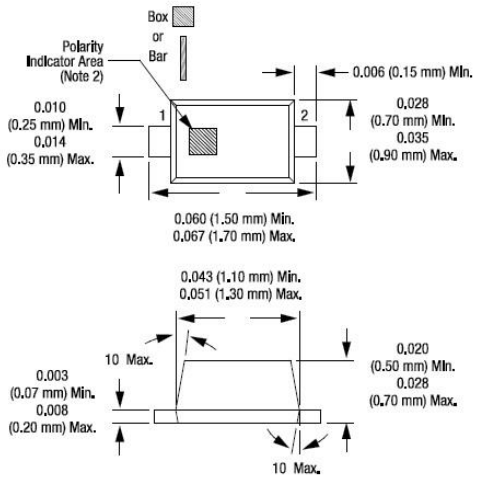

Figure 95: SC-79 Package Dimensions (Source: Datasheet Skyworks SMS7630-079

For each rectenna application the parasitic elements of the packaged diode were considered. Avago Technologies, Skyworks and MA/Com manufacture numerous high frequency diodes that are used for rectification purposes. The datasheets and application notes of the diode manufacturer (in this case, Avago Technologies), provide the parameters for use in system design. Examples of the characteristics and applications parameters and as well there use in other rectenna applications are illustrated in [15], [13], [18], [19], 20] for the HSMS 2820, [1], [3], [5], [21] (remote RF battery charging) for the HSMS 2850, and [x] for the HSMS 2852. The electrical parameters of several diodes are illustrated the table below.

Table 10: SPICE Model Parameters

Electrical Parameters of High Frequency Schottky Diodes				
Parameter	**SMS7630**	**MA4E2054**	**HSMS 2862**	**Units**
Is	5.00E-06	3.00E-08	5.00E-08	A
Rs	20	11	6	Ohms
N	1.05	1.05	1.08	-
TT	1.00E-11	0	-	s
Cjo	0.14	1.30E-13	0.18	pF
M	0.4	0.5	0.5	-
EG	0.69	0.69	0.69	eV
XTI	2	-	2	-
Fc	0.5	-	-	-
Bv	1	5	7	V
IBV	1.00E-04	1.00E-05	1.00E-05	A
Vj	0.34	0.4	0.65	V

As with the WRCS system, the impedance of several diodes is calculated using ADS in order to determine the feasibility of rectification within the desired band of operation, 8 – 12 GHz in this case. However, unlike the diode in the WRCS system, the physical dimensions of the diode of are of primary concern in order for the diode to fit at the feeding point of the rectenna. The ADS circuit as well as the impedance of the diodes is shown in the table below.

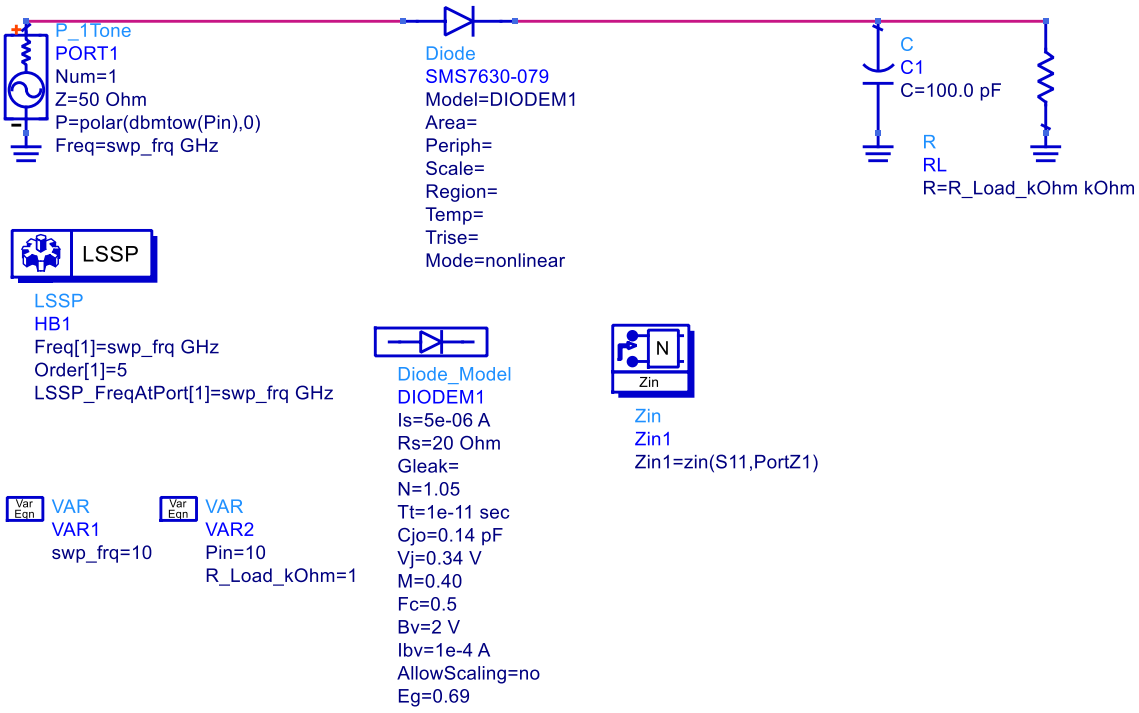

Figure 96: ADS circuit for input impedance calculation with an input power of 10 dBm, a load of 1 kOhm, and a DC Pass filter of 100 pF.

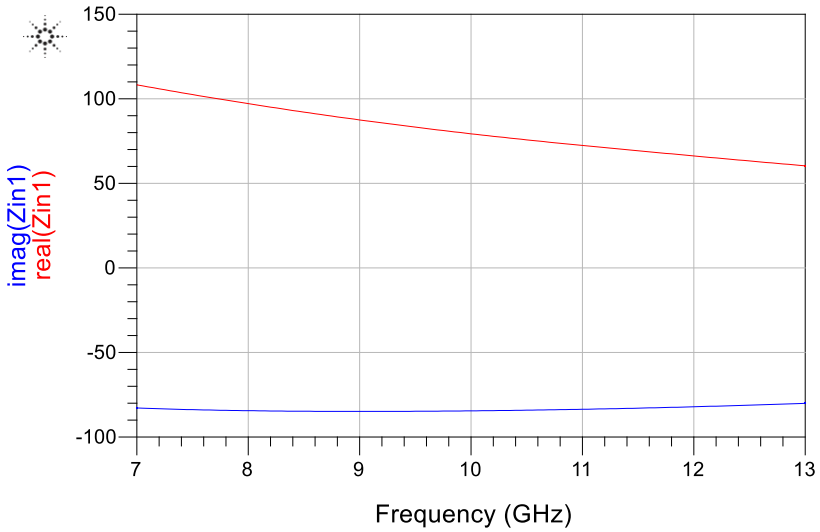

Figure 97: Input impedance of the SMS 7630-079 rectification circuit.

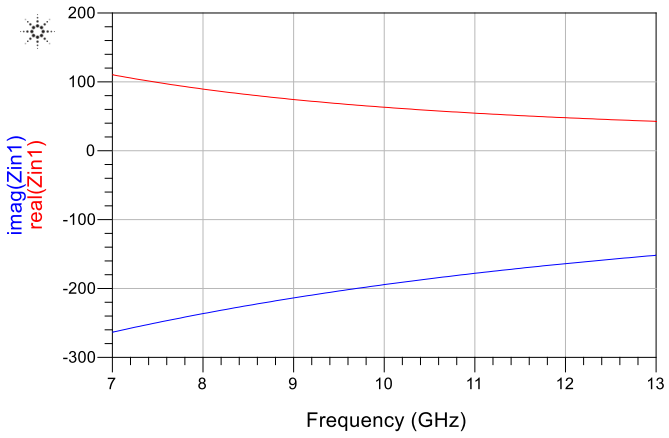

Figure 98: Input impedance of the MA4E2054 rectification circuit.

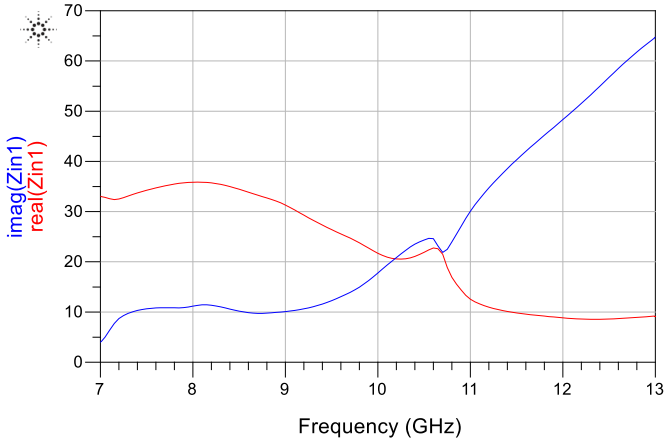

Figure 99: Input impedance of the HSMS 2862 rectification circuit.

5.4 Broadband Rectenna Design and Simulations

The topology of the spiral antenna design is shown in the figure below.

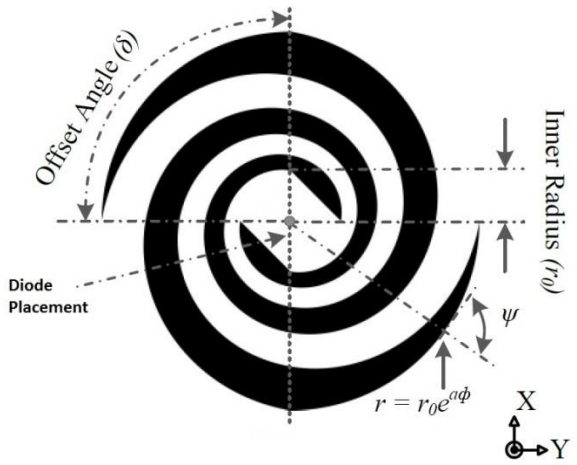

Figure 100: Spiral Antenna (Adapted from [40] for diode placement)

To accommodate the design of the Wilkinson Rectenna Communication System, the spiral antenna was designed to operate within the range of 8-12 GHz. The spiral antenna was designed based on length of the diode which is 3.13 mm. The inner radius was thus defined to be 1.6 mm. The number of turns is 1.25. The offset angle was selected to be 90 degrees. After several iterations, the expansion coefficient was selected as 7.88. Because the maximum frequency of operation of the spiral is based on the radius at the input of the spiral (inner radius), the maximum frequency of operation is greater than the desired frequency [39].

The spiral antenna was designed to operate in the X-band to allow for radar guns to replenish the charge of a battery. A figure of the designed spiral is shown in the figure below.

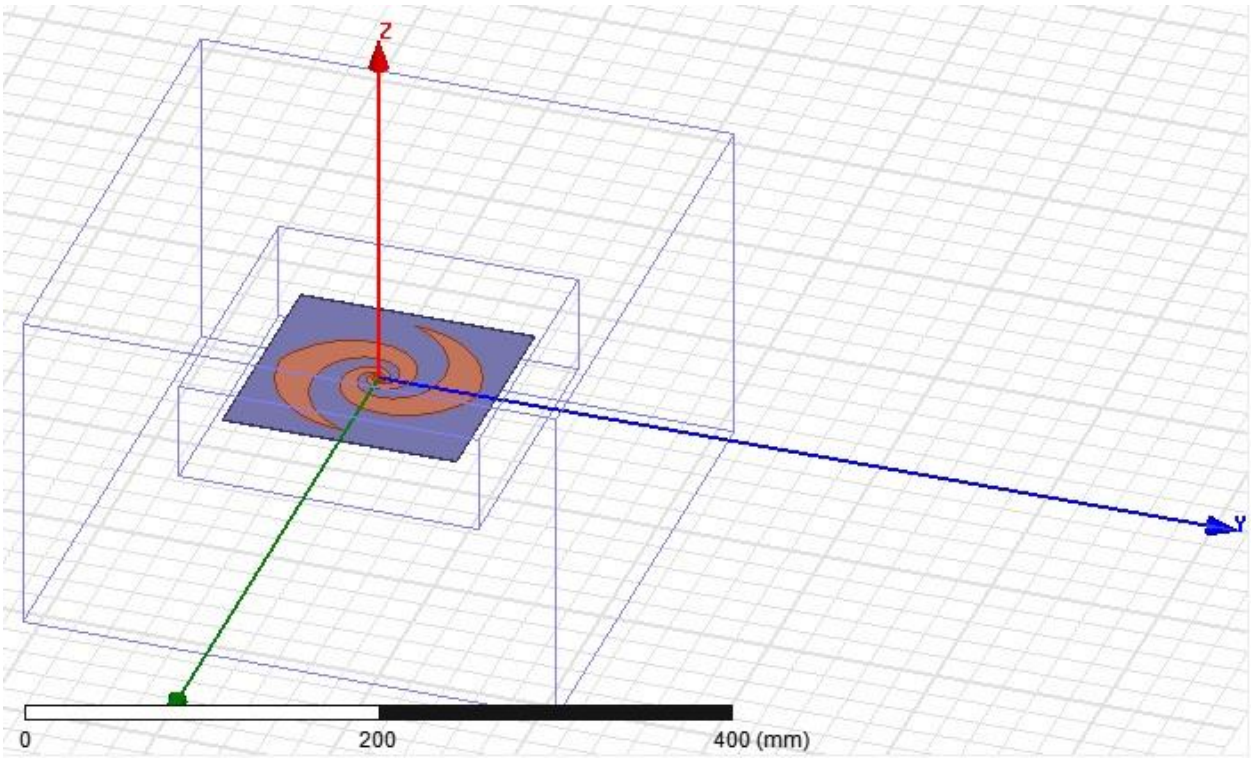

Figure 101: Spiral Antenna designed to operate between 8 - 12 GHz

The simulated 3D gain is shown in the figures below.

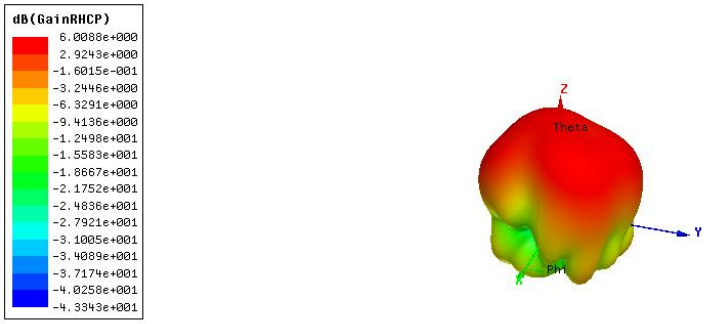

Figure 102: Simulated RHCP gain.

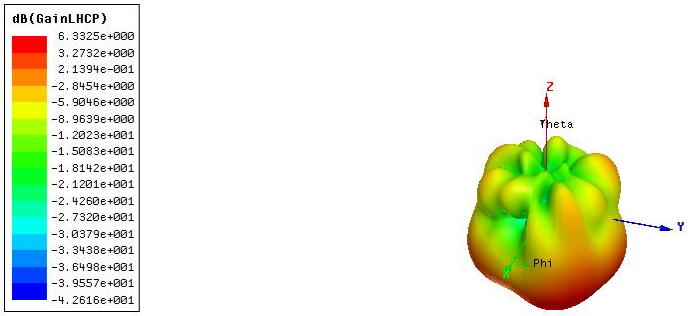

Figure 103: Simulated LHCP gain.

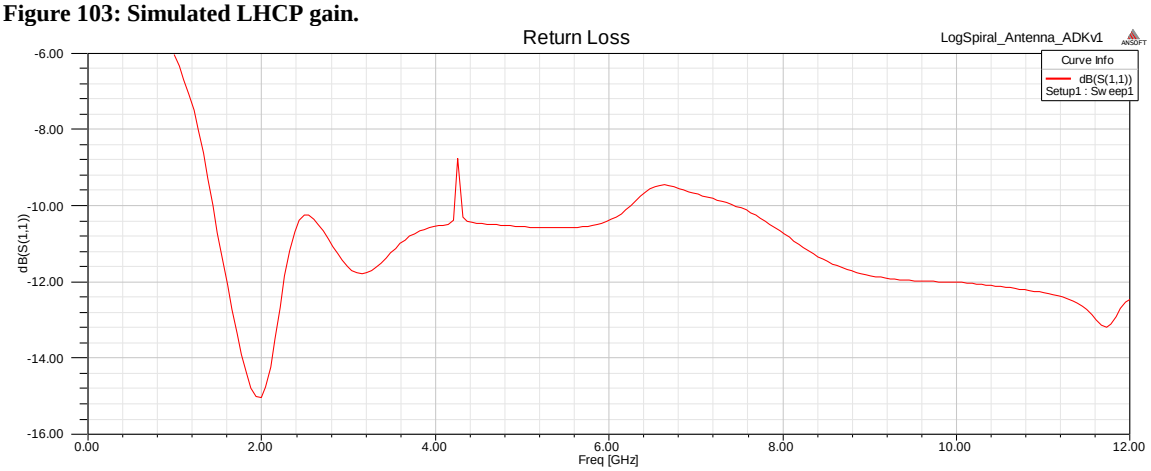

Figure 104: Return Loss of a spiral antenna operational at 8 - 12 GHz

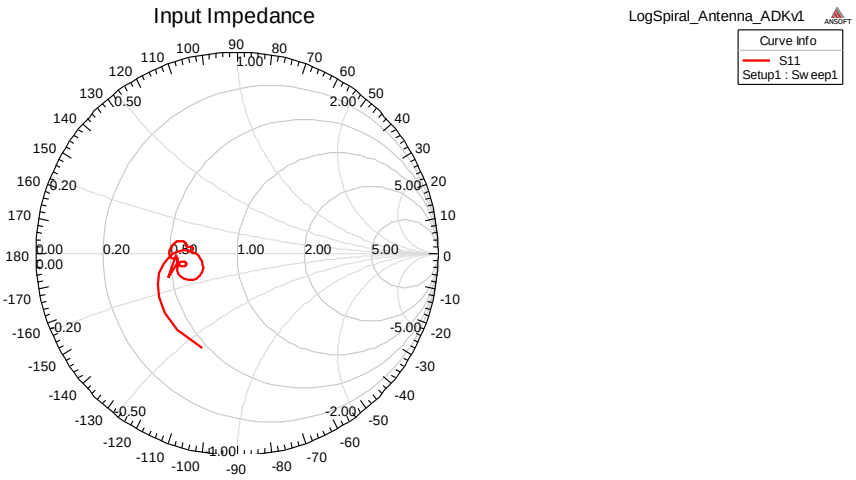

Figure 105: Input impedance of spiral antenna designed to operate between 8 - 12 GHz

The spiral rectenna was simulated in ADS and is shown in the figure below.

Figure 106: ADS Circuit for Spiral Rectenna with 10 dBm input power and a 1 kOhm load.

As can be seen from the DC Voltage figure below, the rectified voltage of the spiral rectenna is relatively constant between 8 and 10 GHz. At 10 GHz, the rectified voltage is 0.64 V.

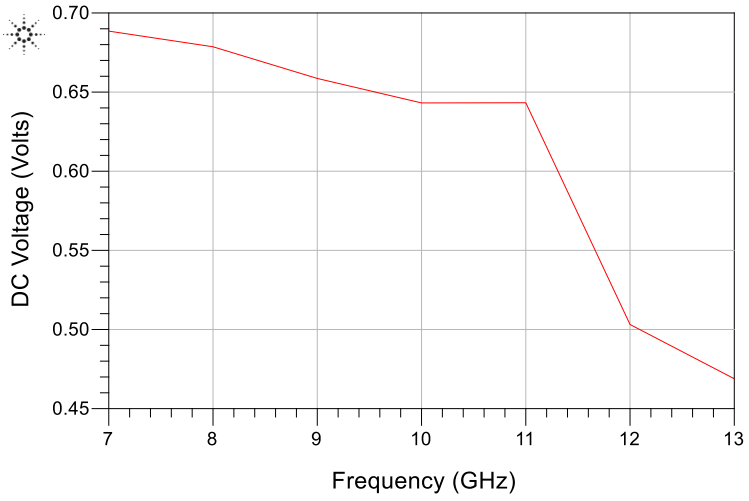

Figure 107: Rectified voltage for the Spiral Rectenna with SMS 7630-079, input power of 10 dBm, and load of 1kOhm.

The circuit for the Skyworks spiral rectenna as well as the resulting rectified are shown in the ADS schematic and figures below. The DC voltage rectified by the spiral rectenna is between 0.35 V for a 0 dBm input power and 0.95 V for a 20 dBm input power.

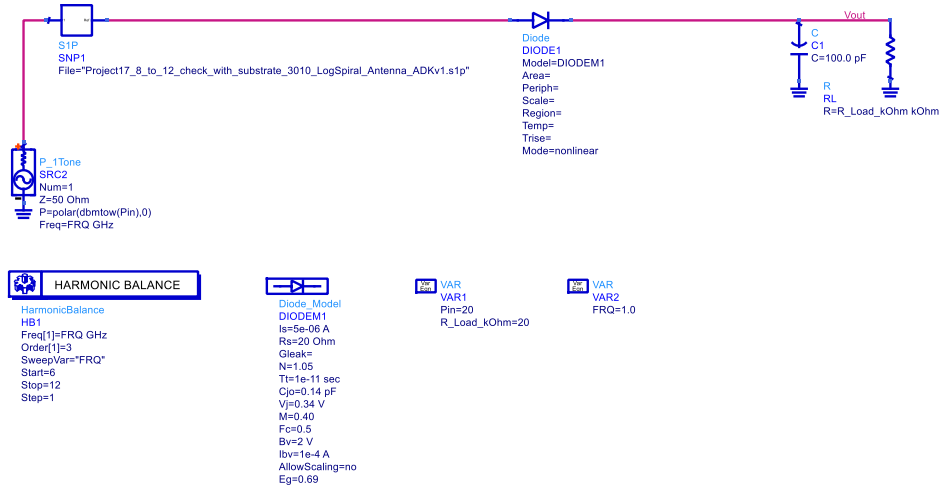

Figure 108: Spiral Rectenna ADS Circuit Layout – Skyworks SMS7630-079

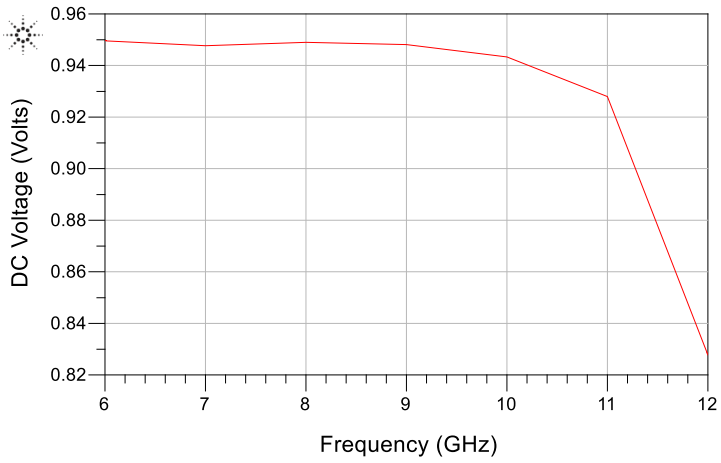

Figure 109:DC Voltage for the Skyworks SMS7630-079 with a 20 dBm input power

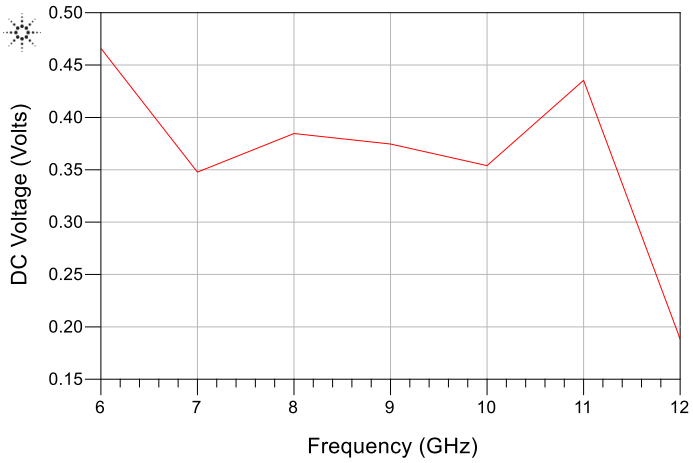

Figure 110: DC Voltage for the Skyworks SMS7630-079 with a 0 dBm input power

As can be seen from the simulated results, the amount of voltage rectified for a single broadband spiral rectenna is not significant (between 0.35 V for 0 dBm input power and 0.95 V for 20 dBm input power).

5.5 Conclusion

A single spiral rectenna alone is not desirable for rectification unless it is coupled with another source of rectification, such as a spiral rectenna array or the WRCS system. In addition, the space required for such an array may not be desirable for RFID systems since an array of spiral rectennas would require additional space not available in typical RFID designs. Additional options may include, circularly polarized patch antennas or standard rectangular patch microstrip array configurations. Such options would allow the antenna engineer to increase the amount of rectified voltage to provide additional power to the WRCS system.

5.6 References

[1] J.A. Hagerty, W. H. McCalpin, R. Zane, Z. B. Popovic, "Recycling Ambient Microwave Energy With Broad-Band Arrays", IEEE Transactions On Microwave Theory and Techniques, 2004, Vol. 52.

[2] J.A. Hagerty, N. D. Lopez, B. Popovic, Z. Popovic, "Broadband Rectenna Arrays for Randomly Polarized Incident Wave", s.l. : IEE.

[3] D. Bouchouicha, F. Dupont, M. Latrach, L. Ventura, "Ambient RF Energy Harvesting", International Conference on Renewable Energies and Power Quality, Granada, 2010.

[4] D. Bouchouicha, F. Dupont, M. Latrach, L. Ventura, "An Experimental Evaluation of Surrounding RF Energy Harvesting Devices", Proceedings of the 40th European Microwave Conference, Paris, September 2010.

[5] M.F. Abdul Khalid, M.A. Haron, A. Baharudin, A.A. Sulaiman, "Design of a Spiral Antenna for Wi-fi Applications", IEEE International RF and Microwave Conference Proceedings, 2008.

[6] D.K. Kotter, S.D. Novack, W.D. Slafer, P. Pinhero, "Solar Nantenna Electromagnetic Collectors", Proceedings of ES2008 Energy Sustainability, ASME, Jacksonville, Florida, 2008.

[7] E. Gschwendtner, W. Wiesbeck, "Ultra-Broadband Car Antennas for Communication and Navigation Applications", IEEE Transactions on Antennas and Propagation, Vol. 51, No. 8, August 2003.

[8] P. Mookiah, D. Piazza, and K. R. Dandekar, "Reconfigurable spiral antenna array for pattern diversity in wideband MIMO communication systems," presented at the IEEE Antennas and Propagation Society Int. Symposium., Jul. 2008.

[9] R. Bansal, *Fundamentals of Engineering Electromagnetics*, pg. 295, CRC Press, Boca Raton, 2006.

[10] Y.T. Lo, S.W. Lee, *Antenna Handbook: Theory, Applications, and Design*, pgs. 9-72- 9-79, Van Nostrand Reinhold Company Inc., New York, 1988.

[11] T.A. Milligan, *Modern Antenna Design*, McGraw-Hill, New York, 1985.

[12] K.F. Lee, *Principles of Antenna Theory*, John Wiley & Sons, New York, 1985.

[13] *Antenna Standards Committee of the IEEE Antennas and Propagation Society*, IEEE Standard Definitions of Terms for Antennas, IEEE, New York, 1993.

[14] V.H. Rumsey, "Frequency Independent Antennas,"1957 IRE National Convention Record, pt. 1, pp. 114-118.

[15] V.H. Rumsey, *Frequency Independent Antennas*, Academic Press, New York,1966.

[16] T.A. Milligan, *Modern Antenna Design*, Second Edition, New Jersey, 2005.

[17] W. Fu, "Broadband Nested Antenna", Doctoral Thesis, RMIT, 2010.

[18] Y.T. Lo, S.W. Lee, *Antenna Handbook: Theory, Applications, and Design*, Van Nostrand Reinhold Company Inc., New York, 1988.

[19] M. McFadden, W. R. Scott Jr., "Analysis of the Equiangular Spiral Antenna on a Dielectric Substrate," *IEEE Trans. Antennas Propag.*, vol. 55, 2007.

[20] M. McFadden, "Analysis of the Equiangular Spiral Antenna", PhD Thesis, Georgia Institute of Technology, Atlanta, GA, 2009.

[21] S. Kim, M.M. Tentzeris, G. Jin, S. Nikolaou, "Inkjet Printed Ultra Wideband Spiral Antenna Using Integrated Balun on Liquid Crystal Polymer (LCP)", IEEE - Antennas and Propagation Society International Symposium (APSURSI), pg. 1-2, 2012.

[22] H. G. Booker, “Slot aerials and their relation to complementary wire aerials (Babinet’s Principle),” *J. Inst. Electr. Eng.*, vol. 93, pp. 620–626, 1946.

[23] C.A. Balanis, *Antenna Theory: Analysis and Design*, Third Edition, Wiley, New York, 2005.

[24] C.S.R. Fernando, “A Parametric Study of Equiangular Spiral Antenna (Arm type)”, Fourth International Conference on Industrial and Information Systems, ICIIS 2009, December 2009.

[25] Y.T. Lo, S.W. Lee, *Antenna Handbook Antenna Theory Volume II*, Van Nostrand Reinhold, New York, 1993.

[26] J.L. Volakis, C. Chen, K. Fujimoto, *Small Antennas: Miniaturization Techniques & Applications,* McGraw Hill, New York, 2010.

[27] G.S. Clute, “Very Broadband VHF/UHF Omnidirectional Antenna Design Study”, Masters Thesis, Air Force Institute of Technology, 1989.

[28] L.T. Yong, “Broadband Counterwound Sprial Antenna For Subsurface Radar Applications, Masters Thesis”, Naval Postgraduate School, Dec. 2003.

[29] I. Yildiz, “Design and Construction of Reduced Size Planar Spiral Antenna in the 0.5 – 18 GHz Frequency Range”, Masters Thesis, Middle East Technical University, October 2004.

[30] J. Thaysen, K.B. Jakobsen, J. Appel-Hansen, “A Logarithmic Spiral Antenna for 0.4 to 3.8 GHz”, *Applied Microwave & Wireless*, pp. 32-45, Feb 2001.

[31] F.J.T. Moreira, “Broadband Feed for a Parabolic Antenna for Satellite Tracking”, Masters Thesis Draft, Faculdade de Engenharia da Universidad do Porto, January 2011.

[32] J.D. Dyson, “The Equiangular Spiral Antenna,”, *IRE Transactions on Antennas and Propagation*, 1959:181-187.

[33] J.L. Volakis, *Antenna Engineering Handbook*, McGraw-Hill, New York, 2007.

[34] H. Nakano, K. Kikkawa, N. Kondo, Y. Iitsuka, J. Yamauchi, "Low-Profile Equiangular Spiral Antenna Backed by an EBG Reflector", IEEE Transactions on Antennas and Propogation, Vol. 57, No. 5, May 2009.

[35] P. Mookiah, D. Piazza, and K. R. Dandekar, "Reconfigurable spiral antenna array for pattern diversity in wideband MIMO communication systems," presented at the IEEE Antennas and Propagation Society Int. Symposium., Jul. 2008.

[36] Y.T. Lo, S.W. Lee, *Antenna Handbook: Theory, Applications, and Design*, Van Nostrand Reinhold Company Inc., New York, 1988.

[37] J.A. Hagerty, "Nonlinear Circuits And Antennas For Microwave Energy Conversion", PhD Thesis, University of Colorado, 2003.

[38] F.B. Helmbrecht, "A Broadband Rectenna Array for RF Energy Recycling", Technische Universitat Munchen, September 2002.

[39] D. Aristizabal, "Electromagnetic Characterization of Miniature Antennas for Portable Devices", Masters Thesis, University of South Florida, October 30, 2006.

[40] Y. Amin, "Printable Green RFID Antennas for Embedded Sensors", PhD Thesis, KTH School of Information and Communication Technology, Sweden, January 10, 2013.

6 CONCLUSIONS AND FUTURE WORK

The Wilkinson Rectenna Communication System was studied, fabricated and tested and yielded the desired rectification and communication results as expected. A voltage of approximate 1.7 volts was measured and provided for the powering of low power communication devices, while still allowing the device to function as a communication system with a received power of 5.17 dBm. The system is also capable of being utilized as an energy harvesting device at 5.8 GHz while in sleep mode. The WRCS system allows for remote wireless power transmission in systems that do not allow for ease of battery replacement based on the location of the wireless communication device or cost of replacing the battery.

Future work can focus on developing larger rectenna arrays to generate more DC voltage for powering high power devices. Because many of the communication systems that use rectennas are in harsh environments (roads, bridges, etc.), studies can be done to test the effects of the environment on the WRCS system. The harmonics generated by the diode could be studied and methods could be developed to improve the system by eliminating the harmonics by adding a sufficiently sized bandpass filter. A DC bandpass filter can be studied to see the effects the RF signals having on the load and to reduce the amount of RF signal provided to the load. A forced phase difference could also be studied and added to the circuit to generate voltage primarily based upon the phase difference instead of power difference.